Renal-specific and inducible depletion of NaPi-IIc/Slc34a3, the cotransporter mutated in hereditary hypophosphatemic rickets with hypercalciuria, does not affect phosphate or calcium homeostasis in mice

---

Dissertation

zur

Erlangung der naturwissenschaftlichen Doktorwürde

(Dr. sc. nat.)

vorgelegt der Mathematisch-naturwissenschaftlichen Fakultät

der Universität Zürich

von

Myakala Komuraiah

aus

Indien

Promotionskomitee

Prof. Dr. Carsten A. Wagner

Prof. Dr. Jürg Biber

Dr. Natividad Hernando

Dr. Daniel Fuster

Zürich, 2014

Contents

1. Zusammenfassung

Die homöostatische Kontrolle von systemischem Phosphat (Pi) wird weitgehend durch die Balance von renaler Reabsorption von Pi aus dem Ultrafiltrat und intestinaler Absorption von Pi aus der Nahrung aufrecht erhalten. Die renale Reabsorption von Pi findet hauptsächlich in den proximalen Tubuli statt wofür die Na/Pi-Kotransporter Slc34a1/NaPi-IIa, Slc34a3/NaPi-IIc und Slc20a2/Pit-2 verantwortlich sind. Diese Transportproteine sind in der apikalen Membran lokalisiert und werden durch verschiedene Hormone reguliert, wie z.B. durch das Parathormon (PTH) oder durch den "fibroblast growth factor 23" (FGF23). Aufgrund der Daten die von NaPi-IIa und NaPi-IIc defizienten Mausmodellen erhalten wurden geht hervor, dass NaPi-IIa quantitativ die Hauptrolle bei der renalen Reabsorption von Pi spielt, wohingegen NaPi-IIc eine wohl eher geringere Rolle spielt und eventuell auf junge Tiere beschränkt ist. Im Gegensatz zu der Maus, wurden beim Menschen verschiedene Mutationen im NaPi-IIc Gen beschrieben, welche mit dem Krankheitsbild HHRH (hereditary hypophosphatemic rickets with hypercalciurie) assoziert sind.

Das Ziel der vorliegenden Arbeit war es ein Mausmodell zu generieren, in welchem das NaPi-IIc Gen nierenspezifisch und induzierbar ausgeschaltet werden kann. Dieses Modell basiert auf dem loxP:Cre Rekombinase-System. Transgene Mäuse, welche homozygote Träger des gefloxten NaPi-IIc ($NaPi\text{-}IIc^{f/f}$) Gens waren, wurden mit Pax8rtTA/LC1 Tieren verpaart. Damit wurden Mäuse erhalten in denen die Expression der Cre-Rekombinase nierenspezifisch durch Doxycyclin (Doxy) induziert werden konnte.

Zu Beginn der Experimente wurde die Cre Aktivität in 3 bis 4 Wochen alten Mäusen durch die Gabe von 2 mg/ml Doxy im Trinkwasser während 10 Tagen induziert. Als Negativkontrollen dienten Wurfgeschwister. Urinproben wurden während den letzten 24 Stunden des Versuchsprotokolls gesammelt und am Ende wurden Blut, Nieren und Ileum entnommen. Diese Behandlung führte zu einer kompletten Reduktion von NaPi-IIc mRNA und Protein in den Nieren. Allerdings war die Ausscheidung von Pi im Urin bei allen Doxy behandelten Tieren erhöht, mit gleichzeitiger reduzierter Ausscheidung von Na^+ - und K^+ - Ionen. Dies deutete darauf hin, dass die Behandlung mit 2 mg/ml Doxy entweder zu

unspezifischen renalen Effekten führte, oder möglicherweise eine intestinale Veränderung bewirkte.

Um die Dosierung von Doxy zu optimieren wurden NaPi-IIc$^{+/+}$ und NaPi-IIc$^{f/f}$ Mäuse zunächst während 10 Tagen entweder mit 1, 0.5 oder 0.25 mg/ml Doxy behandelt, gefolgt von einer Erholungsperiode von 15 Tagen mit normalem Trinkwasser. Bei Tieren, die 1 respektive 0.5 mg/ml Doxy erhielten war die Ausscheidung von Na^+ -Ionen im Urin immer noch reduziert, aber nicht mehr in Mäusen die mit 0.25 mg/ml behandelt wurden. In NaPi-IIc$^{f/f}$ Mäusen wurde die Expression von NaPi-IIc mRNA durch die Gabe von 1 respektive 0.5 mg/ml Doxy beinahe komplett unterdrückt, wohingegen 25% der Expression der NaPi-llc mRNA nach einer Dosis von 0.25 mg/ml erhalten blieben. Aufgrund dieser Resultate wurde ein neues Doxy Dosierungsprotokoll erarbeitet, nach dem die Tiere zunächst für 5 Tage mit 0.5 mg/ml Doxy und anschliessend für weitere 5 Tage mit 0.25 mg/ml Doxy behandelt wurden. Nach einer 15-tägigen Erholungsphase wurden die Tiere erneut untersucht. Als Indikator für unspezifische Effekte wurde wieder die Konzentration von Na^+ -Ionen im Urin gemessen. Die Ausscheidung von Na^+-Ionen im Urin bei behandelten Tieren war vergleichbar zu den Kontrollen, was darauf schliessen liess, dass dieses Induktionsprotokoll keine unspezifischen renalen Effekte hervorrufte. Die folgenden Experimente wurden deshalb mit diesem optimierten Protokoll durchgeführt.

Die Expression von NaPi-IIc mRNA und NaPi-llc Protein waren vergleichbar in NaPi-IIc$^{+/+}$ Kontrollmäusen die entweder mit Doxy oder nur mit Saccharose im Trinkwasser behandelt wurden. Erwartungsgemäss führte die Behandlung mit Doxy zu einer 50%-igen beziehungsweise 90%-igen Reduktion der Menge von NaPi-llc mRNA und Protein in NaPi-IIc$^{f/+}$ und NaPi-IIc$^{f/f}$ Tieren. Allerdings hatte das Fehlen von NaPi-llc in den Nieren der NaPi-IIc$^{f/f}$ Mäusen keinen Effekt auf die Na/Pi-Kotransport Aktivität in isolierten renalen Bürstensaummembranen und es wurden auch keine Aenderungen der Mengen der anderen renalen Na/Pi-Kotransporter, NaPi-IIa und Pit-2 beobachtet. Ebenso blieb die Menge von NaPi-IIb in Enterozyten unverändert. Dies deutete darauf hin dass keine Kompensation durch andere Na/Pi-Kotransporter in NaPi-IIc defizienten Mäusen stattfindet.

In Mäusen mit NaPi-IIc defizienten Nieren waren die Ausscheidung von Pi im Urin und die Plasmakonzentration von Pi normal. Die Konzentrationen der phosphaturischen Hormone PTH und FGF23 waren unverändert. Die Konzentrationen von Ca^{2+} im Plasma und Urin sowie des zirkulierenden $1,25(OH)_2D_3$ waren ebenfalls unverändert. Die Expression der 1α-Hydroxylase und der 24-Hydroxylase mRNA waren vergleichbar in NaPi-$IIc^{+/+}$ und NaPi-$IIc^{f/f}$ Mäusen.

Die Daten, die mit den induzierbaren nierenspezifischen NaPi-IIc defizienten Mäusen erhalten wurden, sind nur teilweise übereinstimmend mit den Beobachtungen, die für konstitutiv NaPi-IIc defiziente Mäuse beschrieben wurden. Obwohl in konstitutiv NaPi-IIc defizienten Mäusen die Pi Ausscheidung im Urin und die Plasmakonzentration von Pi ebenso normal blieben, ging die konstitutive Defizienz von NaPi-IIc mit einer Hyperkalzämie und Hyperkalziurie, sowie einer erhöhten Konzentration von $1,25(OH)_2D_3$ einher. Dies lässt darauf schliessen, dass nach einer konstitutiven Deletion des NaPi-llc Gens, das Fehlen von NaPi-IIc in extrarenalen Geweben zu den beobachteten Änderungen des Calcium-Haushaltes führt.

Zusammengefasst haben wir ein Maussmodell generiert, bei welchem das Na/Pi-Kotransporter NaPi-llc Gen SLC34a3 nierenspezifische und induzierbar inaktiviert werden kann. Die Analyse dieses Mausmodells zeigte, dass im Gegensatz zum Menschen, die renale Reabsorption von Pi durch NaPi-IIc minimal ist. Das hier beschriebene neue Mausmodell (floxed NaPi-IIc) erlaubt es, die noch weitgehend unbekannte Rolle von NaPi-IIc in verschiedenen Organen neben der Niere zu untersuchen.

2. Summary

Homeostatic control of inorganic phosphate (Pi) is largely achieved by renal reabsorption and intestinal absorption of Pi. Renal reabsorption of Pi takes place preferentially in the proximal tubules and is mediated by the Na/Pi-cotransporters Slc34a1/NaPi-IIa, Slc34a3/NaPi-IIc and Slc20a2/Pit-2. The abundance of these cotransporters is regulated by several hormones including parathyroid hormone (PTH) and fibroblast growth factor23 (FGF23). Based on constitutively deficient NaPi-IIa and NaPi-IIc mouse models, it has been postulated that NaPi-IIa plays a major quantitative role in the renal reabsorption of Pi in rodents, whereas the contribution of NaPi-IIc is considered to be less important and probably restricted to young animals. However, in humans several mutations have been identified in the NaPi-IIc gene that cause hereditary hypophosphatemic rickets with hypercalciuria (HHRH).

The aim of this study was to generate a renal-specific and inducible mouse model deficient of NaPi-IIc to investigate the contribution of this cotransporter to Pi reabsorption in young animals. This model is based on the loxP: Cre recombinase system. Mice harboring both floxed-NaPi-IIc alleles (NaPi-IIc$^{f/f}$) were bred with Pax8rtTA/LC1 mice in which the renal-specific expression of Cre-recombinase can be induced by doxycycline (Doxy). Further mating resulted in homozygous (NaPi-IIc$^{f/f}$) and heterozygous mutants (NaPi-IIc$^{f/+}$) as well as wild type (NaPi-IIc$^{+/+}$) mice that also expressed Pax8 and Cre.

Initially, Cre activity was induced in 3 to 4 weeks old mice by providing them water supplemented with 2 mg/ml Doxy in 2% sucrose for 10 days; as negative control, littermates drank 2% sucrose. Urinary samples were collected during the last 24 hours and at the end of the experimental protocol blood, kidney and ileum were extracted. The treatment with Doxy led to no changes in the expression of NaPi-IIc mRNA and protein in NaPi-IIc$^{+/+}$ mice. However, it resulted in a 50% reduction of the cotransporter mRNA and protein in NaPi-IIc$^{f/+}$ animals and almost full depletion in NaPi-IIc$^{f/f}$ mice compared to sucrose treated controls. Notably, the urinary excretion of Pi was increased in both NaPi-IIc$^{+/+}$ and NaPi-IIc$^{f/f}$ Doxy treated mice, whereas excretions of Na^+ and K^+ were reduced in all the groups of mice treated with Doxy compared to controls. These findings suggested that the treatment with 2

mg/ml Doxy produced some non-specific effects, either in the kidney or secondary to intestinal changes possibly due to effects on the gut flora.

Hence, in order to optimize the dosage of Doxy, NaPi-IIc$^{+/+}$ and NaPi-IIc$^{f/f}$ mice were treated with 1, 0.5 or 0.25 mg/ml Doxy for 10 days, followed by a recovery period of 15 days during which mice drank normal tap water. The excretion of Na^+ was still reduced in NaPi-IIc$^{+/+}$ mice that received 1 and 0.5 mg/ml Doxy, but not in mice subjected to 0.25 mg/ml. In NaPi-IIc$^{f/f}$ mice, the mRNA expression of NaPi-IIc was almost completely depleted upon 1 and 0.5 mg/ml Doxy induction, but 25% of mRNA still remained at the dosage of 0.25 mg/ml. Therefore, we setup a final Doxy treatment protocol consisting of 5 days administration of 0.5 mg/ml Doxy followed by 5 days with 0.25 mg/ml Doxy and a final recovery period of 15 days during which mice received normal drinking water. At the end of the protocol, we measured the concentration of Na^+ in urine as an indicator for non-specific effects. The excretion of Na^+ was comparable in all the groups of mice treated with either Doxy or sucrose, indicating that the final induction protocol did not produce non-specific effects. All subsequent experiments were performed with this optimized protocol.

The expression of NaPi-IIc mRNA and protein was comparable in NaPi-IIc$^{+/+}$ mice drinking Doxy or sucrose, whereas the Doxy treatment reduced by 50% and 90% the expression of the cotransporter mRNA and protein in NaPi-IIc$^{f/+}$ and NaPi-IIc$^{f/f}$ animals, respectively. The absence of NaPi-IIc in the kidneys of NaPi-IIc$^{f/f}$ mice did not affect the Na/Pi-cotransport activity in renal brush border membrane vesicles (BBMVs). Moreover, the expression of other renal Na/Pi-cotransporters, namely NaPi-IIa and Pit-2, remained unaffected. Similarly, the abundance of NaPi-IIb in intestinal BBM did not changed upon removal of NaPi-IIc. This suggests the absence of compensatory changes of other Na/Pi-cotransporters in NaPi-IIc depleted mice.

The urinary excretion of Pi and the concentration of Pi in plasma were normal upon depletion of NaPi-IIc in the kidney. Moreover, the circulating levels of the phosphaturic hormones PTH and FGF23 remained unchanged. The concentration of Ca^{2+} in plasma and urine as well as circulating levels of $1,25(OH)_2D_3$ also remained unchanged. Furthermore, the

mRNA expression of the 1α-hydroxylase and 24-hydroxylase were comparable in NaPi-IIc$^{+/+}$ and NaPi-IIc$^{f/f}$ mice.

The data that we obtained with the renal-specific and inducible NaPi-IIc deficient mice are only partially in agreement with observations reported in constitutive NaPi-IIc deficient mice. Thus, in constitutive NaPi-IIc depleted mice the urinary excretion and plasma Pi are normal, similar to our renal-specific model. However, the constitutive depletion of NaPi-IIc resulted in hypercalcemia and hypercalciuria as well as in increased 1,25$(OH)_2D_3$. Together these findings suggested that depletion of NaPi-IIc in some extra-renal tissues might explain the changes in Ca^{2+} homeostasis in the constitutive NaPi-IIc knockouts. Moreover, the absence of changes in Pi and Pi-related parameters in both the constitutive and renal-specific NaPi-IIc deficient models suggests that unlike in humans, NaPi-IIc has a minor role in the renal reabsorption of Pi in mice.

In conclusion, we have generated a renal-specific and inducible NaPi-IIc deficient mouse model. This study indicated that unlike in humans, the reabsorption of Pi by NaPi-IIc is minimal in mouse kidney. The inducible system (floxed NaPi-IIc: Cre recombinase) will allow us to further investigate the role of NaPi-IIc in different organs other than in the kidney.

3. Introduction

3.1 Phosphate (Pi) homeostasis and its importance

Phosphate (H_2PO4^-, $HPO4^{2-}$; abbreviated as Pi) is an inorganic anion present in all the body fluids and is present in organic and inorganic forms. Pi is essential for all living organisms and plays a pivotal role in most biological processes, including cellular energy metabolism, nucleic acid synthesis, cellular signaling, cell membrane integrity, enzymatic activities, mineralization of bone, and lipid metabolism. Therefore, it is important to maintain the extracellular concentration of Pi in balance within a narrow range. In humans, the plasma Pi concentration ranges between 0.8 to 1.5 mM and in rodents between 2 to 4 mM. In both species these values varies with age. At the physiological pH of 7.4, the monovalent (H_2PO4^-) and divalent ($HPO4^{2-}$) phosphate are present in a ratio of 1:4. Pi makes up approximately 1% of total bodyweight. The skeleton is the major storage organ of Pi in the body and contains approximately 10g of Pi per 100 g dry fat-free tissue, whereas muscle contains 0.2 g and the brain 0.33 g of Pi per 100 g dry fat free tissues, and approximately 1% is present in the extracellular fluid (Figure 1). In the skeleton Pi complexes with calcium in the form of hydroxyapatite crystals, which are the main inorganic constituent of the mineralized bone matrix. In mammals, Pi is obtained from dietary sources and is absorbed in the intestine in the form of $H_2PO_4^-$ or HPO_4^{2-} Pi ions.

The maintenance of the extracellular concentration of Pi depends on intestinal absorption, on the exchange between intracellular and extracellular pools from bone and skeletal muscles and on the reabsorption and excretion by the kidneys. Under normal physiological conditions, small intestinal absorption of Pi approximately equals the sum of fecal and renal excretion per day (Figure 1). Renal excretion does not always remain constant because of the daily changes of hormones and metabolic factors that regulate the Pi homeostasis.

Given the extensive distribution of Pi in the body, decreased levels of Pi in the serum may lead to clinical symptoms such as weakening of muscle, rhabdomyolysis, functional alterations of leukocytes and defects in bone mineralization leading to rickets or osteomalacia. On the other hand, elevated serum Pi levels as observed in patients with

chronic renal failure contribute to the pathogenesis of secondary hyperparathyroidism and may lead to vascular calcification [1].

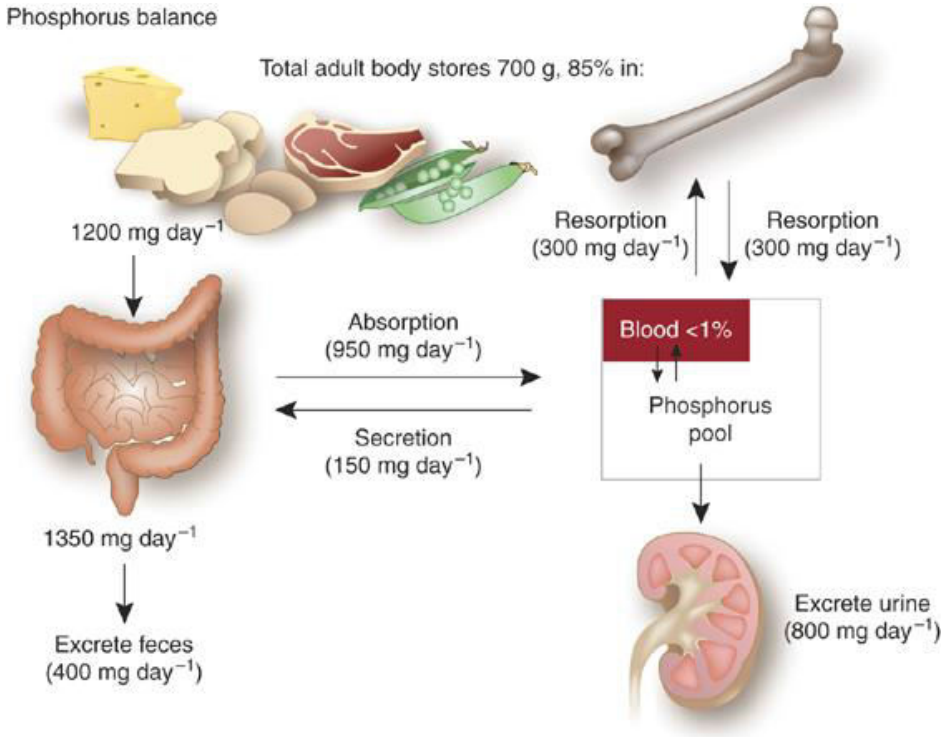

Figure 1 Phosphate homeostasis under normal physiological condition. The maintenance of constant serum phosphate levels by the intestinal absorption of phosphate from daily diet and renal excretion. The movement of phosphate into bone also helps to maintain serum phosphate levels [2]. (Image taken from: Keith A. Hruska et al., 2008, Kidney International).

3.2 Epithelial transport of phosphate

In the small intestine and in renal proximal tubules absorption or reabsorption of Pi represents a transepithelial transport process, which in principle, can occur transcellularly or paracellularly. Transcellular uptake of Pi is mediated by secondary active Na-dependent Pi-cotransporters which depend on the Na^+-gradient maintained by the Na^+/K^+ ATPase pump which is localized at the basolateral membrane [3]. In both intestine and kidney, transcellular transport of Pi is mediated by members of the SLC34 and SLC20 families of solute carriers. The SLC34 family includes NaPi-IIa (Slc34a1), NaPi-IIb (Slc34a2) and NaPi-IIc (Slc34a3) and the SLC20 family includes Pit-1 (Slc20a1) and Pit-2 (Slc20a2). All these Na/Pi-cotransporters are specifically localized at the apical (brush border) membrane (BBM) with an exception that NaPi-IIb expression was also observed in basolateral membrane of proximal tubules [4]. In intestinal epithelial cells, transport of Pi is mediated by NaPi-IIb, Pit-1 and Pit-2 whereas in the kidney, transport is mediated by NaPi-IIa, NaPi-IIc and Pit-2 (Figure

2A and 2B) [5-8]. However, in both epithelia the identity of the basolateral transporter that transfers Pi in-to the interstitium is not known yet.

In small intestine, the possibility of Pi absorption via a paracellular route has also been observed [9-11]. The paracellular barrier is formed by the interaction between complementary adhesive proteins of adjacent cells which form the tight junctions. These tight junction proteins include claudins and occludins which allow the permeation of selected ions across the epithelium. Until now, many claudins have been identified and were shown to determine the paracellular permeability of ions [12-16]. However, transport of Pi through the tight junction barrier has not been yet characterized. Sabbagh et al. has shown in NaPi-IIb deficient mice fed with low Pi diet followed by a phosphorus bolus that serum Pi levels increased less than in wild type [17]. This suggests that, transport of Pi absorption via the paracellular route might have a higher contribution.

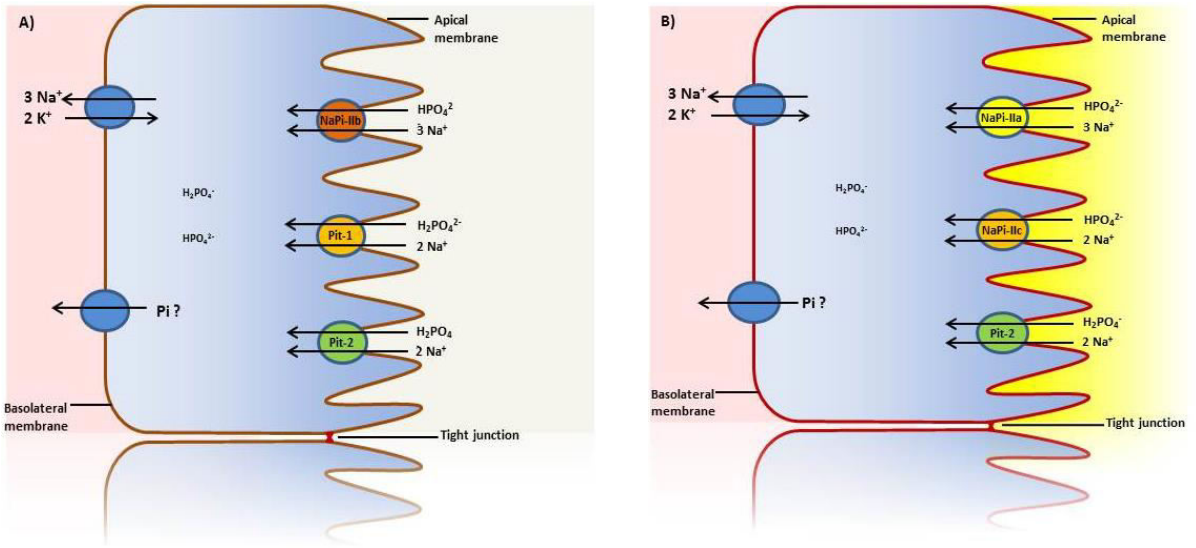

Figure 2 Transport of Pi across the epithelial cells of the intestine and kidney. A) In intestine, transport of Pi is mediated by the Na/Pi- cotransporters NaPi-IIb, Pit-1 and Pit-2. B) In renal proximal tubules, transport of Pi is mediated by NaPi-IIa, NaPi-IIc and Pit-2. All the Na/Pi- cotransporters are expressed at the apical (brush border) membrane of the epithelial cells. The identity of the protein responsible for the transport of Pi through the basolateral membrane is still unknown.

3.3 SLC34 Na/Pi-cotransporters

The SLC34 solute carrier family consists of three isoforms: NaPi-IIa (SLC34A1), NaPi-IIb (SLC34A2) and NaPi-IIc (SLC34A3) [18]. These three isoforms represent the main secondary active transport proteins for Pi (re)absorption in mammalian intestine and kidney. Although

predominantly expressed in epithelial cells of small intestine and proximal tubules these Na/Pi-cotransporters are also expressed in different organs such as the lung, liver, bone, salivary and mammary glands and testis.

SLC34 isoforms are an unique class of membrane proteins that do not share any structural homology with other transporter proteins. Based on the biochemical approach of cysteine scanning mutagenesis and electrophysiological methods, SLC34 proteins have been proposed to be functional monomers [19]. Later, using a modified split-ubiquitin membrane yeast two-hybrid system (MYTH), it was also observed that SLC34 proteins may dimerize via protein-protein interactions with the help of PDZ-binding motifs [20]. Recently Fenollar Ferrer et al. [21] suggested based on homology modelling that the SLC34 isoform NaPi-IIa structure may consist of two inverted repeat units (RU1, RU2) plus a C-terminal region with the extension of two transmembrane helices (Figure 3). These two units containing conserved inverted repeat motifs separated by a large extracellular loop consist of two N-linked glycosylation sites and a disulfide bond. RU1 and RU2 are composed of residues 86-256 and 335-489. Both C-terminal and N-terminal regions are also important components of the protein and are localized in the cytoplasm. There are several residues predicted as coordination sites for Na+ and Pi interaction for each transport cycle. These residues when mutated (S164, T195, S196 in RU1 and Q417, S418, S419 in RUC2), alter phosphate transport characteristics [18, 21].

Based on the information obtained with the SLC34A1 and SLC34A3 proteins, the C-terminal end is involved in protein-protein interactions that take part in the translocation, trafficking and regulation of the transporters by different physiological factors.

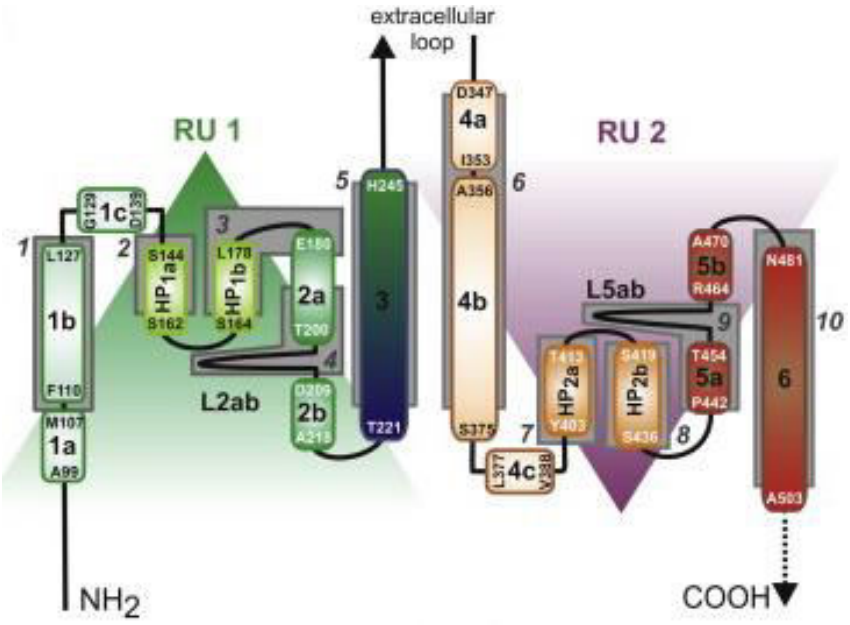

Figure 3 Topology model of SLC34 isoform NaPi-IIa. The model consists of two structural repeat units (RU1 and RU2) are indicated green and red containing transmembrane helices (*numbered*). The conserved repeat motifs separated by large extracellular loop. (Image taken from: Fenollar-Ferrer et al, 2014)

The kinetic properties of all three isoforms have been studied after expression in oocytes of *Xenopus. laevis* by electrophysiology and tracer flux studies using radioactive Pi (summarized in Table 1). All SLC34 family members preferentially transport divalent Pi ($HPO4^{2-}$) and require Na^+ ions as driving cosubstrate to import Pi into cells [22]. Recently it was shown that Li^+ -ions are partially able to substitute for at least one of the Na^+ -ion during the transport cycle (Table 1)[23]. The transport capacity of SLC34 transporters depends on the extracellular pH, which determines the distribution of extracellular monovalent/divalent Pi. Moreover, the kinetic properties of these transporters are influenced by protons due to competition with Na^+ binding [24]. The rate of Pi influx is higher at pH 7.4 for all three isoforms, and all isoform that have similar Km- values for Pi (0.1 mM) and for Na^+ (approximately 40 mM) [25] with the exception of mammalian NaPi-IIb has different apparent Pi affinity (10 µM) [26, 27].

SLC34 isoforms can be distinguished based on their functional properties. NaPi-IIa and NaPi-IIb transport one net-positive charge into the cell per transport cycle, therefore these two proteins are electrogenic whereas no net-charge is transported by NaPi-IIc, an electroneutral transporter (Table 1). The electrogenic isoforms are sensitive to the membrane potential and transport rate is a function of membrane potential. In contrast, electroneutal NaPi-IIc is

insensitive to the membrane potential. The transport capacity of electrogenic isoforms for Pi is approximately 100- folds higher compared to NaPi-IIc [22, 28, 29]. Voltage clamp flurometric studies on NaPi-IIa and NaPi-IIb indicated that 2 Na^+ ions bind sequentially followed by binding of Pi and the third Na^+ before the rate-limiting reorientation of the fully loaded carrier occurs [30]. For NaPi-IIc, to complete transport cycle 3 Na^+ bind but only 2 Na^+ are translocated into the cytosol [31]. The order of substrate release to the cytosol has not been demonstrated yet.

There are several reports indicating that SLC34 Na/Pi-cotransporters can be inhibited by specific inhibitors which are able to block the transport process. Arsenate is a structural analogue to Pi and competitively inhibits the NaPi-IIb mediated transport in the small intestine whereas it shows low affinity towards NaPi-IIa and NaPi-IIc in the kidney [27]. Phosphonoformic acid (PFA) is another competitive inhibitor of all SLC34 isoforms and blocks the Na/Pi-cotransport in the small intestine and kidney [25, 32]. In contrast, PFA has very low affinity for the SLC20 transporters [33, 34].

Family	**SLC34**			**SLC20**
Isoform	NaPi-IIa (Slc34a1)	NaPi-IIb (Slc34a2)	NaPi-IIc (Slc34a3)	Pit-1/Pit-2 (Slc20a1/2)
Pi species preference	$HPO4^{2-}$	$HPO4^{2-}$	$HPO4^{2-}$	H_2PO4^-
Driving substrate	Na^+ (Li^+)	Na^+ (Li^+)	Na^+	Na^+, Li^+
Electrogenicity (charge/cycle)	1	1	0	1
Stoichiometry (Na:Pi)	3:1	3:1	2:1	2:1
Presteady-state currents	Yes	Yes	No	n.d
$K_{0.5}^{Pi}$ (µM)	50, 54	250, 7, 29, 31	70, 80	120, 24, 25
$K_{0.5}^{Na}$ (mM)	40, 50	25, 42, 46, 67	48, 43	50
pH dependence (pH↓)	Strong	Strong, weak	Strong	Weak
Arsenate (K_i^{As}) (mM)	1.08	0.05	1.01	3.61 (3.95)
PFA (K_i^{PFA}) (mM)	1.05	0.16	0.9	2.71 (4.63)

Table 1 Kinetic properties of SLC34 and SLC20 proteins expressed in *Xenopus laevis* oocytes [18] (Adapted from: Forster IC et al, 2012)

3.3.1 Sodium dependent phosphate cotransporter-IIa (NaPi-IIa)

NaPi-IIa is encoded by the gene SLC34A1 and it was the first SLC34 Na/Pi cotransporter identified in mammalian kidney [5]. NaPi-IIa translocate one net positive charge into the cell per cotransport cycle. NaPi-IIa preferentially transports HPO_4^{2-} and mediates transport with a stoichiometry of 3 Na^+ -ions to 1 HPO_4^{2-} (Table 1).Therefore, NaPi-IIa is electrogenic (Table 1). The apparent substrate affinity (Km) of human and rat NaPi-IIa are approximately 100 µM and 40 mM for divalent Pi and Na^+ ions, respectively [35, 36].

Many studies have been performed to unravel a structural model of mammalian NaPi-IIa Na/Pi-cotransporter. NaPi-IIa protein consists of 640 amino acids [37-41]. The disulfide bond between extracellular glycosylation sites is not required for NaPi-IIa transport function [37, 38]. The C-terminal tail contains a conserved PDZ (post-synaptic density protein PSD95, Drosophila disc large tumor suppressor DIgA, and zonula occludens-1 protein ZO-1) binding motif represented by the last three residues (TRL) (Figure 3). The TRL motif acts as PDZ binding motif and is important for protein-protein interactions, that have been suggested to play a role in the apical sorting and/or regulation [42]. Gisler et al. [43] screened cDNA libraries from adult mouse kidney using the Yeast two-hybrid (Y2H) method and identified several proteins that interact with the PDZ binding motif (TRL) of the cotransporter. These interacting proteins include the Na^+/H^+ exchanger regulatory factors 1, 2 (NHERF1 and NHERF2), PDZK1/NaPi-Cap1 (NHERF3) and PDZK2/NaPi-Cap2 (NHERF4) as well as Shank2E [43, 44]. All these proteins colocalize with NaPi-IIa in the BBM of proximal tubular cells [43].

NHERF-1/2 consist of two PDZ domains [44] and their carboxyl regions contain a Moesin-Ezrin-Radixin-Merlin (MERM) binding domain, which connects them to cytoskeleton proteins [45]. NHERF-3/4 consist of four PDZ domains and interact with cytoskeleton proteins via association with NHERF-1. The first PDZ domain of NHERF-1/2 is involved in interaction with NaPi-IIa whereas interaction of NHERF-3/4 with NaPi-lla depends on the third PDZ domain [46].

The interaction of all these proteins with NaPi-IIa depends on the presence of the TRL motif. After transfection of a TRL-truncated NaPi-IIa in OK cells, expression of NaPi-IIa was partly blunted and accumulation of the protein in the cytoplasm was observed [47, 48]. In mice,

depletion of NHERF-1 results in a reduced abundance of NaPi-IIa at the BBM which is associated with hypophosphatemia and hyperphosphaturia [49]. Together, these studies suggest that the interaction of NHERF-1 with the C-terminal region of NaPi-IIa might be critical for NaPi-IIa targeting to the membrane. Interestingly, BBM expression of NaPi-IIa and urinary excretion of Pi was not altered in PDZK-1 deficient mice [50].

Shank2E also belongs to the PDZ protein family and has been shown to interact with NaPi-IIa via its single PDZ domain [51]. In rats, expression of Shank2E was detected in proximal tubular BBM and in isolated membrane fractions. In addition, Shank2E colocalized with GFP-tagged NaPi-IIa in OK cells and specifically binds to the TRL region of NaPi-IIa[51].

In addition to these PDZ-proteins, Reining et al. [52] demonstrated a role of the GABA(A) receptor-associated protein (GABARAP) in determining the apical abundance of NaPi-IIa. In a GABARAP deficient mouse model, the BBM expression of NaPi-IIa is increased, which leads to increased renal Pi uptake and reduced Pi excretion. In addition, expression of NHERF-1 was also upregulated in these mice. However, the molecular mechanism of how GABARAP affects NaPi-IIa expression is unknown.

3.3.1.1 Expression of NaPi-IIa and its contribution to renal Pi handling

Based on early micro-puncture studies in rats, it was proposed that the reabsorption of Pi takes place in superficial and juxtamedullary nephrons [53, 54]. Later on, the expression of NaPi-IIa mRNA was detected in isolated proximal tubules and the protein was observed in proximal tubular BBM by immunofluorescence [55]. The highest mRNA expression was found in proximal convoluted tubular segments, less in the straight proximal tubules [55]. Abundant NaPi-IIa mRNA and protein expression has been detected mostly in juxtamedullary nephrons [55, 56]. This suggested an important role of NaPi-IIa in the reabsorption of Pi in the proximal tubule. To study the ontogeny of NaPi-IIa expression, Taufiq et al. [57] investigated the expression of the cotransporter in rats of various ages. Interestingly, they observed highest protein expression in weaning rats as compared with adult rats without changes in mRNA levels. The uptake of Pi was also observed in BBM which was parallel to the expression of NaPi-IIa in these animals [57]. In contrast, the abundance of NaPi-IIa was decreased in BBM of weaned rats [58]. In addition, the expression of NaPi-IIa was lower in

the BBM of superficial nephrons whereas expression was higher in the juxtamedullary nephrons [58]. This internephron (superficial and juxtamedullary nephrons) heterogenic expression of NaPi-IIa after weaning might be related to the requirement for dietary Pi in an age dependent manner [58].

Most notably, the homozygous gene deletion of Slc34a1 in mice (NaPi-IIa$^{-/-}$) leads to severe phenotypic changes such as phosphaturia with hypophosphatemia [59]. In addition, NaPi-IIa$^{-/-}$ mice exhibited hypercalcemia, hypercalciuria and reduced serum FGF23 and PTH with elevated active 1,25 dihydorxy vitamin D (1,25$(OH)_2D_3$). The impaired Ca^{2+} metabolism might be an effect of increased serum 1,25$(OH)_2D_3$ which is known to increase the abundance of TRPV6 a channel involved in the absorption of Ca^{2+} in the small intestine [60]. Transport studies in NaPi-IIa$^{-/-}$ mice indicated that the Pi uptake was reduced by 70% in isolated renal BBMVs compared to BBMVs isolated from wild type mice [59]. This data suggested that NaPi-IIa critically contributes to the reabsorption of Pi in mouse kidney. Hypercalciuria is one of the known risk factors for inducing nephrocalcinosis. Therefore, kidneys of adult NaPi-IIa$^{-/-}$ mice were examined for calcification, von Kossa staining indicated mineral (Ca^{2+} and Pi) deposits in kidney sections from NaPi-IIa$^{-/-}$ and calcification was further detected by microcomputed tomography of intact kidneys [61].

Heterozygous mutations in the SLC34A1 gene were reported in three patients with hypercalciuria, hypophosphatemia and nephrolithiasis [62]. In one patient, the mutation results in a residue substitutions at position 48 (A48F) and in the two other patients, substitution at position 147 (V147M) is evident. These mutations are located in the N-terminal tail and second TMD of NaPi-IIa, respectively. As all three patients were heterozygous the authors proposed that mutations might have dominant negative effects that lead to reduced transport activity of NaPi-IIa. However, these findings could not be reproduced independently using the X. laevis oocyte expression system [63]. Recently, a homozygous in-frame duplication of 21 bp in NaPi-IIa from two related patients was identified and this mutation leads to severe Pi wasting with rickets and renal Fanconi`s syndrome [64]. Together, these data indicate that NaPi-IIa might have a dominant role in renal Pi handling in both humans and rodents.

3.3.2 Sodium dependent phosphate cotransporter-IIc (NaPi-IIc)

NaPi-IIc is encoded by the SLC34A3 gene and has been identified as a growth related protein that consists of 599 amino acids. NaPi-IIc was cloned from human and rat cDNA using expressed sequence tags (EST) [7]. To analyze the transport properties of NaPi-IIc, Segawa et al [7] expressed NaPi-IIc in *Xenopus laevis* oocytes and proposed that NaPi-IIc transports two Na^+ ions along with one HPO_4^{2-} ion (2:1). Therefore, transport mediated by NaPi-IIc is electroneutral [7, 22]. The sequence of substrate binding and translocation into the cell for NaPi-IIc is different from other two SLC34 proteins. Kinetic studies of NaPi-IIc using the oocyte expression system suggested that 3 Na^+ ions bind to the carrier protein but only 2 Na^+ ions are released inside the cytoplasmic space [31].

Sequence comparison indicated that there is a high degree of sequence identity, especially high in the TMDs, between NaPi-IIa and NaPi-IIc [7]. This suggests that there may be minor differences in the amino acid sequence which profoundly affect the electrophysiological properties of NaPi-IIa and NaPi-IIc. To identify which residues are responsible for the electroneutrality NaPi-IIa/NaPi-IIc chimeras were constructed, followed by single and triple mutants and their transport features were analyzed in oocytes. These studies allowed the identification of 3 residues within the third TMD that are critical for electrogenicity: Gly195, A 218 and A 224 of NaPi-IIc are replaced by Asp 224, Ala 218 and Ala 224 in the equivalent position of NaPi-IIa [22].

In contrast to NaPi-IIa, TRL motifs are absent in C-terminal region of NaPi-IIc. Recently Ito et al. [65] identified an internal WLHSL motif within the C-terminal tail of mouse NaPi-IIc. The deletion of this WLHSL motif leads to failure of apical sorting when constructed chimeras were expressed in OK and MDCK cells [65]. Several proteins interact with NaPi-IIc and are involved in stabilization and cargo sorting to the plasma membrane. Based on the two-hybrid system, NHERF-1 and 3 were found to interact with NaPi-IIc. Interaction with NHERF-1 depends on an internal PDZ binding motif and the first PDZ domain of NHERF-1. The association with NHERF-3 requires the last 3 residues of NaPi-IIc (QQL) and the second PDZ domain of NHERF-3. The interactions with these two proteins were confirmed in OK cells and rat kidney cortex by coimmunoprecipitation [66]. In renal BBMVs of rats fed with low Pi diet, the yield of coprecipitation of NaPi-IIc-NHERF3 complexes was increased whereas the

amount of NaPi-IIc-NHERF1 complexes was unchanged [66]. This different pattern of coprecipitation indicates that the interactions of NaPi-IIc with these two partners may be different. Thus, NHERF1 interaction may be required for basal level of NaPi-IIc expression at the apical membrane whereas NHERF3 may be required for the response to low Pi diet [66]. In addition, the cellular localization and transport activity of truncated NaPi-IIc lacking the last three amino acids (QQL) at the C-terminal tail are similar to the full length protein [66]. This suggests that these three amino acids may not be required for membrane expression in contrast to NaPi-IIa.

3.3.2.1 Expression of NaPi-IIc and its contribution to renal Pi handling

The abundance of NaPi-IIc in proximal tubules is predominant in weaning rodents and diminishes with age [7]. It was also found that age regulates the expression of NaPi-IIc mRNA and that Pi uptake was higher in oocytes injected with mRNA isolated from kidneys of young rats compared to adult animals [7]. In addition, Na/Pi-cotransport induced in oocytes expressing mRNA from young rats is still observed even after depletion of NaPi-IIa transcript. In oocytes expressing mRNA from adult animals, depletion of NaPi-IIa mRNA fully abolished the Pi uptake whereas depletion of NaPi-IIc had no effect [67]. These results demonstrate the importance of NaPi-IIc in young animals. In terms of protein levels, abundant expression of NaPi-IIc was found in renal BBM of the S1 segment of proximal convoluted tubules (PCT) of weaning rats. In contrast, the abundance was massively reduced in adult rats [7]. Recently it has also been shown that NaPi-IIc is expressed exclusively in the S1/S2 segments of the proximal convoluted tubule (PCT) in mouse kidney [68].

Unlike NaPi-IIa, the constitutive depletion of NaPi-IIc in mice does not affect the circulating levels and renal excretion of Pi. The uptake of Pi into renal BBMVs of NaPi-IIc$^{-/-}$ mice is similar to renal BBMVs isolated from wild type mice even though the expression of NaPi-IIa remains unchanged [69]. This data demonstrated that, in mice, NaPi-IIc plays a minor role in Pi reabsorption in the kidney after weaning. As in NaPi-IIa$^{-/-}$ mice, 1,25$(OH)_2D_3$ is higher in serum of constitutive NaPi-IIc$^{-/-}$ mice, which leads to increased serum and urinary excretion of Ca^{2+}. In addition, serum FGF23 levels were significantly lower in NaPi-IIc$^{-/-}$ mice. Based on these data it has been suggested that NaPi-IIc may be involved in Ca^{2+} metabolism and regulation of the 1,25$(OH)_2D_3$ - FGF23 axis [69]. However, the mechanisms that lead to these

changes are unknown. Recently, it has been shown that NaPi-IIc mRNA is expressed in several tissues other than kidney. Although the highest expression was found in the kidney, lower levels were also found in ovary, testis and spinal cord [70]. However, the expression of NaPi-IIc at the protein level in extra renal tissues has not been analyzed.

Recently a NaPi-IIa/NaPi-IIc double knockout (DKO) mouse model has been characterized and showed greater changes in the phenotype than the single deficient mice [71]. The excretion of Pi is increased in DKO mice compared to NaPi-IIa deficient mice and DKO mice suffered from severe hypercalcemia and hypercalciuria, at levels higher than those of single deficient mice [71]. The changes in Pi and Ca^{2+} balance associated with rickets in DKO mice. These severe biochemical changes in DKO mice are similar to the phenotype observed in patients with HHRH. Considering these data, it cannot be ruled out that NaPi-IIc plays a minor contribution to renal reabsorption of Pi in mice.

Several studies have revealed that diverse mutations in the human NaPi-IIc gene (SLC34A3) (Figure 4) lead to hereditary hypophosphatemic rickets with hypercalciuria (HHRH). Patients with HHRH have higher renal Pi excretion, hypercalciuria and increased plasma $1,25(OH)_2D_3$, which leads to defects in bone mineralization [72]. Expression of mutated human NaPi-IIc in *X. laevis* oocytes results in reduced Na/Pi-cotransport activity. These data indicated that, unlike in rodents, NaPi-IIc plays a very important role in renal Pi reabsorption in humans.

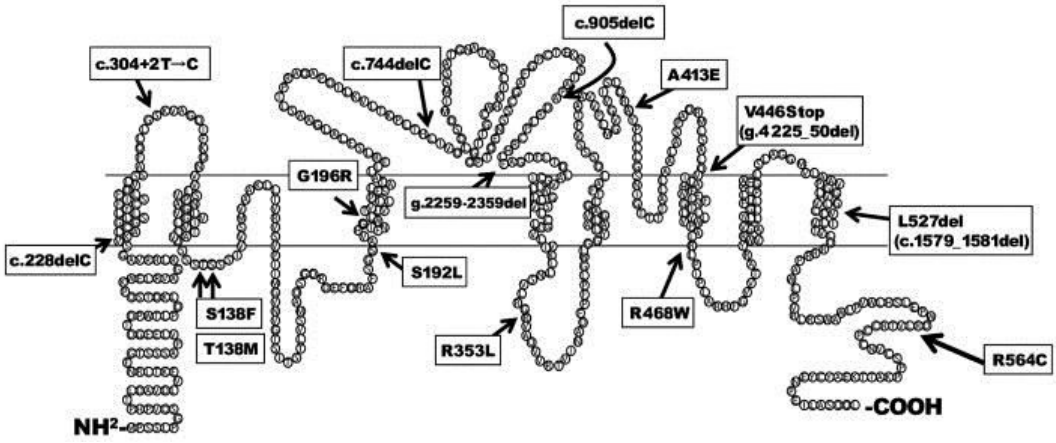

Figure 4 The predicted structural model of human NaPi-IIc showing different mutations identified in patients with hereditary hypophosphatemic rickets with hypercalciuria (HHRH) [73]. Image taken from: Segawa H et al., 2009.

3.3.3 Sodium dependent phosphate cotransporter-IIb (NaPi-IIb)

NaPi-IIb is encoded by SLC34A2 and was cloned in 1998 on the basis of a homologous sequence of EST clones isolated from a mouse embryo [6]. The transport characteristics of NaPi-IIb have been analyzed in voltage clamp studies after expression of NaPi-IIb cRNA in*Xenopus laevis* oocytes. The mouse and rat NaPi-IIb exhibits substrate affinities of approximately 10 µM and 40 mM for divalent Pi and Na^+ at pH 7.4. Changes in pH do not alter the Na/Pi-cotransporter activity. NaPi-IIb is an electrogenic transporter and mediates the transport of 3 Na^+ together with 1 $HPO4^{2-}$ [6].

3.3.3.1 Expression of NaPi-IIb in different tissues and its importance in Pi handling

The expression of NaPi-IIb at the protein level was first found in the apical BBM of the small intestine [6]. However, NaPi-IIb shows a wider range of tissue distribution and immunohistological studies have shown its expression in lungs, hepatocytes, salivary glands, epididymis, mammary glands, testis and recently also in kidney [74-76]. In lungs, NaPi-IIb is expressed in the apical membrane of type-II alveolar cells and may be involved in the synthesis of surfactants. In the liver, it has been proposed that NaPi-IIb mediates the uptake of Pi from the primary bile. In salivary glands, the expression of NaPi-IIb was found in the apical side of the duct cells whereas expression was observed predominantly at the basolateral membrane of acinar cells [75]. In c-ros KO mice, expression of NaPi-IIb in the epididymis is required for sperm production and involved in male fertility [76]. Recently, NaPi-IIb was localized in the basolateral side of renal proximal tubules in rats fed with high Pi diet [4]. In addition, NaPi-IIb mRNA has also been identified in lymphoid tissue, placenta, uterus, prostate, pancreas, thyroid and colon [6, 74, 75].

The expression of NaPi-IIb is essential during embryonic development. In mice, constitutive depletion of NaPi-IIb results in embryonic lethality likely due to a defect of the transport of Pi from the maternal circulation to the fetus [77]. Sabbagh et al. [17] generated a conditional NaPi-IIb deficient mice. The depletion of NaPi-IIb (NaPi-$IIb^{-/-}$) in adult mice leads to increased fecal excretion of Pi with hypophosphaturia, but serum Pi levels remain unchanged. The hypophosphaturia was explained by an increased expression of NaPi-IIa associated with decreased FGF23 in NaPi-$IIb^{-/-}$ mice [17]. In addition, the uptake of Pi was reduced by 90% in

BBMVs isolated from the ileum of NaPi-IIb$^{-/-}$ mice. Furthermore, low Pi diet followed by Pi bolus results in approximately 50% reduced overall Pi absorption in NaPi-IIb$^{-/-}$ mice compared to wild type mice [17]. These findings suggest that NaPi-IIb plays a major role in the absorption of Pi in the small intestine. However, the relative contribution of transcellular versus paracellular mechanisms for overall intestinal Pi absorption remains unknown.

As mentioned above, NaPi-llb is also present in alveolar type ll cells and testis and mutations in NaPi-IIb lead to pulmonary alveolar and testicular microlithiasis in humans [78]. This suggests an important role of NaPi-IIb in the regulation of Pi balance in lungs and testis. However the role of NaPi-llb in these two organs remains to be clarified.

3.4 SLC20 Na^+ coupled phosphate cotransporters

The solute carrier family SLC20 consists of two members Pit-1 (SLC20A1) and Pit-2 (SLC20A2). Originally, both Pit-1 and Pit-2 were identified as retroviral receptors for Gibbon ape leukemia virus (Glvr-1; Pit-1) and for rat amphotropic virus (Ram-1; Pit-1) [79, 80] but later on Na-dependent Pi transport of these proteins was demonstrated.

The transport kinetics suggest that SLC20 proteins preferentially transport monovalent Pi ($H_2PO_4^-$) together with two Na^+ with a Na^+:Pi stoichiometry of 2:1 (Table 1) [34]. This transport kinetics is the most important feature which distinguishes the SCL20 transporters from the SLC34 members. The typical substrate binding affinity of SLC20 proteins for Pi is ≥100 µM and for Na^+ approximately 50 mM. It was shown for Pit-1 that, lithium (Li^+) ions can replace Na^+ ions as a driving substrate although the transport rate was reduced (Table 1) [34]. Unlike SLC34 proteins that are pH sensitive, the rate of maximum transport for Pit-1 remains constant over changes of 3 pH units between 5 to 7.4. In addition, studies on Pit-2 expressed in *X. laevis* oocytes demonstrated that decreasing the pH from 7.5 to 6 leads to an increase in the Pi transport influx suggesting that protons might be replacing Na^+ ions or that the availability of monovalent Pi increases [33, 81].

The current structural topology of SLC20 proteins is based on bioinformatic tools and biochemical (epitope tagging, cysteine scanning) and in vitro glycosylation methods. The predicted topology suggests that SLC20 isoforms consist of 12 transmembrane helices with

extracellular amino (-NH_2) and carboxy (-COOH) termini (Figure 5). Structural topology shows one extracellular glycosylated loop and a large intracellular linker region present between transmembrane segments 7 and 8 (Figure 5).

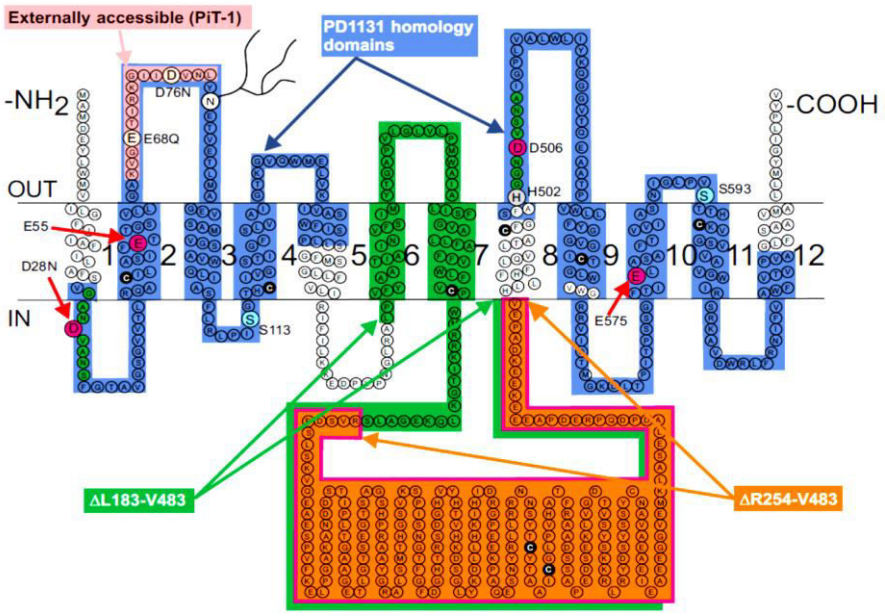

Figure 5 Topology and structure-function features of SLC20 proteins. This topology model for mammalian SLC20 proteins is based on the human PiT-2 sequence. The 12 predicted TMDs were assigned according to Salaun et al., 2001. The model was drawn using TOPO2 software. Residues important for SLC20 function that have been identified by mutagenesis (Bottger & Pedersen, 2004; Salaun, et al., 2004; Bottger & Pedersen, 2005) are shown enlarged. *Blue*: PD1131 homology domains (amino acid blocks that are conserved among all the family members has been identifies) (Salaun et al., 2001). Two regions involving the large intracellular loop have been deleted: the ΔL183-V483 deletion causes loss of transport function with partially compromised viral receptor function (*green*) and the ΔR254-V483 leaves transport function intact but compromises viral receptor function 46 (*orange*) (Bottger & Pedersen 2011). Acidic residues important for transport function (D28, E55, D506, E575) (*red*) and those not critical for transport function (E68, D78, E91) (*pink*) are indicated. The protein is N-glycosylated at Asp-81. A region in the 1st extracellular loop of PiT-1, also conserved in PiT-2 was subjected to SCAM, and sites accessible from the external medium have been identified [18]. (Image taken from: Forster IC et al., 2012).

3.4.1 Expression and role of Pit-1 and Pit-2 in Pi handling

Expression of SLC20 Na/Pi-cotransporters has been found ubiquitously in all tested mammalian tissues including intestine, kidney, liver, brain, heart, thymus, parathyroid gland, bone and vascular smooth muscles [8, 82-85]. Similar to SLC34 proteins, the distribution of SLC20 transporters within same tissues varies in different species. For example, in mice, abundant expression of Pit-2 was observed in the jejunum [82] whereas its expression was lower in rat small intestine [86]. In mouse and rat kidneys, expressions of both Pit-1/2 were detected at the level of mRNA [87, 88].

Under normal dietary conditions, Pit-1 protein is localized along the apical BBM of rat intestine. The highest expression of Pit-1 protein was found in the duodenum and jejunum, whereas lower levels of Pit-2 were found across all segments of the small intestine [83]. In mice, the precise intestinal expression of Pit-1 remains unknown, whereas Pit-2 expression was found at the level of mRNA and protein in the ileum, where the transporter is located at the apical BBM [89]. This suggests that the differential distribution of Pit-1/2 across the small intestine might be species specific.

In mouse and rat kidneys, expressions of both Pit-1/2 were detected at the level of mRNA [87, 88] . While SLS20 transporters have been shown to be expressed in several organs, their physiological relevance in each organ is not known. Recently Beck et al. [90] generated a mouse model deficient for Pit-1, which resulted in embryonic lethality due to impaired liver development, bone marrow function and growth retardation [90]. This suggests that Pit-1 may have an impact on early stages of fetal development. Pit-2 has not yet been characterized by using gene deficient animal models. As mentioned above, Miyamoto and his colleagues [73] characterized a mouse model deficient in both Slc34a1 and Slc34a3. They observed hypophosphatemia with hyperphosphaturia, but a residual amount of Pi is still reabsorbed in the kidney, which may be mediated by Pit-1 and Pit-2 [71]. Apparently, the relative abundance of SLC20 transporters mRNA in the kidney is very low and, in terms of preserving Pi balance, SLC20 Na/Pi-cotransporters might be responsible only for 5% Pi (re)absorption in kidney and intestine [91]. In humans, familial idiopathic basal ganglia calcification is probably caused by the loss of Pit-2 function. In these patients several mutations have been identified in Pit-2 that leads to loss of functional protein. Thus, Pit-2 absence might results in deposition of Pi in the basal ganglia, a brain region that express higher levels of Pit-2 [92].

Increased expression of Pit-1 mRNA was observed in parathyroid gland of $1,25(OH)_2D_3$ deficient rats and also in animals fed with low Pi diet [84]. Furthermore, Pit-1 expression was also found in bone derived osteoclasts and osteoblasts and may have a role in bone remodeling [93]. Moreover, calcification in vasculature was observed along with increased Pit-1 mRNA levels upon treatment with high Ca^{2+} and PDGF [94] [95]. In contrast, a reduced

effect on calcification in smooth muscle cells was observed in response to stimuli after inhibition of Pit-1 expression [96]. In patients with Werner syndrome (WS), soft tissue calcification is one of the important clinical symptoms. The overexpression of Pit-1 that was observed in fibroblasts and skin may be associated with tissue calcification in WS patients [97]. Another pivotal role of Pit-1 is that it may participate in cell proliferation and the control of cell death (apoptosis) as shown in human leukemic cells (U937) and HeLa cells, an effect that seems to be dependent of its Pi transport activity [98]. The depletion of Pit-1 mRNA by small hairpin RNA (Sh-RNA) in HeLa and HepG2 cell lines results in diminished cell proliferation and blunted mitosis which lead to the postponing of the cell cycle [86].

Pit-1 is regulated in response to different stimuli. In vitro studies indicated that the calcification of human vascular smooth muscle cells (VSMC) by high Pi influx leads to phenotypic changes of VSMC to osteoblast-like cells. Li and colleagues [99] observed that the increased Pit-1 expression in response to bone morphogenic protein 2 (BMP-2) leads to enhanced Pi uptake in human VSMC [99]. BMP-2 is a cytokine known to be involved in bone mineralization by inducing osteoblastic cell differentiation. Moreover, Pit-1 is also regulated by insulin-like growth factor-1 (IGF-1) in rat osteoblasts, human osteogenic cells and VSMC without changes on Pit-2 expression [100, 101]. Together these data demonstrate the clinical importance of Pit-1.

3.5 Phosphate handling by the kidney

In mammals, control of extracellular Pi largely depends on active reabsorption of Pi from the primary urine that is produced by filtration of the blood in the glomeruli. Active reabsorption occurs through a transcellular process located in the proximal tubules along which approximately 80% of filtered Pi is reabsorbed. There is no clear evidence for Pi reabsorption in the loop of Henle but a small amount of Pi may be reabsorbed in the distal tubules [102]. However, this mechanism has not been characterized yet.

Renal proximal tubular epithelial cells are characterized by numerous microvilli which increase the luminal surface and are the site of active reabsorption of filtered components. The transport of Pi into proximal tubular cells depends on the presence of Na^+ ions [103]. The reabsorption of Pi is mediated by members of the SLC34 (NaPi-IIa; NaPi-IIc) and SLC20

(Pit-2) families of solute carriers [104] which are localized at the brush border membrane (BBM) of proximal tubular epithelial cells (Figure 6).

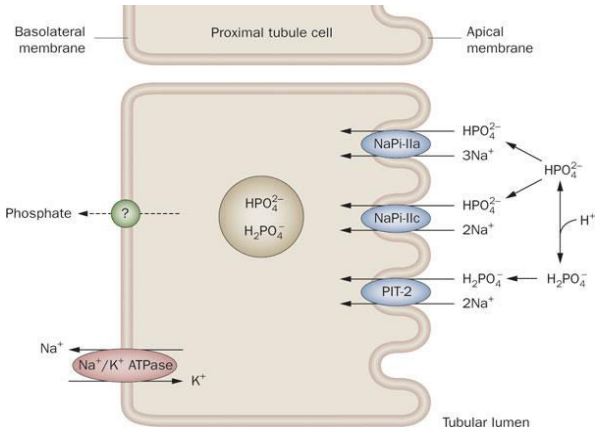

Figure 6 Na^+ dependent Phosphate (Pi) cotransporters in the BBM of proximal tubular epithelial cell. The transport of Pi is mediated by SLC34 (NaPi-IIa, NaPI-IIc) and SLC20 (Pit-2) cotransporters. These cotransporters mediate a secondary active transport of Pi using the electrochemical gradient of Na^+ as driving force [105]. Image taken from: Alizadeh Naderi, A. S. & Reilly, R. F. 2010, *Nature Reviews.*

Under normal dietary conditions NaPi-IIa is predominantly expressed in the S1 segment of juxtamedullary nephrons and its expression decreases in S2/S3 segments [55]. NaPi-IIc is expressed in S1 segments of superficial and juxtamedullary nephrons, but has not been detected in S2/S3 segments [106]. In addition, Pit-2 has also been identified in S1 segment and weakly in S2 segment of both superficial and juxtamedullary nephrons.

3.6 Physiological regulation of Na/Pi-cotransport in the kidney

The extent of reabsorption of Pi by the proximal tubular cells depends on the abundance of Na/Pi-cotransporters which are localized at the BBM. Numerous studies have described the control of Pi reabsorption in the proximal tubule under different physiological conditions. Thus far, all studies indicated that proximal tubular reabsorption of Pi is regulated by an alteration of the abundances of Na/Pi-co transporters in the microvilli that depends on the rate of protein synthesis, trafficking into the apical membrane and rate of endocytosis. These processes are controlled by many hormonal and metabolic factors (listed in Table 2) by mechanisms that are only partially understood. In the following sections, the impact on renal handling of Pi of some of these factors is discussed in more detail.

Decreased reabsorption ⬇	Increased reabsorption ⬆
High phosphate diet	Low phosphate diet
Hypokalemia	High potassium diet
Parathyroid hormone	1, 25dihydroxy vitamin D
Fibroblast growth factor – 23	Parathyroidectomy
Dopamine	Growth hormone
Glucocorcoids	Insuline
Estrogen	Thyorid hormone
Metabolic acidosis	Metabolic alkalosis
Calcitonin	
Epidermal growth factor	
Hypercalcemia	Hypocalcemia

Table 2 Regulation of Pi reabsorption in proximal tubule in response to hormonal and non-hormonal factors

3.6.1 Dietary phosphate

Dietary intake of Pi is a major regulator of renal Pi reabsorption. Renal reabsorption of Pi is increased in low dietary Pi condition whereas it is reduced in response to high Pi diet. Adaptive changes to the content of Pi in the diet are observed after few hours (acute adaptation) as well as several days (chronic adaptation) after dietary restrictions [7, 8, 107]. In renal BBM vesicles isolated from animals fed with low Pi the rate of Na/Pi-cotransport is higher compared to BBMVs isolated from animals fed a high Pi-diet. Changes in Pi reabsorption are achieved by membrane insertion or retrieval of NaPi-IIa, NaPi-IIc and Pit-2 into or from the apical membrane [7, 8, 11, 107].

Intake of dietary Pi differentially regulates the Na/Pi-cotransporters in the BBM. The abundance of NaPi-IIa changes within few hours after dietary switches, whereas regulation of NaPi-IIc and Pit-2 abundance is much slower. In response to high Pi-diet NaPi-IIa is endocytosed and degraded in lysosomes whereas a decrease of the abundance of the NaPi-IIc cotransporter occurs via a different mechanism that is still not understood [108]. The increased abundance and translocation of NaPi-IIa and NaPi-IIc is a microtubule-dependent mechanism [108, 109].

To address the relative contribution of the different Na/Pi-cotransporters to the dietary adaptive changes, wild type and NaPi-IIa deficient mice were chronically and acutely

challenged with high and low Pi diets. This study suggests that NaPi-IIa is responsible for the acute phase of adaptation [110]. Moreover, the abundance of NaPi-IIa was increased after 4 hours switch from high to low Pi even though FGF23 levels remained higher [110]. It is known that the stability of Na/Pi-cotransporters at the BBM is dependent on the interacting PDZ binding proteins. Phosphaturia was observed with decreased NaPi-IIa expression at BBM in NHERF-1 deficient mice challenged with chronic low Pi diet [111, 112]. Chronic treatment, but not acute feeding, may also result in changes of mRNA levels, at least in the adult mice [113]. In weaning mice, chronic low Pi dietary intake leads to higher NaPi-IIa protein abundance without mRNA changes, whereas NaPi-IIc expression increases at mRNA and protein levels [114].

The mechanism(s) that elucidate rapid changes of the renal abundance of Na/Pi-cotransporters due to altered intake of dietary Pi is (are) not known. Recently it has been shown that administration of a Pi bolus into the rat duodenum was associated with higher Pi excretion after 15 minutes without changes in the serum PTH and FGF23 [115]. This rapid adaptive response in the kidney suggested the presence of Pi sensor or sensing mechanism in the kidney or extra renal tissues, e.g. in the small intestine.

3.6.2 Parathyroid hormone

Parathyroid hormone (PTH) is synthesized by the chief cells of the parathyroid gland. The production and secretion of PTH is a tightly regulated mechanism and depends on the extracellular Ca^{2+} concentration. The secretion of PTH is regulated by the Ca^{2+} sensing receptor (CaR) and $1,25(OH)_2D_3$. Activation of the CaR reduces the PTH levels via transcriptional and post-translational mechanisms through different intracellular signaling pathways [116]. PTH secretion is also inhibited by $1,25(OH)_2D_3$ by blocking the transcription [117]. In addition to its primary effect on Ca^{2+} homeostasis, it is well known that PTH acts on the kidney to decrease Pi reabsorption by reducing the apical abundance of Na/Pi-cotransporters (Figure 7) without changing the mRNA levels [118].

In rodents, it has been demonstrated that NaPi-IIa is almost completely removed from the apical membrane within 1 hour after PTH addition, whereas a decrease of the NaPi-IIc abundance is slower and observed only after 4 to 8 hours [118-120]. In addition, Pit-2

abundance is also reduced 30 minutes after PTH infusion [106]. Tracking-racer image spectroscopy analysis showed that PTH induced internalization of both NaPi-IIa and NaPi-IIc requires myosin VI (a motor protein in microvilli) [121]. PTH treatment leads to rapid internalization of NaPi-IIa via clathrin coated pits. Internalized NaPi-IIa, but not NaPi-IIc and Pit-2, is subsequently degraded in the lysosomes [106, 119, 120, 122].

PTH did not stimulate the internalization and degradation when NaPi-IIa was mutated at a KR motif located in the last cytoplasmic loop (Figure 3) [123]. As the KR motif is absent in NaPi-IIc, this could explain the different internalization rates of both cotransporters in response to PTH. PTH acts on a G-protein coupled receptor (PTHR1) that is located at both the apical and the basolateral membranes of the proximal tubular cell. The PTH signal from the apical side results in activation of Gq/phospholipase C/protein kinase C. Signaling of PTH receptors located at the basolateral side leads to activation of Gαs/adenylate cyclase, which increases cyclic adenosine monophosphate (cAMP) levels leading to activation of PKA. Activation of both signaling cascades leads to internalization of NaPi-IIa from the BBM [124, 125]. Furthermore, inhibition of ERK1/2 partially prevented the PTH induced down regulation of NaPi-IIa, suggesting the involvement of the MAPK pathway [126]. NHERF-1 is a NaPi-IIa interacting partner involved in the stabilization of the cotransporter at the BBM. Immunohistochemical analysis suggested that the endocytosis of NaPi-IIa in reponse to PKC activation is impaired in NHERF1$^{-/-}$ deficient mice [127]. Upon PTH administration, NHERF-1 is phosphorylated at a serine residue (S77) located in the first PDZ domain and it has been suggested that this phosphorylation of, NHERF-1 leads to a dissociation of the NaPi-IIa/ NHERF-1 complex and thereby allows the endocytosis of NaPi-IIa [48].

3.6.3 Dietary potassium

Potassium (K^+) deficiency is one of the factors that regulate Pi reabsorption in the kidney. Low dietary K^+ leads to increased Pi excretion that is paralleled by decreased Na/Pi-cotransport activity in renal BBMVs. Breusegem et al. [128] observed hypophosphatemia with increased Pi excretion in the urine of low K^+ fed animals compared to controls. They also found decreased abundance of NaPi-IIc and Pit-2 at protein and mRNA levels in K^+ deficient rats and mice. Moreover, the Na/Pi-cotransport activity was also decreased in these animals. The decreased abundance of these two transporters might contribute to

phosphaturia although NaPi-IIa abundance was increased [128]. The reduced transport activity suggests the contribution of NaPi-IIc and Pit-2 to Pi reabsorption in the kidney. Paradoxically, the decreased transport activity is associated with an increased abundance of NaPi-IIa and Pit-1 proteins [129]. Furthermore, low K^+ diet leads to increased levels of several lipids in renal BBM (sphingomyeline, glycosylceramide and ganglioside GM3) and decreased lipid fluidity [129]. Interestingly, when glycosylceramide synthesis was inhibited, increased BBM transport activity was observed in animals fed with control and low K^+ diet, although the abundance of NaPi-IIa protein as well as its mRNA expression remains unchanged. Therefore, K^+ deficiency might lead to alterations in the lipid composition of BBM that regulate posttranscriptionally the abundance and activity of NaPi-IIa [129]. Analysis based on scanning fluctuation correlation spectroscopy showed that the diffusion of NaPi-IIa in the BBM occurred slowly but the cluster size increased in mice fed low K^+ diet [130].

3.6.4 1,25 dihydroxy vitamin D

Although active 1,25 dihydorxy vitamin D ($1,25(OH)_2D_3$) plays a major role in Ca^{2+} homeostasis it is also involved in Pi homeostasis. Proximal tubular epithelial cells express two enzymes, 1α-hydroxylase (Cyp27b1) and 24-hydroxylase (Cyp24a1), that regulate $1,25(OH)_2D_3$ metabolism. The anabolic enzyme 1α-hydroxylase converts the inactive 25-hydroxy vitamin D3 to the active form $1,25(OH)_2D_3$, whereas 24-hydroxylase inactivates the active form. The synthesis of $1,25(OH)_2D_3$ is regulated mainly by PTH and FGF23 (Figure 7). PTH acts on the proximal tubule to increase the expression of 1α-hydroxylase. In contrast to PTH, FGF23 impairs the $1,25(OH)_2D_3$ synthesis by inhibiting the 1α-hydroxylase mRNA expression and by increasing 24-hydroxylase mRNA [131, 132] (Figure 7).

In $1,25(OH)_2D_3$ deficient rats, the abundance of NaPi-IIa protein and mRNA were decreased in the juxtamedullary cortex of kidney whereas expression was unchanged in superficial cortex [133]. Moreover, the injection of $1,25(OH)_2D_3$ into $1,25(OH)_2D_3$ deficient rats leads to increased Na/Pi-cotransport activity due to an increase of the abundance of NaPi-IIa mRNA and protein [133]. Furthermore, the abundance of NaPi-IIa in BBM was reduced in vitamin D receptor (VDR) deficient mice compared to wild type [134].

$1,25(OH)_2D_3$ treatment in TPTX rats increased the serum level of FGF23, suggesting an indirect of action of $1,25(OH)_2D_3$ on renal Pi handling[135].In mice, treatment with $1,25(OH)_2D_3$ leads to increased expression of FGF23 in bone [136]. Together, these data demonstrate the presence of negative feedback mechanism between these two hormones associated with a kidney-intestine-bone axis that regulates the Pi homeostasis (Figure 7).

3.6.5 Metabolic acidosis

Besides the many functions of Pi, Pi is an important urinary buffering component for keeping acid base balance [137]. Metabolic acidosis (MA) increases the excretion of Pi into urine. During metabolic acidosis, there is an increased resorption of Pi from the bone which along with increased H^+ excretion and absorption of bicarbonate (HCO_3^-) in the proximal tubule contributes to balance acid-base status. It was also reported that MA is compensated by ammonia (NH_3) and citrate excretion which act together with Pi as a buffer system to increase the excretion of H^+ along the nephron [138]. In rats, induction of chronic MA led to a massive reduction of Pi uptake into isolated renal BBM vesicles. Reduced transport activity was associated with downregulation of NaPi-IIa mRNA and protein abundance [139]. Microarray gene profiling analysis in the kidney of mice challenged with chronic acid load also showed decreased expression of NaPi-IIa and NaPi-IIc mRNAs [138] whereas the expression of Pit-1/Pit-2 mRNAs was higher in acid loaded mice [68]. However, the protein abundance of NaPi-IIa and NaPi-IIc increased in acid loaded mice despite the higher Pi excretion [68] . The increased abundance of both cotransporters is associated with higher Na/Pi-cotransport into BBM vesicles isolated from acid loaded mice which is in contrast to the observations made with rats. These findings suggest that the phosphaturia induced by MA is independent of the abundance of NaPi-IIa/NaPi-IIc, and may be due to inhibition of Na/Pi-cotransporters by the high concentration of H^+ in the lumen of proximal tubule.

3.6.6 Phosphatonins

In 1994, Cai and Econs identified factors called phosphatonins that are responsible for severe Pi wasting in the urine. They observed inhibition of Pi reabsorption and altered $1,25(OH)_2D_3$ metabolism in patients with tumor-induced osteomalacia (TIO) [140, 141]. Incubation with supernatant from tumor cell cultures lead to inhibition of Na/Pi-cotransport in OK cells. In contrast to PTH action these phosphatonins did not increase cAMP levels and

their activity was also not inhibited by PTH receptor antagonists [140]. The phosphaturic factors include fibroblast growth factor-23 (FGF23), secreted frizzled related protein-4 (sFRP-4), matrix extracellular phosphor-glycoprotein (MEPE) and fibroblast growth factor-7 (FGF7) [115, 142].

3.6.6.1 Fibroblast growth factor23 (FGF23)

FGF23 is a bone-derived peptide hormone which is synthesized in osteoblasts and osteocytes [143]. Expression of FGF23 has also been found in several other tissues, including the small intestine, heart, liver and parathyroid gland. FGF23 has been identified as the gene mutated in patients with autosomal dominant hypophosphatemic rickets (ADHR), a Pi wasting genetic disease. Based on the positional cloning, several "gain of function" mutations of FGF23 were identified in ADHR patients. These mutations lead to the absence of a furin proconvertase site, and thereby to resistance to inactivation by proteolysis [144, 145]. The proteolytic resistance results in elevated intact FGF23, which triggers phosphaturia,and blocks 1α-hydroxylase release resulting in lower levels of circulating 1,25(OH)2D3 and rickets.

The synthesis of FGF23 by the bone is known to be regulated by $1,25(OH)_2D_3$ [136]. In dialysis patients, treatment with $1,25(OH)_2D_3$ led to increased circulating FGF23. Similarly, administration of $1,25(OH)_2D_3$ to mice lead to increased serum FGF23 along with increased mRNA expression in bone [136, 146]. Moreover, it was also demonstrated in mice that chronic high Pi dietary intake resulted in elevated FGF23 levels in serum and low levels under low Pi diet [115]. Increased serum FGF23 negatively regulates the synthesis of active vitamin D by inhibiting the 1α-hydroxylase mRNA (Figure 7). This correlation of both FGF23 and $1,25(OH)_2D_3$ metabolism suggests the presence of a feedback loop between bone-kidney axes (Figure 7).

Intraperitoneal administration and intravenous injection of recombinant FGF23 in mice resulted in low serum Pi and a dose-dependent increased fractional excretion of Pi [147]. Implantation of plasmids containing FGF23 into nude mice also results in hypophosphatemia and Pi wasting in urine [145]. In addition, FGF23 decreased the expression of 1α-hydroxylase mRNA (Cyp27b1) and rickets were observed by morphological analysis in long bones [145].

In agreement with this findings, incubation of OK cells with FGF23 results in inhibition of Na/Pi-cotransport activity [148]. Similar findings were observed in transgenic mice overexpressing FGF23, which show reduced abundance of NaPi-IIa in the BBM [149]. Conversely, these phenotypic changes were reversed in FGF23 deficient mice, for which higher $1,25(OH)_2D_3$ levels in serum were reported [132].

FGF23 induces phosphaturia by downregulating the expression of NaPi-IIa, NaPi-IIc and Pit-2 [150]. However, the time course of FGF23 to reduce the abundance of each cotransporter is not known. This effect of FGF23 involves its binding to fibroblast growth factor receptor-1 (FGFR-1) and probably to FGFR-4 in the presence of klotho as coreceptor [151]. FGF23 reduces the abundance of Na/Pi-cotransporters at least partially via the MAPK pathway [150, 152, 153]. The highest expression of FGFR-1, -4 and klotho complexes were observed in the distal tubules compared to proximal tubules, whereas the biological actions of FGF23 are in the proximal tubule [154-156]. The mechanisms underlying the differential effects of FGF23 to regulate the Na/Pi reabsorption in vivo are unclear. There are two conflicting theories through which FGF23 acts on the kidney to downregulate the Na/Pi-cotransporters. The administration of FGF23 in mice leads to activation of phospho-ERK1/2 only within distal tubules [153]. However, microperfusion studies in isolated proximal tubules showed reduced BBM abundance of NaPi-IIa in response to FGF23 [157]. Thus, FGF23 actions on the proximal tubule may be indirect, possibly via stimulation of distal tubule and release of paracrine factors that regulate the proximal tubular reabsorption of Pi (i.e., distal-to-proximal tubular feedback mechanism) [158]. As discussed for PTH regulation, FGF23 induced downregulation of NaPi-IIa seems to involve phosphorylation of NHERF-1 [159].

Klotho belongs to the family of β1 glycosidases and the extracellular domain of klotho shares 40% sequence homology with mammalian lactase glycosylceramidase. In the kidney, as mentioned earlier that the highest expression was found in the distal tubule but was also observed in the proximal tubules [155]. The expression of klotho has also been described in several endocrine organs including the parathyroid gland, pancreas, ovaries, testis and placenta. This broad tissue distribution explains its role in several tissues. Kuro [160] identified klotho as an age suppressor gene in mice [160]. Mice deficient in klotho exhibited

premature aging syndromes associated with growth retardation, osteopenia, vascular calcification, skin atrophy and sarcopenia [161].

Membrane klotho acts as a co-receptor for FGF23 binding to FGF receptors and is required for biological activity of FGF23 in the kidney. Thus, klotho deficient mice exhibited not only premature aging but also hyperphosphatemia with tissue calcification and elevated FGF23 levels [160]. In addition, klotho deficient mice exhibited increased abundances of NaPi-IIa and NaPi-IIc, although FGF23 was elevated. Initially it was described that FGF23 acts on the distal tubule and inhibits the Pi reabsorption in proximal tubules via paracrine function [158]. However, microperfusion studies in isolated proximal tubules showed reduced BBM abundance of NaPi-IIa in response to FGF23 [157]. In support of this, the expression of klotho in the proximal tubules was also demonstrated [162].

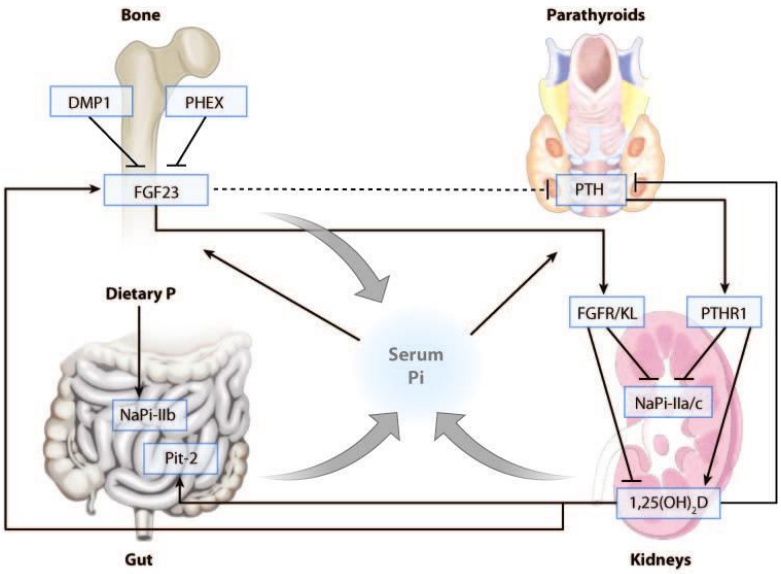

Figure 7 Factors effecting the regulation of phosphate homeostasis. Pi is absorbed in the intestine from diet and stored into bones. The reabsorption and excretion of Pi occurred by the kidney. $1,25(OH)_2D_3$ is synthesized in the kidney and stimulates the absorption of Pi in the intestine. FGF-23 produced in bone and increases the renal Pi excretion by downregulting NaPi-IIa and NaPi-IIc. FGF-23 also inhibits the synthesis of $1,25(OH)_2D_3$ and may inhibit the parathyroid hormone (PTH) secretion. PTH inhibits the Pi reabsorption and stimulates the synthesis of $1,25(OH)_2D_3$ [116]. Image taken from: Bergwitz & Juppner, 2010, Annual Review of Medicine.

3.7 Phosphate absorption in the intestine

Dietary Pi is absorbed in the small intestine and released into the circulation. The absorption of Pi across the epithelium probably occurs both transcellularly and paracellularly. Besides

NaPi-IIb, Pit-1 and Pit-2 mRNAs are also expressed in the small intestine and NaPi-llb and Pit-2 proteins have been detected in the apical membrane of enterocytes [74].

The segmental distribution of NaPi-IIb along the small intestine is species specific. In mice, the expression of NaPi-IIb (mRNA and protein) is highest in distal intestine (ileum) and gradually decreases in the jejunum [163]. In contrast, in rats the highest expression of NaPi-IIb and Pi absorption was observed in the jejunum and the duodenum and is almost absent from the ileum [164]. In humans maximal Pi- uptake was observed in BBMVs isolated from the jejunum [165].

The ontogenic expression of NaPi-IIb in the small intestine of mice and rats was also reported. The transport of Pi was higher in intestinal BBM vesicles isolated from young (14-day old) mice compared to adults. These changes were paralleled by increased expression of NaPi-IIb mRNA and protein in young mice [166]. The expression decreases progressively with age and this reduction has been associated with an increase in the N-glcosylation status [167]. However, there is no clear evidence whether age dependent regulated glycosylation also plays a role in the regulation of other SLC34 transporters. These effects were paralleled by age-dependent downregulation of NaPi-IIb at the protein and mRNA levels [166, 168].

The deletion of NaPi-IIb (NaPi-IIb$^{-/-}$) leads to increased fecal excretion of Pi with hypophosphaturia but no change of serum Pi. Hypophosphaturia was explained by an increased expression of NaPi-IIa in kidney, thereby maintaining the normal serum Pi [17]. In intestinal BBM vesicles isolated from NaPi-IIb$^{-/-}$ mice the Na^+-dependent uptake of Pi was reduced by 90%. The remaining Pi uptake may be mediated by Pit-1 and Pit-2. These findings suggest that NaPi-IIb plays a major role in the Pi absorption in the small intestine. However, the relative contribution of sodium dependent and independent transport mechanisms for overall Pi absorption remains unknown.

Transepithelial transport of Pi in the small intestine might also be mediated by a paracellular pathway. The overall transport within the region may also depend on the time course of Pi transit along the segments. Intestinal Pi absorption was comparable in the presence or absence of 1,25$(OH)_2D_3$ in the rats fed with Pi bolus [169]. This suggests that the absorption

of Pi might occur through the paracellular transport mechanism which may depend on intake of dietary Pi.

3.8 Regulation of Na/Pi-cotransport in the small intestine

In contrast to the renal reabsorption of Pi less is known about the regulation of small intestinal Pi absorption. Several studies described the regulation by dietary Pi and $1,25(OH)_2D_3$; these two factors will be discussed in the following paragraphs. Several other factors, such as metabolic acidosis, glucocorticoids, estrogens, epidermal growth factor, matrix extracellular phosphoglycoprotein and FGF23 also modulate the Pi absorption by indirect or direct mechanisms [167, 170-174]. The relative role of these different factors under normal physiological condition may require additional studies.

3.8.1 Dietary phosphate and 1,25dihydroxy vitamin D

The administration of low Pi diet in mice leads to increased abundance of NaPi-IIb, in parallel with higher Na/Pi cotransport activity in BBMVs isolated from the small intestine [175]. In addition, low Pi diet stimulates the expression of renal 1α-hydroxylase, and thereby the synthesis of $1,25(OH)_2D_3$ is increased [175]. Although $1,25(OH)_2D_3$ also regulates the abundance of the cotransporter, the expression of NaPi-IIb was increased in VDR deficient as well as in 1-α hydroxylase deficient mice challenged with low Pi diet [134, 175]. This suggests that low dietary Pi can induce the expression of NaPi-IIb in the intestine independent of changes in $1,25(OH)_2D_3$.

The expression of NaPi-IIb mRNA and the intestinal Na/Pi-cotransport were also increased in rats fed with low Pi diet compared to rats on a control diet [176]. Interestingly, it was also observed that the abundance of NaPi-IIb changed differently across the segments of the small intestine in response to changes in diet. Thus, NaPi-IIb expression was increased in the jejunum but not in the duodenum of rats treated with low Pi diet for 7 days. Similarly, the Na/Pi-cotransport activity was increased in BBMV isolated from the jejunum. Moreover, rats adapted to low Pi diet and then acutely switched to high Pi diet exhibited an increased Na/Pi-cotransport and abundance of NaPi-IIb in the duodenum but not in the jejunum [83]. Hence, these data suggest that the acute or chronic changes in dietary Pi regulate NaPi-IIb in a segmental specific way along the small intestine. Furthermore, hyperphosphatemia with

phosphaturia was observed within one hour after administration of different concentrations of dietary Pi in humans [177]. These postprandial changes in serum Pi levels suggest that fast adaptive changes occurred in response to dietary Pi.

$1,25(OH)_2D_3$ is an important hormone known to regulate Pi absorption across the small intestine. $1,25(OH)_2D_3$ binds to the vitamin D receptor (VDR) and enhance the expression of NaPi-IIb at the level of mRNA and protein [178]. In adult $1,25(OH)_2D_3$ deficient rats, the uptake of Pi in intestinal BBMVs was increased after $1,25(OH)_2D_3$ treatment. In addition, Pit-2 mRNA was also increased in these rats [176]. Treatment of suckling rats with $1,25(OH)_2D_3$ also resulted in increased Pi uptake in the BBMVs. This increase was higher than the one observed in adult rats. Moreover, NaPi-IIb mRNA increased in young but not in adult rats upon $1,25(OH)_2D_3$ treatment [166]. Similarly, the expression of NaPi-IIb was increased after the administration of $1,25(OH)_2D_3$ into mice whereas NaPi-IIb expression and Na^+/Pi transport activity was reduced in the VDR deficient mice [134, 178]. Recently it was reported that the $1,25(OH)_2D_3$ analog ED71 (1,25 dihydroxy-2β-(3-hydroxypropyloxy) vitamin D) increased NaPi-IIb mRNA in $1,25(OH)_2D_3$ replete rats. In addition, oral administration of ED71 in mice leads to enhanced NaPi-IIb mRNA and protein levels [179]. These evidences strongly support the presence of a $1,25(OH)_2D_3$ induced transcellular Na/Pi-cotransport mechanism in the small intestine.

3.9 Genetic diseases associated with Pi homeostasis

Mutations in SLC34 and SLC20 Na/Pi-cotransporters have been identified in patients with severe Pi wasting phenotypes, bone mineralization defects, or soft tissue calcification. Some of these clinical disorders are discussed below.

In bone, there are several cascades of proteins consisting of PHEX, 7B2/PC2, BMP-1 and DMP-1 that regulate transcriptionally or posttranscriptionally the expression of FGF23. In addition, GALNT3 glycosylates FGF23 leading to higher resistance against proteolysis.

3.9.1 X-linked hypophosphatemia (XLH)

XLH is an inherited Pi wasting dominant disorder that results in changes in biochemical parameters which includes hypophosphatemia, increased serum FGF23 levels and abnormal $1,25(OH)_2D_3$ levels with normal PTH levels. Patients with XLH are characterized by hypophosphatemia, rickets and tooth abscesses. These symptoms are similar to those of patients with ADHR. The gene responsible for XLH is PHEX, which encodes a protein that belongs to the family of M13 zinc metallopeptidases. PHEX is known to be expressed in osteocytes and osteoblasts and is thought to regulate the synthesis and degradation of FGF23 [180]. Inactivating mutations in PHEX lead to a loss of functional protein and failure to promote degradation of FGF23. In addition, inactivation of PHEX also increases transcription of FGF23. Both mechanisms lead to higher circulating level of FGF23. Patients with XLH show higher FGF23 levels in serum, which leads to an impaired Pi reabsorption. Similar changes were also observed in Hyp mice which represent an animal model for XLH [181]. The abundance of NaPi-IIa protein is reduced by approximately 50% in Hyp mice compared to wild type.

3.9.2 Autosomal dominant hypophosphatemic rickets (ADHR)

Gain of function mutations in the FGF23 gene are responsible for ADHR. The proteolysis and inactivation of FGF23 occurs at the subtilisin-like proprotein convertase (SPC) site Arg_{176}HisThrArg179/Ser_{180} (RXXR/S motif) which cleaves the FGF-like domain from the C-terminal tail. The mutation in this specific site at Arg_{176}Gln, Arg_{179}Gln and Arg_{179}Trp results in FGF23 that is resistant to proteolysis. ADHR is a Pi wasting disorder characterized by higher circulating levels of FGF23, hypophosphatemia and abnormal serum $1,25(OH)_2D_3$ levels without any changes in the serum calcium and PTH [182]. In general, patients with ADHR show clinical symptoms including bone fractures, pain in bones, osteomalacia and tooth abscesses. Apparently, adult and young patients with ADHR exhibit different symptoms. Children with ADHR exhibit severe bone pain, weakness and fractures. In adult patients maximum tubular reabsorption of Pi per glomerular filtration rate (TmP/GFR) was lower, and they also exhibited bone deformities and pseudofractures [182]. The progression of the ADHR in patients depends on the circulating levels of FGF23 and correlates with severity [183]. As mentioned above (Section 3.6.6.1) that transgenic mice over expressing FGF23

leads to decreased abundance of NaPi-IIa in the kidney [149]. In contrast, hyperphosphatemia was observed in the absence of FGF23 in mice [132].

3.9.3 Autosomal recessive hypophosphatemic rickets (ARHR)

Inactivating mutations in dentin matrix protein (DMP1) lead to ARHR [184, 185]. The biochemical phenotypic changes observed in patients with ARHR were comparable to ADHR and XLH affected individuals. DMP-1 belongs to the family of SIBLING proteins and is highly expressed by osteocytes [186]. In ARHR patients' FGF23 was elevated in serum and increased expression was similar to patients with PHEX mutation. The deletion of DMP1 in mice results in severe hypophosphatemia, increased serum FGF23 and defects in bone mineralization associated with diminished osteocyte maturation [186-188]. These data indicated that DMP1 participates in the regulation of hydroxyapatite formation as well as in the regulation of FGF23 synthesis. DMP1 deficient mice exhibit a phenotype comparable to Hyp mice.

3.9.4 Tumor-induced osteomalacia (TIO)

TIO is an acquired disorder associated with loss of Pi in urine. Most tumors originate from the mesenchymal tissue in TIO patients [189]. Several studies have observed that FGF23 mRNA and circulating protein was increased in tumors isolated from TIO patients. Hence, increased FGF23 inhibits Pi reabsorption in the kidney which results in biochemical and bone phenotype. These changes are parallel to the phenotypes observed in patients with ADHR, XLH and ARHR, and were reverted after surgical removal of tumors from TIO patients [190].

3.9.5 Fibrous dysplasia of McCune-Albright syndrome (MAS/FD)

This syndrome is caused by gain of function mutations in GNAS1. MAS is characterized by hypophosphatemia and renal Pi wasting with increased FGF23 levels in serum. Patients with MAS develop hypophosphatemic rickets with replacement of bone with fibrous tissue leading to swelling of bone [191]. Patients with MAS also show pigment patches on the skin, bone fractures and early puberty.

3.9.6 Hereditary hypophosphatemic rickets with hypercalciuria (HHRH)

Hereditary hypophosphatemic rickets with hypercalciuria was identified by Tieder et al. [192] in patients for the first time. HHRH is a rare autosomal recessive syndrome characterized by hypophosphatemia due to impaired renal reabsorption of Pi, hypercalciuria, increased serum $1,25(OH)_2D_3$, rickets, and osteomalacia. To identify the gene carrying the mutation associated with HHRH, Bergwitz et al. [193, 194] performed homozygosity mapping and nucleotide sequence analysis. They identified patients carrying homozygous single nucleotide mutations in the SLC34A3 gene. Moreover, compound heterozygous missense and deletion mutation were also reported in unrelated individuals with HHRH. Heterozygous mutations do not show the disease phenotype [194]. Up to now 20 different types of mutations have been identified throughout the SLC34A3 gene that cause HHRH (Figure 4). These mutations are thought to cause a loss of NaPi-IIc at the BBM, due to defects in trafficking, or reduced stability of the mutated protein [195]. However, mice with constitutive deletion of NaPi-IIc exhibited hypercalcemia, hypercalciuria and increased $1,25(OH)_2D_3$, but they did not display hypophosphatemia or hypophosphaturia and rickets [69]. Together these observations suggest that, unlike in rodents, NaPi-IIc has a major contribution to Pi homeostasis in humans.

3.9.7 Renal Fanconi syndrome

Renal Fanconi syndrome is a generalized disturbance of proximal tubular functions with many different genetic and acquired forms. It is characterized by excessive wasting of glucose, amino acids, uric acid, bicarbonate in the urine. Patients with this syndrome also suffer from rickets due to a massive excretion of Pi. Recently a homozygous in-frame duplication of 21-bp in SLC34A1 was reported in two siblings from an Israeli family that had autosomal recessive hypophosphatemic Fanconi syndrome and rickets. This mutation leads to impaired trafficking to the membrane and therefore inactivation of NaPi-IIa [64]. This provides information regarding a role of NaPi-IIa in renal reabsorption of Pi in humans.

3.9.8 Familial idiopathic basal ganglia calcification (IBGC)

IBGC, also known as Fahr's disease, is an inherited autosomal dominant syndrome. It is a neurodegenerative disorder characterized by calcification (calcium phosphate deposits) of vascular tissue in the basal ganglia of the brain region. Typical neuropsychiatric clinical symptoms include parkinsonism, psychosis, dementia, dystonia, tremor, ataxia, seizures and headache. Recently Wang et al. [92] identified different mutations in Pit-2 (SLC20A2) in different families affected by IBGC. These mutations associated with the loss of Pit-2 function [92]. The Pit-2 transcript is known to be expressed abundantly in the basal ganglia of the brain region. In addition, mutational analysis data reported that 41% of IBGC patients exhibited mutations in Pit-2 and these mutations were non-sense, deletion, missense and site directed [196]. These data indicate that Pit-2 might be responsible for Pi handling in the brain. The tissue specific importance of these mutations in Pit-2 remains unclear.

3.10 Contribution of NaPi-IIa and NaPi-IIc to Pi reabsorption in the kidney

Several studies indicated the importance of Na/Pi-cotransporters to Pi reabsorption in the kidney (see introduction). Based on these studies it is important to consider the species and developmental stages of animals to investigate the relative contribution of Na/Pi-cotransporters in the kidney. Inhibition of NaPi-IIa by RNase H-mediated hybrid depletion using *X.laevis* oocytes as expression system suggest that NaPi-IIa mediates most of the Na/Pi- cotransport activity in the adult rat kidney whereas NaPi-IIc seems to have a minimal contribution [7]. In agreement with this observation, the highest abundance of NaPi-IIa was observed in weaning animals whereas it expression was reduced gradually in older animals [57]. In contrast, the relative abundance of NaPi-IIc is higher in weaning animals compared to adult animals [7]. The uptake of Pi is higher in renal BBM isolated from young animals and declines with age, suggest the renal reabsorption of Pi is an age-regulated process [67]. Furthermore, the different pattern of regulation of NaPi-IIa and NaPi-IIc in response to dietary Pi, PTH and FGF23 (see introduction) suggests the presence of different signaling mechanisms. NaPi-IIa deficient mice show hyperphosphaturia with hypophosphatemia, which suggests that, the reabsorption of Pi is largely mediated by NaPi-IIa. Indeed the uptake of Pi in isolated BBMVs was reduced by 70% in NaPi-IIa$^{-/-}$ mice compared to wild type

animals, although NaPi-IIc expression was increased [59]. The remaining 30% Pi uptake in NaPi-IIa$^{-/-}$ mice should be mediated by other Na/Pi-cotransporters expressed in the kidney, i.e. NaPi-IIc and/or Pit-2 [197]. Furthermore, NaPi-IIa$^{-/-}$ mice displayed reduced PTH and FGF23 with hypercalcemia and hypercalciuria associated with higher levels of circulating 1,25$(OH)_2D_3$ resulting in increased Ca^{2+} absorption in the small intestine [198]. Constitutive NaPi-IIc deficient mice (NaPi-IIc$^{-/-}$) mice are characterized by hypercalcemia and hypercalciuria without disturbances in serum Pi levels [69]. A double knockout (DKO) mouse model deficient for NaPi-IIa and NaPi-IIc shows a more severe hypophosphatemia than NaPi-IIa$^{-/-}$ mice [71], suggesting that the, relative contribution of both cotransporters to Pi handling is nonredundant. The data from gene deficient mouse models suggests that, NaPi-IIa has a major quantitative role to Pi reabsorption whereas NaPi-IIc is considered to play a minor role or is restricted to young animals.

4. Aim of the study

To date, it is known that, in mice, NaPi-IIa plays a major role to maintain Pi homeostasis by reabsorbing the bulk of Pi from primary urine. NaPi-IIc and/or other proximal tubular apical Na/Pi-cotransporters appear to have minimal contribution to Pi reabsorption. However, in humans, NaPi-IIc might be more important as suggested by the genetic defects in NaPi-IIc that lead to hereditary hypophosphatemic rickets with hypercalciuria (Figure 4).

In mice, the relative contribution of NaPi-IIa and NaPi-IIc to renal Pi reabsorption is based on deficient models in which these cotransporters have been knocked out in a constitutive manner. These mouse models however could not explain the relative contribution of these cotransporters to Pi reabsorption in the kidney. In this situation, compensatory changes may have a masking initial effect on Pi handling. Therefore, our aim was to investigate the renal contribution of NaPi-IIc and we generated and characterized a mouse model in which NaPi-IIc can be knocked out in a tissue specific (here kidney) and in an inducible manner.

5. Material and Methods

5.1 Generation of renal-specific and inducible NaPi-IIc knockout mice

A floxed-NaPi-IIc gene was generated by gene-targeting strategy in embryonic stem cells (ESC). Briefly, a targeting vector was constructed (Figure 9A) to replace the NaPi-IIc genomic sequence by homologous recombination upon injection into ESC. The targeting vector consisted of floxed Slc34a3 genomic sequence along with a neomycin resistant cassette (PGK-neo) and the thymidine kinase gene from herpes simplex virus (HSV-TK). Two loxP sites were inserted in 5` to 3` direction between within introns 3 and 12. This loxP flanked sequence has about 2.3 Kb (Figure 9A), and encodes residues 58 to 447 of the NaPi-IIc protein. As a positive selection marker the neomycin resistant gene driven by the phosphoglycerate kinase promoter (PGK-neo) was inserted downstream of the 5` homologous arm of NaPi-IIc and upstream of the floxed fragment. The PGK-neo was flanked by the two frt sites. As negative selection marker the HSV-TK was inserted downstream of the 3` homologous arm. Both the 5` and 3` homologous arms consist of around 1.9 kb.

To allow homologous recombination, the vector was linearized with *PacI* and transfected by electroporation into 129SV ESC. ESC clones that survived in G148 but not in ganciclovir were then analyzed by Southern blots using 5` and 3` probes to further confirm the homologous recombination (Figure 9A, B). The 5` probe consisted of the last 700 bp of the 5` homologous arm. The 3` probe consisted of 550 bp located at the middle of 3` homologous arm. In brief, we performed the restriction digestion with *KpnI* or *EcoR1* of the genomic DNA isolated from 4 selected clones and from untransfected ESC. The digested DNA was separated on an agarose gel and transferred to nitrocellulose membranes. Then, hybridization was done according to the standard protocol using ^{32}P labeled probes. In addition, PCR was performed to confirm the presence of loxP sites on the same DNA samples. The presence of 5` loxP site was detected with a sense primer that anneals to the loxP sequence flanking exon 4 (S1: CTTCGTATAGCATACATTATAC) and an antisense primer that anneals to intron 12 (AS1: GCATGAGATGACCACAGG). The PCR reaction to detect the 3` loxP site was performed with a sense primer anneals within the sequence of intron 3 (S2: GGAGATCCTGTGCTCTG) and

antisense primer that anneals to the loxP sequence located in exon 12 (AS2: CTTCGTATAATGTATGCTATAC).

The selected recombinant clone was microinjected into C57BL/6 mice blastocysts. Chimeric offsprings were produced upon blastocysts implantation into NMRI pseudopregnant female mice. The transfection of the targeting vector in ESC, blastocyst injection, and implantation were performed in collaboration with Dr. E. Hummler from the Transgenic Animal Facility of the University of *Lausanne (TAF UNIL)*. Floxed- heterozygous mice were bred with 64FlpeB6 mice in order to delete the neo-cassette. Floxed-homozygous mice devoid of the neo-cassette were bred with Pax8rtTA/LC1 double transgenic mice (kindly provided by Dr.Koester, University of Heidelberg). In this model the renal expression of Cre-recombinase (under the control of the Pax8 promoter) can be induced by doxycycline (Doxy) (Figure 8). Further mating resulted in the generation of conditional homozygous (NaPi-IIc$^{f/f}$) and conditional heterozygous mutants (NaPi-IIc$^{f/+}$) as well as wild type (NaPi-IIc$^{+/+}$) mice positive for both Pax8-rtTA and Cre.

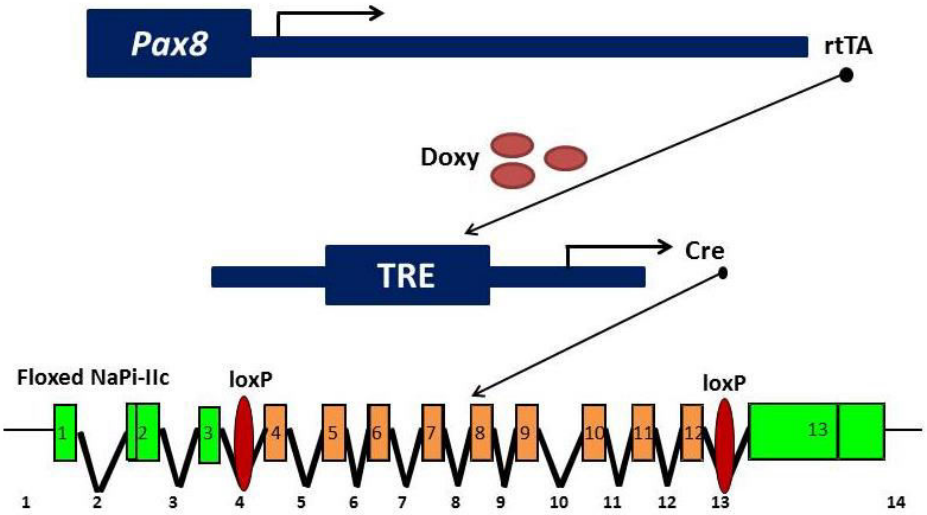

Figure 8 Pax8-rtTA-mediated, doxycycline-induced Cre-recombinase (Cre) expression in the kidney of NaPi-IIc$^{f/f}$ mice. The Pax8 promoter controls the expression of the reverse tetracycline-dependent transactivator (rtTA). In the presence of doxycycline (Doxy) as a cofactor rtTA binds and transactivates the tetracycline-responsive element (TRE) which is a bidirectional P_{tet} promoter. Upon binding of Doxy, rtTA activates the TRE and induces the expression of Cre. The Doxy induced activation of Cre should result in the removal of the Floxed NaPi-IIc sequence flanked by loxP sites [199]. (Image adapted from Traykova-Brauch et al., 2008, Nature Medicine).

5.2 Genomic DNA isolation and genotyping

Genomic DNA was isolated from ear biopsies. Each ear biopsy was incubated in a digestion solution (750µl) containing 50 mM Tris-HCl (pH 8.0), 100 mM EDTA, 100 mM NaCl, 1% SDS, 0.5 mg/ml Proteinase K (Roche, Germany). The incubation was performed at 37^0C overnight. After incubation, the samples were gently mixed and 250µl of 5.5 M sodium chloride were added. Upon centrifugation at 13000 rpm for 10 min at 4^0C the supernatants (800 µl) were collected and transferred to fresh tubes. Isopropanol (530 µl) was added to each tube and mixed gently. Samples were centrifuged at 13,000 rpm for 15 min at 4^0C. The supernatant was removed and the pellet washed with 70% ethanol (750 µl) and centrifuged again at 13,000 rpm for 20 min at 4^0C. Ethanol was removed carefully using a vacuum pump and the pellet was air dried until ethanol was evaporated completely. The dry pellet was resuspended in 50 µl of a buffer containing 10 mM Tris, 1 mM EDTA (TE) and pH 7.4 adjusted with HCl. The samples were incubated for 2 hours at 37^0C in an Eppendorf mixer and the resuspended genomic DNA was stored at -20^0C.

Genotyping was performed by PCR using genomic DNA as a template. Genotyping of NaPi-IIc was done with a forward primer annealing within exon 3 and a reverse primer that anneals on the exon 4 (Figure 9A, C). The presence of Cre and Pax8-rtTA was analyzed with the primers described in the original manuscript (see Table 3). The template DNA was amplified with TaKaRaLa Taq polymerase (RR002A, TAKARA Bio Inc.). The PCR reaction mixture contained dNTPs (10µM), $MgCl_2$ (25µM), forward and reverse primer (10 µM; Microsynth AG). The amplification was performed using a thermo cycler (Robocycler 40) and the following reaction conditions were applied: 95°C for 2 min / 40 cycles of 94^0C for 1 min / 55^0C for 1 min / 68^0C for 1 min followed by 72^0C for 5 min and holding at 4°C. The PCR reactions were mixed with loading dye (Thermo scientific) and loaded on 1% agarose gel. Then, the amplified product together with a DNA ladder (1 kb; Fermentas) was separated by gel electrophoresis and observed under the ultraviolet light. The lengths of PCR fragments were recognized by comparing to DNA ladder.

Gene	Forward (FW) and reverse (RV) Primers
Slc34a3	FW: 5` - GAAGAACGCTGACCAACTG - 3` RV: 5` - CTCACTGCCTAGTAGCTG – 3`
Cre	FW: 5` - TCGCTGCATTACCGGTCGATGC - 3` RV: 5` - CCATGAGTGAACGAACCTGGTCG - 3`
Pax8	FW: 5` - CCATGTCTAGACTGGACAAGA - 3` RV: 5` - CTCCAGGCCACATATGATTAG - 3`

Table 3: List of primers used for genotyping

5.3 Experimental study with mice and sample collection

Mice were kept in accordance with the Swiss Animal Welfare Laws and project license restrictions with the approval of the local veterinary authority (Kantonales Veterinäramt Zürich). Expression of Cre-recombinase was induced in the 3 genotypes (NaPi-IIc$^{+/+}$, NaPi-IIc$^{f/+}$, NaPi-IIc$^{f/f}$) of both genders by providing Doxycycline (Sigma, Switzerland) in the drinking water sweetened with 2% sucrose, whereas the controls drank 2% sucrose alone. The Doxy was prepared freshly every two days and was protected from light by wrapping the bottles with black plastic. To optimize the amount of Doxy required to induce the expression of Cre recombinase the following protocols were used.

Protocol 1: Mice received drinking water supplemented with either 2% sucrose alone or in combination with 2 mg/ml Doxy for 10 days.

Protocol 2: Mice received drinking water supplemented with either 2% sucrose alone or in combination with different concentrations of Doxy (1 mg/ml, 0.5 mg/ml and 0.25 mg/ml) for 10 days. After treatment, all mice drank normal tap water for two additional weeks (recovery period).

Protocol 3: Mice received drinking water supplemented with either 2% sucrose alone or in combination with 0.5 Doxy for 5 days followed by 0.25 mg/ml during the next 5 days. After treatment, all mice received normal tap water for two additional weeks (recovery period). As discussed below, this was the final protocol.

The treatment with Doxy was initiated after weaning (3-4 weeks old) and throughout the experiment mice were fed with standard diet (KLIBA, SA) containing 0.8% Pi. Three days

before the end of the treatment or recovery period, mice were placed in individual metabolic cages, having free access to food and liquid (Doxy, sucrose or water). After two days of adaptation to the new housing conditions, last 24 hours urine was collected under mineral oil. Then, animals were anesthetized with a mixture of 10% ketamine and 10% xylazin in 0.9% sodium chloride. The blood was collected from vena cava and immediately centrifuged (in the presence of heparin) at 8000 rpm. for 6 min to separate plasma. Then kidneys and ileum mucosa were collected. All the samples were immediately frozen in liquid nitrogen and stored at -80°C.

5.4 Analysis of urine and blood parameters

5.4.1 Determination of Pi in urine and plasma

Concentration of Pi in urine and plasma was determined according to the Fiske and Subbarow method (Fiske & Subbarow., 1925). Urinary samples were diluted 1:50 in milliQ water. Plasma Pi was determined without prior dilution of the samples.

To prepare the Pi standards, lyophilized Pi (Randox® Laboratories, United Kingdom) was dissolved in 5 ml of milliQ water to obtain a Pi concentration of 11.70 mM. From this stock, serial dilutions were made resulting in concentrations of 5.85, 2.92, 1.46, 0.73, 0.36 and 0.18 mM. All the urinary, plasma and standard samples were prepared in triplicates.

All samples (10 µl) were mixed with 90 µl of 20% TCA and shortly vortexed. Then, 900 µl of milliQ water were added and the tubes vortexed shortly again. Samples were incubated on ice for 10 min followed by centrifugation (13'000 rpm) for 20 min at 4°C. Supernatants (125 µl) were transferred into a 96-well plate (Nunclon™ Surface, Denmark). Then, 50 µl of ammonium molybdate (1.25 gm dissolved in 2.5 N H_2SO_4) and 12.5 µl of Fiske & Subbarrow reducer (Sigma F5428-25; 1 g/6.3 ml of milliQ water) were added to each well. The plate was gently rotated to mix the solutions and incubated at room temperature (RT) for 15-20 min. The absorbance was read at 620 nm in a micro plate reader (µQuant™, BioTek Instriments, USA). The standard curve was obtained by plotting the standard concentrations versus the corresponding absorbance. Urinary or plasma Pi concentrations were calculated from the slope value of graph.

5.4.2 Determination of creatinine (Cr) in urine

Urinary creatinine was determined according to the Jaffé method (63) for standardization of excretion by kidneys. Before performing the assay, the following reagents, standard concentrations of creatinine and urinary dilutions were prepared.

Reagent A: 4.4 g of NaOH, 9.5 g trisodium phosphate ($Na_3PO_4.12H_2O$) and 9.5 g sodium tetraborate ($Na_2B_4O_710H_2O$) in 500 ml milliQ water with pH >10.

Reagent B: 5 % sodium dodecyl sulfate (SDS: Fluka, Germany) in milliQ water

Reagent C: 1.4% crystal picric acid (Sigma) in milliQ water.

Creatinine standards were prepared by serial dilutions in milliQ water to given final concentrations of 12, 10, 6, 3, and 1.5 mg/dl.

Prior to the assay, a working solution was prepared by mixing equal volumes of reagent A, B and C. Urine samples were diluted 1:20 in milliQ water. All the standards and urine samples were prepared in triplicate.

Briefly, 10 µl of urine and standard samples were pipetted into a 96-well plate (Nunclon™ Surface, Denmark) and 150 µl of working solution were added to each well. The plate was rotated gently to mix the contents and incubated at RT for 30 minutes. The intensity of colour was read at 505 nm with a micro plate reader. Upon addition of 10 µl of 30% acetic acid samples were further incubated at RT for 5 minutes. The absorbance was read again at 505 nm. Final absorbance was calculated by subtracting the second from the first reading. The standard curve was obtained by plotting standard concentration versus the corresponding absorbance. The concentrations of creatinine in the urine samples were obtained from the slope value of graph.

5.4.3 Determination of Ca^{2+} in urine and plasma

The concentration of Ca^{2+} in urine and plasma was measured with the Qauntichrom™ Calcium Assay Kit (DICA-500, Bioassay System). All the reagents (reagent A and reagent B) and Ca^{2+} standard stock (20 mg/dl) were provided with the kit. Before beginning with the assay, a working solution was prepared by mixing equal volumes of reagent A and reagent B. The standard stock was diluted in milliQ water to give concentrations of 20, 16, 12, 8, 6, 4

and 2 mg/dl. Urine samples were diluted in 1:3 milliQ water and plasma samples were measured undiluted. Standards and test samples were prepared in duplicates.

To measure the Ca^{2+} concentration, 5 µl of each urine or plasma samples as well as standards were pipetted into a 96-well plate. Immediately, 200 µl of working solution were added and the plate was gently rotated to mix the contents. Upon incubation at RT for 3 minutes, the absorbance was read at 612 nm using a micro plate reader. The absorption of the standards was plotted against the standard concentrations. The Ca^{2+} concentrations in urine and plasma were obtained from the slope value the graph.

5.4.4 Determination of PTH in plasma

The concentration of PTH in plasma was quantified with a mouse 1-84 PTH ELISA (Enzyme-Linked Immuno-Sorbent Assay) kit (Immunotopics). The kit contains streptavidin coated strips that can be fixed in a 96 multi well holder as well as antibodies and wash solutions. According to manufacturer protocol, 20 µl of plasma samples, standards and controls were added in duplicates in the wells of the coated strips. The samples were incubated with 50 µl working antibody solution. This solution contains equal volumes of mouse PTH biotinylated antibody and mouse PTH horseradish peroxidase (HRP) conjugated antibody. The biotinylated antibody recognizes the C-terminal peptide (39-84) of PTH whereas the HRP conjugated antibody recognizes the N-terminal peptide (1-34). Incubation was done at RT for 3 hours in a horizontal rotator (Heidolph promax 1020, FAUST Switzerland) with speed of 180-220 rpm. After incubation, the contents from each well were removed and the samples were washed four times with 350 µl of wash solution to remove unbounded antibodies. Then, 100 µl of ELISA HRP substrate were added into each well and the plate was further incubated at RT for 30 minutes on the horizontal rotator with the same speed as before. This incubation as performed in the dark. The absorbance was read at 620 nm using the micro plate reader. Immediately, the reaction was stop by adding 100 µl of ELISA stop solution and the plate was incubated on the horizontal rotator for 1 minute. The absorbance was read again at 450 nm. The standard curve was generated by plotting the absorbance values read at 620 nm against the standard concentrations (1045, 336, 102, 32 and 0 pg/mL). The concentrations of PTH in plasma were obtained from the slope value of the standard curve.

5.4.5 Determination of FGF-23 in plasma

The concentration of FGF23 (C-terminal fragment) in plasma was determined by using a Mouse/Rat FGF-23 (C-Term) ELISA kit (Immunotopics). All the materials (streptavidin coated strips, standards, controls and wash solutions) were supplied by the kit and the experiment was done according to manufacturer protocol. In brief, 25 µl of plasma, standards and controls were pipetted in duplicates into the streptavidin coated wells (strips) fixed by a holder. Then, each well was filled with 50 µl of antibody working solution which contains equal volumes of biotinylated and HRP conjugated antibody. The plate was then incubated at RT for 3 hours on a horizontal rotator with speed at 180-220 rpm. The unbound antibody solution was decanted and the wells washed 5 times by pipetting 350 µl of wash solution. Then, 100 µl of HRP substrate were added to all wells and the plate further incubated at RT for 30 minutes on the rotator. During this incubation, the plate was kept in the dark. The absorbance was read at 620 nm. Immediately, 50 µl of ELISA stop solution were added to each well and the reaction incubated on the rotator for 1 min at RT before reading the absorbance at 450 nm.

The standard curve was generated by plotting the absorbance values read at 450 nm against the standard concentrations (1000, 300, 100, 30 and 0 pg/mL). The concentrations of FGF-23 in plasma were obtained from the slope value of the standard graph.

5.4.6 Determination of 1,25 dihydroxy vitamin D in plasma

Active 1,25 dihydroxy vitamin D ($1,25(OH)_2D_3$) in plasma was determined with a radio immune assay (RIA) kit (Immunodiagnostic Systems). All the calibrators, controls, reagents and wash buffers were provided with the kit. Briefly described, the assay was performed in three steps: delipidation, extraction of immunopurified active $1,25(OH)_2D_3$, and reaction with the quantification assay. For the delipidation process, 100 µl of plasma samples were diluted with 400 µl of distilled water. Then, 50 µl of delipidation reagent (mix of dextran sulphate and $MgCl_2$) were added to the diluted plasma samples and to the internal controls. Samples were vortexed shortly and centrifuge at 10, 400 rpm (10, 000 g) for 10 minutes.

During the immunopurification step, 100 µl of delipidated samples were transferred into SORB capsules containing a monoclonal antibody to $1,25(OH)_2D_3$ linked to solid phase

particles. SORB capsules were incubated for 3 hours at RT on a foam rack fixed to a rotator, with rotation speed of 10-20 rpm. Then, SORB capsules were left upright on the rack for 5-6 minutes to allow the gel to settle down. After removal of top screw caps and breaking of the bottom stopper, the SORB capsules were placed on glass tubes and immediately centrifuged at 1200 rpm for 1 minute to washout the samples. After two washes with 500 µl of washing buffer the SORB capsules were transferred to borosilicate glass tubes. Immobilised $1,25(OH)_2D_3$ was eluted by adding 150 µl elution buffer into the SORB capsules followed by centrifugation at 1200 rpm for 1 min. The elution step was repeated 2 more times. The eluate containing the purified active $1,25(OH)_2D_3$ was evaporated by passing nitrogen gas through the glass tubes placed in a water bath at 30^0C. After complete evaporation, the samples were dissolved in 100 µl of assay buffer. For the quantification assay, 100 µl of standard calibrated solutions were transferred to glass tubes. Immunopurified samples and standards were incubated with 200 µl sheep anti-$1,25(OH)_2D_3$ antibody for 16-18 hours at 4^0C. For non-specific binding (NSB) determination, 300 µl of assay buffer were incubated in parallel without antibody. After overnight incubation, 200 µl of radioactive ^{125}I-$1,25(OH)_2D_3$ were pipetted to all the tubes including 2 additional tubes as total counts. Samples were incubated for 1 hour at RT. Then, 100 µl of Sac-Cel (cellulose suspended in buffer with 0.09% sodium azide) containing anti-sheep IgG coupled to cellulose were added to all the tubes except total counts, vortex shortly and incubated for 30 minutes at RT. Later, 4 ml of washing solution were added to all the tubes (except total counts) and centrifuged at 2400 rpm for 20 minutes. After complete removal of the supernatants the radioactivity in all the tubes was measured in a gamma counter. The bound radioactivity present in samples is inversely proportional to the concentration of active $1,25(OH)_2D_3$.

The percentage of binding (B/Bo %) was calculated for all samples, calibrators and controls. The standard curve was calculated by plotting the B/Bo % against the standard concentrations. The concentrations of $1,25(OH)_2D_3$ in plasma were obtained from the slope value of the standard graph.

5.5 Determination of cations in urine by ion chromatography

We analyzed the concentration of sodium (Na^+), potassium (K^+) and magnesium (Mg^{2+}) in the urinary samples using ion exchange chromatography (Metrohm ion chromatography, Herisau, Switzerland). In order to remove any sediment in urine, samples were centrifuged at 10, 000 rpm for 7 minutes. Centrifuged urine samples were diluted 1:300 in nitric acid (HNO_3; 1.7 mM). All the dilutions were made in screw cap vials (allTech, Switzerland). Cations in each sample was separated through cation exchanger column (Metrosep C4 150, Metrohm) with flow rate of 0.9-2.0 ml/minute and pressure of 15.0 MPa (150 bar). Samples were eluted from the column by passing a elution buffer containing a mix of HNO3 (1.7 mM) and dipicolinic acid (0.7 mM). For each cation, three different standard concentrations were prepared (Table 4) in 1.7 mM HNO_3.

Sodium (Na^+) (mM)	Potassium (K^+) (mM)	Magnesium (Mg^{2+}) (mM)
4.34	0.51	0.82
1.08	0.12	0.20
0.27	0.03	0.05

Table 4 standard concentrations of each cation

After analysis by ion chromatography system, each peak in the graph represents the concentration of the corresponding cation. The concentration of ions was estimated by calculating the area of each peak. The surface area of each peak was calculated by the software connected to the ion chromatography system and quantified against standard concentrations of each ion.

5.6 Total RNA isolation from kidneys

Frozen kidney (¼) tissue was homogenized with the help of a glas-teflon potter (B.Braun, Melsungen AG, Germany) in 1ml RLT buffer™ (Qiagen, Germany) containing 1% β-mercaptoethanol (Sigma, USA). The total RNA was isolated from 200 µl of homogenized sample according to the manufacturer's protocol (RNAeasy Mini extraction kit from Qiagen,

Germany). Total RNA was eluted with 30 µl of nuclease free water. The concentration of total RNA (ng/µl) was determined by using the Nanodrop® ND-1000 system (ND-1000 version 3.7.1, Thermo Fisher Scientific Inc.). Quality was determined based on the ratio between 260 nm/280 nm.

5.7 Semi-quantitative real time RT-PCR (qPCR)

Prior to performing qPCR, purified total RNA (300 ng) was transcribed to cDNA using random hexamer primers and multi reverse transcriptase enzyme provided with TaqMan® Reverse Transcription Kit (Applied Biosystems). Reverse transcription was performed using the thermo cycler (Robocycler 40) with the following reaction conditions: 25°C for10 min / 48°C for 30 min / 95°C for 5min/ holding at 4°C. The generated cDNA was used as template for PCR. qPCR was performed in a 96-well plate (Applied Biosystems) using TaqMan® Universal master mix containing AmpliTaq Gold® DNA polymerase and dNTPs (Applied Biosystems, USA). Gene expression of NaPi-IIc was analysed with a set of primers (forward and reverse) and probe that anneal to the sequence of the mRNA that should be missing upon removal of the floxed-fragment. The forward primer anneal to exon 8, whereas both the reverse primer and the probe anneal to exon 9. The primers and probes for NaPi-IIc, Cyp24a1 and HPRT (hypoxanthine-guanine phosphoribosyltransferease) were designed using primer-3 software and reference DNA sequence was taken from the mouse genome database (Ensembl). The probes were labelled at the 5` end with a reporter dye (FAM) and at the 3` end with a quencher dye (TAMRA) (Microsynth, Switzerland). The expression of 1α-hydroxylase/Cyp27b1 was quantified using commercial primers and probes (Taqman Gene Expression Assays). The qPCR was performed using the 7500 Fast Real Time PCR System (Applied Biosystems) with the following reaction conditions; 50^0C for 2 min, 95^0C for 10 min and 40 cycles of 95^0C for 15 seconds/ 60^0C for 1 min. The amplification curve was analysed using 7500 Fast Real-Time PCR System Sequence Detection Software v1.4 (Applied Biosystems, USA). The expression of the gene of interest was normalized to the expression of HPRT as housekeeping gene. The relative fold change (R) was calculated according to formula $2^{(Ct\ (HPRT)-Ct\ (gene\ of\ interest))}$ where Ct indicates the cycle number at which the threshold of 0.75 was achieved.

Gene	Forward (FW) and reverse (RV) primers and oligonucleotide (Probe)
Slc34a3	FW: 5` - CAACGGTATTACCAGCAACA - 3` RV: 5` - CTGTCCTCCTCTGGAGATGC – 3` Probe: 5` - GTGGCCTCTTCAGCTCTTGCACAGA - 3`
CYP27b1	Mm01165921_g1 – FAM
CYP24a1	FW: 5` - CCAGCGGCTAGAGATCAAAC - 3` RV: 5` - CACGGGCTTCATGAGTTTCT - 3` Probe: 5` - TACGGGCTGATGATCCTGGAAGGA - 3`
HPRT	FW: 5` - TTATCAGACTGAAGAGCTACTGTAATGATC - 3` RV: 5` - TTACCAGTGTCAATTATATCTTCAACAATC - 3` Probe: 5` - TGAGAGATCATCTCCACCAATAACTTTTATGTCCC - 3`

Table 5 List of primer and probes used for Semi-quantitative real time RT-PCR

5.8 Isolation of brush border membrane vesicles (BBMVs) from kidney

BBMVs were isolated from frozen kidneys according to a previously described method [200]. In brief, for each membrane preparation one and a half kidneys were placed in 12 ml silicon tubes and homogenized in homogenization buffer (2 ml) containing mannitol (300mM), EGTA (5mM), Tris (12mM), pH 7.1 adjusted with HCl. Homogenization was performed using a polytron homogenizer (model PT 10/35, KINEMATICA GmbH, Switzerland) at setting 5 (15000 rpm) for 2 min on ice. After homogenization, ice-cold distilled water (2.8 ml) was added to the tube and vortex shortly. An aliquot (approximately 200µl) of homogenate was frozen for further analysis. Then, 58 µl of 1M $MgCl_2$ were added to the rest of the homogenate and the sample was incubated for 20 min on ice. Upon transfer into 2 ml eppendorf tubes, samples were centrifuged in a SS34 rotor at 4,500 rpm (3000 g_{av}) for 15 minutes at 4^0C. Supernatants were collected in fresh tubes and subsequently centrifuged in the same rotor at 16,000 rpm (30,000g_{av}) for 30 minutes at 4^0C. The pellet was resuspended in membrane buffer (2 ml) containing mannitol (300mM), Hepes (20mM), Tris (12mM), pH 7.4 adjusted with HCl. The resuspension was done by using a syringe equipped with a 22G needle. A final centrifugation was performed at 16,000 rpm (30,000g_{av}) for 30 minutes at 4^0C. The pellet was resuspended again in membrane buffer (300µl) using a syringe equipped with a 25G needle. To inhibit proteases both buffers were mixed with protease inhibitor

cocktail tablets (Complete Mini EDTA free, Roche). The final resuspended pellet is enriched in BBMVs.

5.9 Isolation of brush border membrane vesicles (BBMVs) from intestinal mucosa

Intestinal BBMVs were isolated according to a previously described method from frozen ileum mucosa [200]. In brief, the mucosa was homogenized in the homogenization buffer (200 µl) described above. Homogenization was performed in a micro attached chamber connected to the Omnimixer (model 17106, DIGITANA AG, Horgen, Switzerland) at speed 5 (15000 rpm) for 2 min on ice. Immediately after homogenation 1 ml of ice-cold distilled water and 11 µl of 1M $MgCl_2$ were added. Samples were incubated for 30 min on ice and up on transfer to 2 ml eppendorf tubes centrifuged in a SS34 rotor at 4,500 rpm (3000 g_{av}) for 15 minutes. Supernatants were collected in fresh tubes and centrifuged at 18,500 rpm (32,500g_{av}) for 30 minutes at 4^0C. Pellets were resuspended in the same membrane buffer (100 µl) described above using a syringe equipped with a 22G needle. The pellet is enriched with BBMVs.

5.10 Uptakes of [^{32}P]-HPO_4 and [^{3}H]-D-Glucose into renal BBMVs

Uptake of [^{32}P] $H_2PO_4^-$ into BBMV was performed according to the filtration technique as described [201]. Uptakes were performed in triplicates using three different conditions: in the presence of Na^+ (buffer A), in presence of Na^+ and phosphonoformic acid (PFA) (buffer B) and with Na^+ replaced by K^+ (buffer C). All the buffers contained 0.1 mM KH_2PO_4 and radioactive ^{32}P (NEX011010MC, PerkinElmer, USA) as tracer. The full composition of each buffer is indicated in the Table 4. The uptakes were initiated by mixing 10 µl of BBMV with 40 µl of each buffer. After 1 minute incubation at 25^0C, 20 µl of the reaction mix was transferred to 1 ml of ice-cold stop solution. Samples were vortexed shortly and immediately filtered through nitrocellulose filters (pore size 0.45 µm) that have been prewashed with stop solution. Filtration was performed through a vacuum filtration setup (vacuum pump, vacuum flask and filter support). After filtration, filters were washed with 5 ml ice-cold stop

solution and transferred to scintillation vials. To determine the blank-value, 10 µl of each cocktail buffer were pipetted into 1 ml of cold-stop solution, filtered, washed and placed in vials. In order to calculate the specific activity, 2.5 µl of each of the three uptake buffers were transferred into scintillation vial directly without filtration. Finally, 3 ml of scintillation fluid (Emulsifier-Safe, Perkline Elmer, USA) were added to all the scintillation vials and the radioactivity was measured in a β-counter (Packard Tri-Carb 2900TR).

Buffer A: Mannitol – 300 mM, Hepes – 20 mM, Sodium chloride - 125 mM, KH_2PO_4 - 0.1 mM; adjust to pH 7.4 with Tris.
Buffer B: Mannitol – 300 mM, Hepes – 20 mM, Sodium chloride - 125 mM, PFA – 7.5 mM, KH_2PO_4 - 0.1 mM; adjust to pH 7.4 with Tris.
Buffer C: Mannitol – 300 mM, Hepes – 20 mM, Potassium chloride - 125 mM, PFA – 7.5 mM, KH_2PO_4 - 0.1 mM; adjust to pH 7.4 with Tris.
Stop solution: Mannitol – 100 mM, Sodium chloride - 150 mM, Tris – 5 mM KH_2PO_4 - 5 mM; adjust to pH 7.4 with HCl.

Table 6 Composition of buffers used for phosphate (^{32}P) uptake studies.

The uptake of ^{32}P detected in the presence of Na^+ reflects the total Pi uptake, i.e transport mediated by Na^+-dependent and independent transporters. The Na^+-dependent uptake was calculated by subtracting the values obtained in the absence of Na^+ (Na^+-independent) from those in the presence of Na^+ (total uptake). The SLC34-mediated component of the Na^+-dependent uptake was calculated by subtracting the values measured in the presence of Na^+ plus PFA from those obtained in the presence of Na^+ without the inhibitor, whereas the SLC34-independent component was calculated by subtracting the values in the absence of Na^+ from those obtained in the presence of Na^+ plus PFA.

To determine the uptake of [^{3}H]-D-Glucose BBMVs were incubated for 20 seconds in two different buffers: in the presence of Na^+ (buffer A) or with Na^+ replaced by K^+ (buffer B). The full composition of each buffer is shown in Table 5. Buffer A and B contain 0.1 mM D-glucose and radioactive [^{3}H]-D-Glucose as tracer. The filtration procedure was performed similar to the one described for ^{32}P uptakes. As for the ^{32}P uptakes, blanks and total counts were also

prepared. Blanks and vials for determination of specific activity were processed as indicated for ^{32}P uptakes.

Buffer A: Mannitol – 300 mM, Hepes – 20 mM, Sodium chloride - 125 mM, D-glucose - 0.1 mM; adjust to pH 7.4 with Tris.
Buffer B: Mannitol – 300 mM, Hepes – 20 mM, Potassium chloride - 125 mM, PFA – 7.5 mM, D-glucose - 0.1 mM; adjust to pH 7.4 with Tris.
Stop solution: Mannitol – 100 mM, Sodium chloride - 150 mM, Tris – 5 mM D-glucose - 5 mM; adjust to pH 7.4 with HCl.

Table 7 Composition of buffers used for glucose (^{3}H –D-Glucose) uptake studies

To calculate the transport activity of the BBMVs, we need to know the specific activity of the radioactive substrate, the amount of protein and how much radioactive ^{32}P or ^{3}H was incorporated on the filters. Therefore, the specific activity (cpm/picomoles) was calculated dividing the total counts present in 1 µl of buffer by the amount of cold phosphate contained in 1 µl of buffer. The blank values indicate the amount of radioactive ^{32}P or ^{3}H bound to the nitrocellulose filters in the absence of BBMVs. To determine the correct counts, the blank counts were subtracted from all samples. Final calculation was made by dividing the corrected counts at a given time by the specific activity and the amount of protein. The uptakes are given as picomoles/mg/minute.

5.11 Determination of protein concentration

The concentration of protein in homogenates and isolated BBMV`s was quantified with the Bio-Rad protein assay (Bio-Rad Laboratories, USA) in 96-well plate using bovine serum albumin (BSA) as a standard. In brief, BBMV and homogenate samples were diluted in distilled water (1:5 and 1:10 respectively). Diluted samples and standards were pipetted (5 µl) into a 96-well plate as triplicates. Then, 25 µl of reagent A and 200 µl of reagent B were added in to all the wells. Upon incubation at RT for 15 minutes the absorbance was detected in a spectrophotometer at wavelength of 595 nm. The standard curve was calculated by plotting the absorbance of the standards against the standard concentrations (2, 1, 0.5 and

0.25 mg/ml). The protein concentration in renal homogenates and BBMVs was calculated from the slope of the standard curve.

5.12 Westernblot analysis

Homogenate (40 µg) or BBMV samples (15 µg) were solubilized in Laemmli buffer containing dithiothreitol (DTT, Sigma) and boiled (95^0C) for 2 minutes. The protein samples were loaded and separated on 9% polyacrylamide gel (Tris-HCl at pH 7.4, 0.2% SDS, tetramethylethylenediamine (TEMED) with ammonium persulfate and running buffer: dissolved Tris - 3 g, glycine – 14.4 g, 20% SDS – 5 ml; adjust to 1000 ml of milliQ water). After electrophoresis, the proteins were transferred (Transfer buffer: dissolved Tris - 3 g, glycine – 14.4 g, methanol – 200 ml; adjust to 1000 ml with milliQ water) to polyvinylidene fluoride (PVDF) membranes (Immobilon-P, Millipore, Bedford, MA). After transfer, non-specific antibody binding was blocked by incubating the membranes for 30 minutes with 5% milk powder (Rapilait, Migros, Switzerland) in Tris-buffered saline (TBS) containing 0.1% Tween-20. Membrane blots were then incubated overnight at 4^0C with the following primary antibodies: rabbit affinity-purified anti-NaPi-IIc (1:3000) raised against C-terminal amino acids 588–601 (NH2–CYENPQVIASQQL–COOH; Pineda Antibody services, Berlin, Germany) [68], rabbit polyclonal anti-NaPi-IIa (1:3000) [55], rabbit polyclonal anti NaPi-IIb (1:5000) [6] and mouse monoclonal anti-β-actin (1:12,000; Sigma). After overnight incubation, membranes were washed three times with TBS and blocked for 30 min at RT. Upon three washes with TBS, membranes were incubated for 2 hours at RT with goat anti-rabbit or donkey anti-mouse (1:10,000) secondary antibodies conjugated with horseradish peroxidase (HRP) (GE Healthcare, UK). After 3 times washes for each 10 minutes, secondary antibodies were detected with a chemiluminescent HRP substrate (Millipore). The chemilumenscence signal was detected with a LAS-4000 Fujifilm image analyzer. The signal intensities were quantified using Advanced Image Data Analyzer software (Ray test) and were normalized to β-actin.

5.13 Immunohistochemistry

Mice were anesthetised with isoflurane and perfused-fixed via the left ventricle. The perfusion solution contained 0.9% NaCl, heparin (5000 U/ml), 1% procain-HCl, 3.2% $CaCl_2$. Fixative consisted of freshly prepared 10 ml tissue fixation solution containing 3% paraformaldehyde in 0.1 M sodium-cacodylate. After perfusion with the fixative, kidneys were removed and incubated in the same fixative solution for 1 hour at 4^{o} C followed by the incubation in 1% PFA in 0.1 M sodium-cacodylate for an additional hour. Kidneys were washed 3 times in cold PBS for 5 minutes of each wash, cut in 2 pieces and stored overnight at 4^{0}C in PBS containing 30% sucrose. In the morning kidneys were quickly washed by immersion in cold PBS. The fixed kidneys were embedded with medium O.C.T (Optimal cutting temperature; Miles, Elkart) in issue-tek® cryomolds (Sakura Finetek, CA, USA) and immediately frozen in liquid propane cooled with liquid nitrogen. Samples were stored at -80^{0}C. Consecutive tissue sections (5 µm) were prepared on a cryomicrotome at -20^{o} C and mounted on chromalum/gelatin coated glass slides and kept in cold PBS until they were used for immunostaining.

For immunofluorescence analysis, serial sections were pretreated with blocking solution (1% BSA with 0.02% sodium azide in PBS) for 15 minutes at RT. Immediately after blocking, sections were incubated overnight at 4^{o}C with either affinity purified anti rabbit NaPi-IIc antibody diluted 1:500 or with anti-rabbit NaPi-IIa antibody diluted 1:1000. Primary antibodies were diluted in PBS with 0.02% sodium azide. After overnight incubation, the sections were immersed twice (5 min each time) in hypertonic PBS (18 g sodium chloride in PBS) followed by a single wash in PBS. All the tissue sections were incubated with secondary antibodies for 1 hour at RT. Secondary antibodies (donkey- anti rabbit IgG 1:1000; Invitrogen) were conjugated with Alexa Fluor 594. FITC phalloidin (1:200; Life technologies) and diamino-2-phenylindole (DAPI; 1:1000; Sigma, St Louis, MO) were added together with secondary antibody. Finally, the sections were washed similarly to the step after incubation with primary antibody and mounted in coverslips using mounting medium DaKO-glycergel (DaKO, USA).

All the tissue sections were visualized and images were acquired with a fluorescence microscope (Leica DM 6000, Leica, Wetzlar, Germany) connected with a charged-coupled

device camera (Leica DFC490). Microscopic images with 40X magnification and overlays were processed by Adobe Photoshop.

5.14 Statistical analysis

All statistical analysis was done by using GraphPad Prism 6.0 (GraphPhad Software, USA). All the results from urine or plasma determinations and mRNA expression data were expressed as ±SEM and significance was calculated by one-way ANOVA. The quantified westernblots signal intensities were analysed by unpaired t-test. A P value of < 0.05 was considered as significant. Significance indicated as $*P < 0.05$, $**P < 0.01$ and $***P < 0.001$.

6 Results

6.1 Renal specific and inducible deletion of the NaPi-IIc gene

To generate renal specific and inducible NaPi-IIc/Slc34a3 knockout (KO) mice, we first generated a conditional Slc34a3 allele that was produced by the insertion of loxP sites within introns 3 and 12 of the Slc34a3 gene. To achieve this, the Slc34a3 targeting vector (shown in Figure 9A) replaced the corresponding genomic sequence by homologous recombination in embryonic stem cells (ESC). To confirm the homologous recombination, DNA was isolated from the ESC clones selected based on their neomycin/gancyclovir resistance and digested with *Kpn1* and *EcoR1*. Southern blots were performed with digested DNA samples by hybridization with ^{32}P labeled probes (Figure 9B). In addition, PCR was performed to confirm the presence of loxP sites on the same DNA samples (Figure 9B). Positive embryonic cells were injected into blastocysts and these were implanted in pseudopregnent female mice.

The generated floxed mice were then bred with 64FlpB6 mice in order to delete the neo-cassette from the floxed allele. Neo negative mice harboring both NaPi-IIc alleles flanked by loxP sites were further bred with double transgenic Pax8rtTA-LC1 mice [199]. In this model, the Pax8 promoter controls the expression of the reverse tetracycline-dependent transactivator (rtTA). In the presence of doxycycline (Doxy) as a cofactor rtTA recognizes and activates the tetracycline responsive element (TRE) which is a bidirectional P_{tet} promoter. The activated TRE then induces the expression of luciferase (L) and Cre-recombinase (C). NZL-2 mice contain as reporters the luciferase and β-galactosidase genes. It has been shown earlier that the administration of Doxy to Pax8rtTA/NZL-2 mice leads to expression of β-galactosidase in all renal tubular cells and in a small population of hepatocytes [199]. Therefore, a similar restricted expression of Cre-recombinase was expected in our renal specific Pax8rtTA/LC1 inducible model. A potential expression of Cre in the liver should not be problematic as NaPi-IIc mRNA expression in this organ is very low. Further cross-breeding generated wild type (NaPi-IIc$^{+/+}$), conditional heterozygous (NaPi-IIc$^{f/+}$) and conditional homozygous mice (NaPi-IIc$^{f/f}$) which contain both Pax8rtTA and Cre (Figure 9C).

Genotyping was done by using genomic DNA isolated from ear biopsies as template. To analyse the presence or absence of the loxP sites in the NaPi-IIc alleles, a sense primer that

anneals within the exon 3 and antisense primer that anneals on the exon 4 of NaPi-IIc gene were used. The expected size of the amplified DNA fragments is 710 base pairs (bp) for homozygous NaPi-IIc$^{fl/fl}$ and 615 bp for wild type NaPi-IIc$^{+/+}$ whereas heterozygous NaPi-IIc$^{fl/+}$ mice should show both 615+720 bp amplicons (Figure 9C). To detect the presence of the Pax8rtTA and Cre elements the specific primers described in the original manuscript were used to amplify DNA. The expected sizes of amplified fragments for Cre and Pax8 are around 400 bp (data not shown).

The expression of Cre was induced in both genders and 3 genotypes by administrating Doxy in the drinking water. Induction was initiated immediately after weaning as the expression of NaPi-IIc is highest after weaning and decreases with age [7]. The Doxy induced activation of Cre should result in the removal of the NaPi-IIc sequence flanked by loxP sites. Upon removal of the loxP flanked sequence the truncated mRNA would consist of only exon 1-3 and exon 13 (Figure 9D). This truncated mRNA only encodes for the first 57 amino acids of NaPi-IIc which constitute the intracellular N-terminal region (Figure 9D).

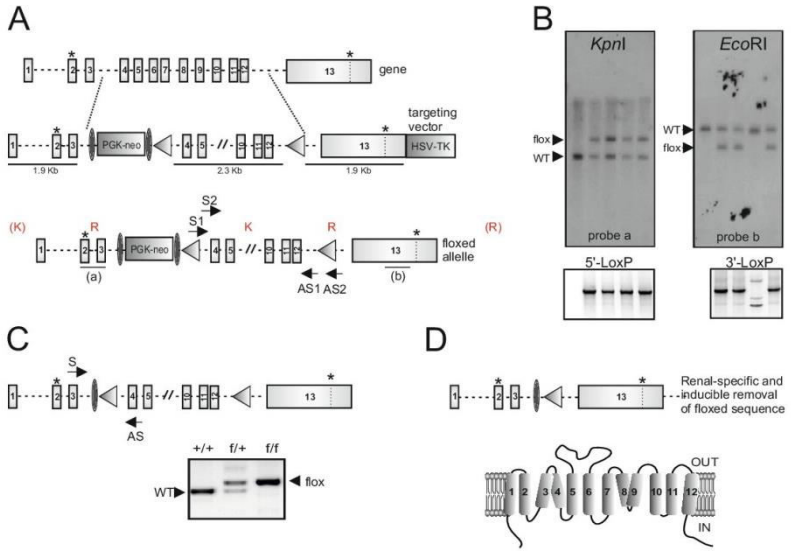

Figure 9 Establishment of a renal-specific and inducible NaPi-IIc deficient mice. Generation of floxed Slc34a3 allele and introduction into embryonic stem cells (ESC) was done by gene-targeting methods. **A**) Structure of the Slc34a3 gene (top), targeting vector (middle) and floxed allele (bottom). The gene consists of 13 exons (E), with the codon for the starting methionine (*) in exon 2 and the stop codon (*) at the end of exon 13. We constructed a conditional Slc34a3 by introducing the loxP sites (shaded triangles) within introns 4 and 13. In addition, a neomycin cassette (PGK-neo) flanked by FRT sites (black ellipses) was inserted upstream of the 5` loxP site and the herpes simplex virus thymidine kinase (HSV-TK) was inserted at the 3` end of the construct. The vector was transfected into ESC. Lines at the bottom of floxed allele (a, b) indicate the position of the probes used for Southern blot, whereas the location of the *Kpn*I (K) and *EcoR*I sites (R) are indicated at the top. The first *Kpn*I and the last *EcoR*I sites are located outside the *Slc34A3* gene. The presence of LoxP sites

was confirmed by PCR using specific primers indicated with arrows. **B**) To confirm the homologous recombination (5` and 3`) genomic DNA was isolated from 4 positive ESC clones that had survived in the presence of neomycin but not ganciclovir and from untransfected ESC. Upon digestion with KpnI (K) or EcoRI (R) the DNA was analyzed by Southern blot (top). PCR was used to confirm the presence of 5` and 3` loxP sites on the same DNA samples (bottom). **C)** Structure of the conditional allele upon removal of the neo-cassette indicating the location of the primers used to discriminate between wild type ($Slc34a3^{+/+}$), conditional heterozygous ($Slc34a3^{f/+}$) or conditional homozygous mice ($Slc34a3^{f/f}$). Genotyping was done by PCR using genomic DNA isolated from ear biopsies **D)** Structure of the gene upon Doxy-induced removal of the floxed-sequence (top) and proposed NaPi-IIc topology (bottom): only the intracellular N-terminus would be expressed in mutant mice.

6.2 Experimental analysis of mice treated with 2 mg/ml doxycycline

Initially, in order to induce Cre-recombinase and to delete the NaPi-IIc gene in floxed-NaPi-IIc mice, the drinking water was supplemented with 2 mg/ml doxycycline (Doxy) plus 2% sucrose; control animals drank 2% sucrose. The drinking protocol lasted 10 days, after which the following experiments were performed.

6.2.1 Gene expression of NaPi-IIc upon doxycycline induction

To analyze if the Doxy-induced activation of Cre resulted in the depletion of NaPi-IIc at the mRNA level in the kidneys of $NaPi\text{-}IIc^{f/f}$ mice, we performed gene expression analysis by semi-quantitative real-time RT-PCR (qPCR). Males and females of all three genotype were investigated. The expression of NaPi-IIc mRNA was normalised to the expression of a housekeeping gene namely the hypoxanthine-guanine phosphorybosyl transferase (HPRT).

The expression of NaPi-IIc mRNA was almost completely abolished in the kidneys of $NaPi\text{-}IIc^{f/f}$ male mice drinking Doxy as compared with the sucrose controls whereas approximately 50% reduction was observed in the $NaPi\text{-}IIc^{f/+}$ mice (Figure 10A). In contrast the expression of the cotransporter was comparable in $NaPi\text{-}IIc^{+/+}$ animals drinking Doxy and sucrose alone (Figure 10A). The changes in the expression of NaPi-IIc in females were similar to those of males (Figure 10B). The extent of the reduction on mRNA expression indicated that Cre-recombinase was successfully induced by a treatment with 2 mg/ml Doxy and that the activated Cre efficiently depleted NaPi-IIc mRNA from the kidney in both genders.

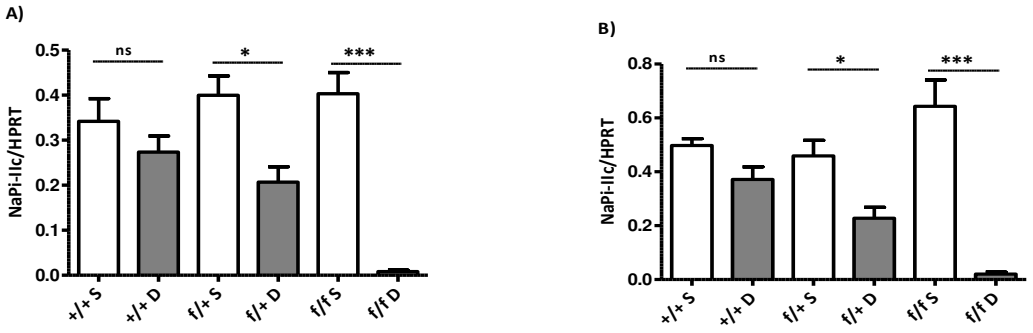

Figure 10 Expression of NaPi-IIc mRNA upon administration of Doxycycline (D) or sucrose (S) to A) males and B) females. Mice received water supplemented either with 2 mg/ml Doxy plus 2% sucrose alone (grey bars) or 2% sucrose (white bars) for 10 days. Kidneys were collected immediately after treatments. Expression of NaPi-IIc mRNA was analyzed in the kidney of NaPi-IIc$^{+/+}$, NaPi-IIc$^{f/+}$ and NaPi-IIc$^{f/f}$ mice (n=6 to 8 per group) and it was corrected by control gene HPRT. The relative expression of NaPi-IIc was calculated and data are presented as mean ± SEM and significance were calculated by ANOVA. *P < 0.05, ***P < 0.001, no significance (ns).

6.2.2 Expression of NaPi-IIc and NaPi-IIa proteins in renal BBM of doxycycline/sucrose treated mice

To investigate if the Doxy treatment also induced the depletion of NaPi-IIc at the protein level, we analysed the expression of NaPi-IIc in renal BBM. The westernblot analysis shows that the expression of the cotransporter was comparable in Doxy and sucrose treated NaPi-IIc$^{+/+}$ male mice (Figure 11A). In contrast, NaPi-IIc was heavily reduced in kidneys from NaPi-IIc$^{f/f}$ male mice treated with Doxy compared to sucrose controls (Figure 11B). The induction with Doxy did not affect the expression of NaPi-IIa in either NaPi-IIc$^{+/+}$ or NaPi-IIc$^{f/f}$ mice as similar amounts were observed in the Doxy and corresponding sucrose controls (Figure 11, A and B). Similar results were observed in females regarding both the expression of NaPi-IIc and NaPi-IIa (data not shown). In all cases actin was used as reference protein and its expression was similar in the Doxy and sucrose groups. Together these results suggested that the Doxy induction effectively downregulated the expression of NaPi-IIc protein by reducing the mRNA expression in the kidney of both male and female mice.

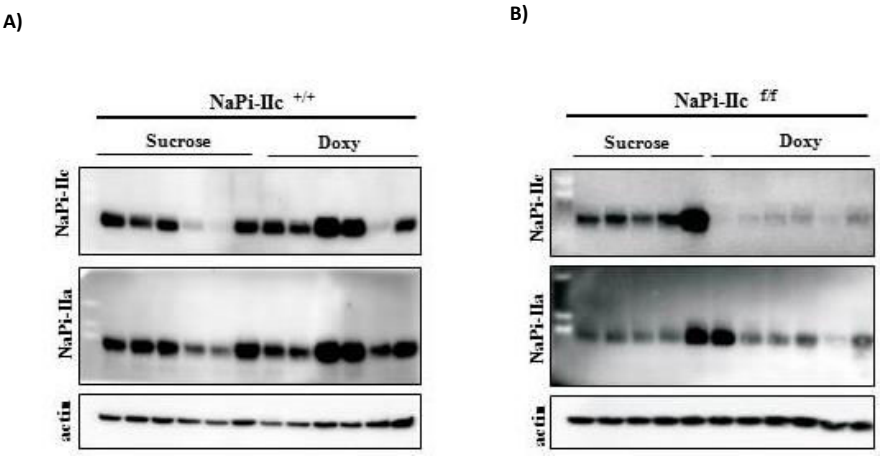

Figure 11 Westernblot analysis of NaPi-IIc and NaPi-IIa in brush border membrane (BBM). BBM were isolated from kidneys of A) male NaPi-IIc$^{+/+}$ mice and B) male NaPi-IIc$^{f/f}$ mice after treatment with either 2 mg/ml Doxy plus 2% sucrose or 2% sucrose alone for 10 days. The expression of actin was used as a control (n=5 to 6 per group).

6.2.3 Urinary excretion of Pi in doxycycline/sucrose treated mice

To investigate if NaPi-IIc deficiency affects the handling of Pi by the kidney, we analysed the concentration of Pi and creatinine in the urine. Surprisingly, Doxy treatment increased the urinary excretion of Pi in wild type males, as we observed significant increased Pi excretion in NaPi-IIc$^{+/+}$ Doxy (+/+ D) compared to NaPi-IIc$^{+/+}$ sucrose (+/+ S) treated controls (Figure 12A). Similarly, the excretion of Pi was significantly increased in NaPi-IIc$^{f/f}$ Doxy (f/f D) treated mice compared to their corresponding sucrose (f/f S) control mice (Figure 12A). Similar changes were also observed in female mice (Figure 12B). These results suggest that the administration of 2 mg/ml Doxy for 10 days had a nonspecific effect which is an independent from the activation of Cre-recombinase.

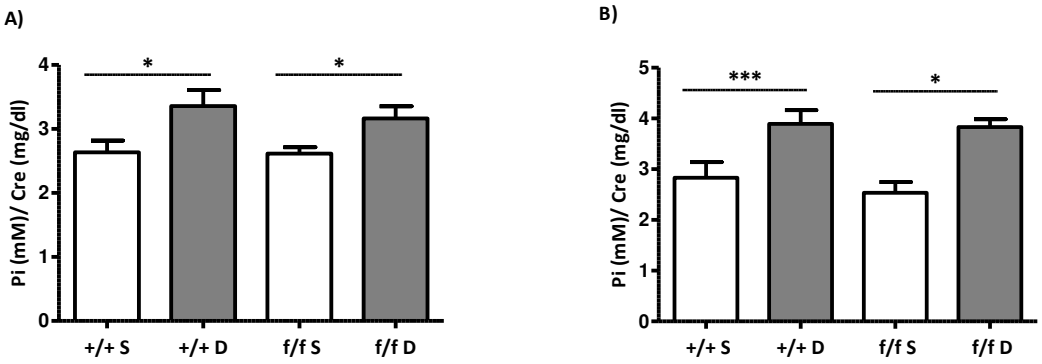

Figure 12 Urinary excretion of Pi in A) males and B) females treated with Doxy (D) or sucrose (S). Mice received water supplemented with either 2 mg/ml Doxy plus 2% sucrose (grey bars) or 2% sucrose alone (white bars) for 10 days. Urinary samples were collected over the last 24 hours of Doxy or sucrose treatment. The concentration of urinary Pi (mM) was

corrected by the creatinine (mg/dl) (n = 6 to 8 mice per group). The data are presented as mean ± SEM and significance were calculated by ANOVA. *P < 0.05, ***P < 0.001.

6.2.4 Urinary excretion of Ca^{2+} in doxycycline/sucrose treated mice

To investigate whether the NaPi-IIc deficiency affects calcium (Ca^{2+}) reabsorption in the kidney, we analysed the concentration of Ca^{2+} in urine. In males, the excretion of Ca^{2+} was significantly increased in NaPi-$IIc^{+/+}$ mice treated with Doxy (+/+ D) compared to their corresponding sucrose (+/+ S) controls (Figure 13A). A similar tendency was also observed in NaPi-$IIc^{f/f}$ Doxy mice (f/f D) compared with sucrose (f/f S) treated controls. In NaPi-$IIc^{f/f}$ and NaPi-$IIc^{+/+}$ females, urinary excretion of Ca^{2+} was increased in Doxy treated mice compared with their control groups (Figure 13B). The increased excretion of Ca^{2+} in all Doxy administered mice indicated again a non-specific effect of Doxy.

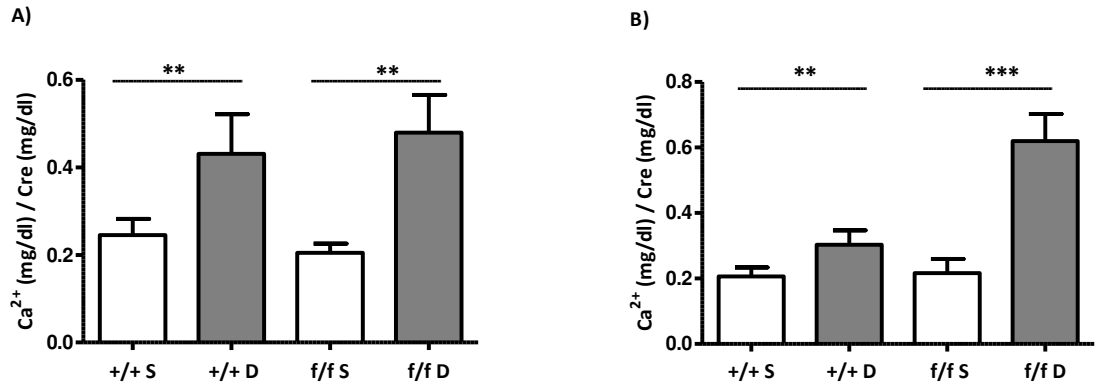

Figure 13 Urinary excretion of Ca^{2+} in A) males and B) females treated with Doxy (D) or sucrose (S). Mice received water supplemented with either 2 mg/ml Doxy plus 2% sucrose (grey bars) or 2% sucrose alone (white bars) for 10 days. The urinary samples were collected over last 24 hours of Doxy or sucrose treatment protocol. The concentration of urinary Ca^{2+} (mM) was corrected by creatinine (mg/dl). The data are presented as mean ± SEM (n = 6 to 8 mice per group) and significances between the groups were calculated by ANOVA. **P < 0.01, ***P < 0.001.

6.2.5 Urinary excretion of Na^+ and K^+ in doxycycline/sucrose treated mice

As shown above, administration of Doxy to both NaPi-$IIc^{+/+}$ and NaPi-$IIc^{f/f}$ mice resulted in increased urinary excretion of Pi and Ca^{2+}. These changes are likely due to non-specific effects of doxycycline. To investigate whether these nonspecific effects of Doxy also impair the excretion of other ions, the urinary excretions of Na^+ and K^+ were also analyzed. The urinary excretion of Na^+ was reduced by approximately 70% in both NaPi-$IIc^{f/f}$ and NaPi-$IIc^{+/+}$

Doxy treated male mice compared with sucrose controls (Figure 13A). Although less, the concentration of K^+ was also reduced significantly in both NaPi-IIc$^{+/+}$ and NaPi-IIc$^{f/f}$ Doxy treated mice (Figure 13B). The changes in Na^+ and K^+ excretions were identical in both males (Figure 14, A and B) and females (data not shown). These data strongly support a nonspecific effect of Doxy although we do not know whether the kidney is the primarily affected organ. Therefore, it was important to optimise the minimal concentration of Doxy and treatment period which can induce Cre-recombinase activity without causing the non-specific effects.

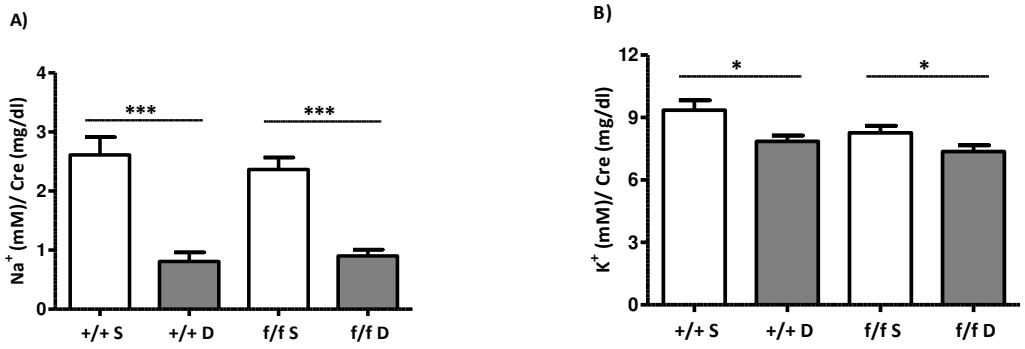

Figure 14 Urinary excretions of A) Na^+ and B) K^+ in male mice treated with Doxy (D) or sucrose (S). Mice received water supplemented with either 2 mg/ml Doxy plus 2% sucrose (grey bars) or 2% sucrose alone (white bars) for 10 days. The urinary samples were collected over the last 24 hours of Doxy or sucrose treatment. The concentration of urinary Na^+ and K^+ (mM) were corrected by creatinine (mg/dl) (n = 6 to 8 mice per group). The data are presented as mean ± SEM and significances between the groups were calculated by ANOVA. *P < 0.05, ***P < 0.001.

6.3 Optimization of doxycycline concentration

In order to find an optimal concentration of Doxy able to induce the knockdown of NaPi-IIc efficiently in the kidney of NaPi-IIc$^{f/f}$ mice without the non-specific effects observed after a treatment with 2mg/ml, we performed a second round of experiments. We administrated water supplemented with different concentrations of Doxy (1, 0.5 and 0.25 mg/ml) plus 2% sucrose or sucrose alone for 10 days to NaPi-IIc$^{f/f}$ and NaPi-IIc$^{+/+}$ male mice. The administration of Doxy was followed by a recovery phase of 15 days during which mice received normal tap water.

6.3.1 Gene expression of NaPi-IIc and urinary excretion of Na^+ in response to several concentrations of doxycycline

We analyzed the expression of NaPi-IIc mRNA in the kidney of NaPi-IIc$^{f/f}$ mice and the concentration of Na^+ in the urine collected from NaPi-IIc$^{+/+}$ mice. The expression of NaPi-IIc mRNA was almost fully depleted in the NaPi-IIc$^{f/f}$ mice that received 1 and 0.5 mg/ml Doxy whereas approximately 25% expression remained in mice receiving 0.25 mg/ml compared with NaPi-IIc$^{f/f}$ mice drinking sucrose (Figure 15A). The urinary excretion of Na^+ was still reduced significantly in the NaPi-IIc$^{+/+}$ mice that received 1 and 0.5 mg/ml Doxy whereas no significant reduction was observed with 0.25 mg/ml (Figure 15B). Together, these data indicated that the protocols with 1 and 0.5 mg/ml Doxy were able to fully deplete NaPi-IIc mRNA expression in NaPi-IIc$^{f/f}$ but still altered the Na^+ excretion in NaPi-IIc$^{+/+}$ mice (Figure 15, A and B). At a concentration of 0.25 mg/ml, Doxy reduced NaPi-IIc mRNA expression only partially in NaPi-IIc$^{f/f}$ mice, whereas it did not lead to any reduction of Na^+ excretion in NaPi-IIc$^{+/+}$ mice. Based on these observations, we setup a final Doxy induction protocol consisting of 5 days administration of 0.5 mg/ml Doxy followed by 5 days with 0.25 mg/ml Doxy. After these 10 days of Doxy administration, mice were left to recover for 15 days drinking normal tap water. The results obtained with this final protocol are described in the next section.

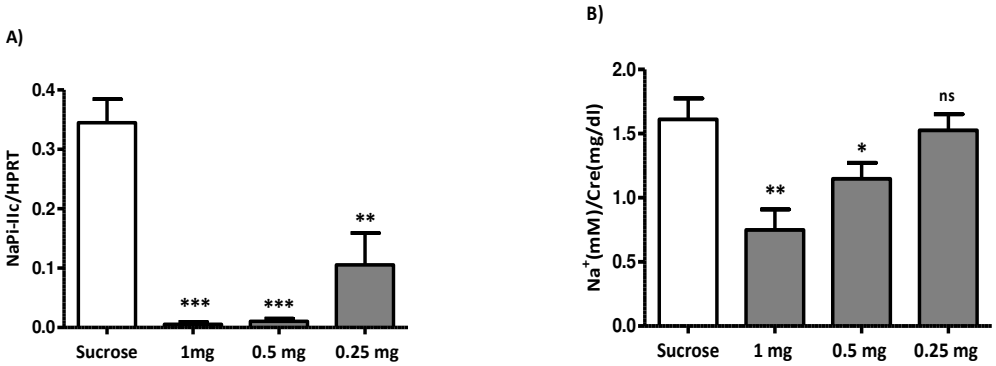

Figure 15 Expression of NaPi-IIc mRNA in the kidneys of NaPi-IIc$^{f/f}$ (A) and urinary excretion Na^+ of NaPi-IIc$^{+/+}$ (B) in response to different dosage of Doxy. Mice received for 10 days either 1, 0.5 and 0.25 mg/ml Doxy in the drinking water supplemented with 2% sucrose (grey bars) or 2% sucrose alone (white bars) followed by 15 days recovery period during which mice received normal drinking water. Urinary samples were collected during the last 24 hours upon which kidneys were harvested. The relative expression of NaPi-IIc was calculated and data are presented as mean ± SEM (n = 6 to 8 per group) and significances between the groups were calculated by ANOVA. *P < 0.05, **P < 0.01, ***P < 0.001, no significance (ns).

6.4 Experimental analysis of mice subjected to the final doxycycline protocol

6.4.1 Urinary excretion of Na^+ and K^+ in doxycycline/sucrose treated mice

In order to test whether the final Doxy protocol affected the urinary excretion of Na^+ and K^+, we measured the concentration of these two cations in urine. In males, the excretion of Na^+ and K^+ were comparable in all the groups of mice (Figure 16, A and B) that received Doxy and their corresponding sucrose controls. Similar results were observed in the female mice (data not shown). This result indicated that the final protocol used for the Doxy treatment did not induce the non-specific effects which we observed with previous protocols.

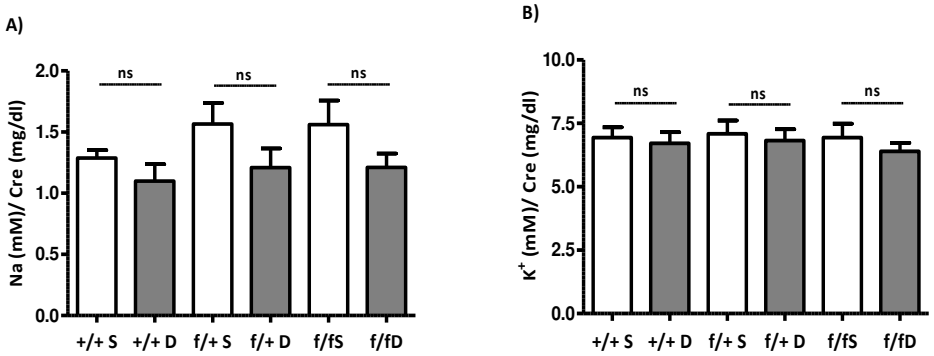

Figure 16 Urinary excretions of A) Na^+ and B) K^+ in male mice treated with Doxy (D) or sucrose (S). Mice received 0.5 + 0.25 mg/ml Doxy in the drinking water supplemented with 2% sucrose (grey bars) or 2% sucrose alone (white bars) for 10 days followed by 15 days recovery period. The concentration of urinary Na^+ and K^+ (mM) were corrected by creatinine (mg/dl). The data are presented as mean ± SEM (n = 6 to 8 mice per group) and statistical significance were calculated by ANOVA. No significant (ns) differences were observed between the groups.

6.4.2 Gene expression of NaPi-IIc upon doxycycline induction

To quantify the depletion of NaPi-IIc at the mRNA level in response to the final protocol of Cre induction, we performed again the gene expression analysis. In males, the expression of NaPi-IIc mRNA was comparable in NaPi-IIc$^{+/+}$ mice drinking Doxy and sucrose. However NaPi-IIc mRNA expression was reduced by 50% in NaPi-IIc$^{f/+}$ and approximately by 90% in NaPi-IIc$^{f/f}$ mice drinking Doxy compared with sucrose treated mice (Figure 17A). In females, NaPi-

IIc mRNA expression was similarly affected as in male mice (Figure 17B). These results suggested that the administration of 0.5 + 0.25 mg/ml Doxy followed by a recovery of 15 days successfully induced the depletion of NaPi-IIc in NaPi-IIc$^{f/f}$ mice without causing non-specific changes such as decreased urinay excretion of sodium ions.

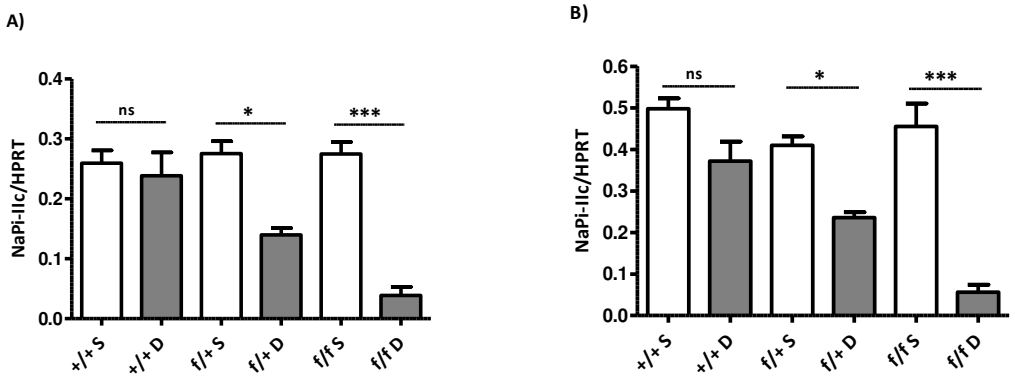

Figure 17 Expression of NaPi-IIc mRNA in kidneys of males (A) and females (B) treated with Doxy or sucrose. Mice received 0.5 + 0.25 mg/ml Doxy in the drinking water supplemented with 2% sucrose (grey bars) or 2% sucrose alone (white bars) for 10 days followed by 15 days recovery period. mRNA expression of NaPi-IIc in NaPi-IIc$^{+/+}$, NaPi-IIc$^{f/+}$ and NaPi-IIc$^{f/f}$ mice was corrected by control gene HPRT. The relative expression of NaPi-IIc was calculated and data are presented as mean ± SEM (n = 8 to 10 per group) and significances between the groups were calculated by ANOVA. *P < 0.05, ***P < 0.001.

6.4.3 Expression of NaPi-IIc in renal brush border membranes and homogenates after doxycycline treatment

To investigate if the final Doxy protocol induced depletion of NaPi-IIc at the protein level, we analysed the expression of NaPi-IIc in renal BBM by westernblots. The abundance of the cotransporter was normalised to the abundance of β-actin. In males, the abundance of NaPi-IIc was similar in NaPi-IIc$^{+/+}$ drinking Doxy and sucrose whereas it was reduced by 50% in NaPi-IIc$^{f/+}$ and by 90% in NaPi-IIc$^{f/f}$ mice treated with Doxy compared with their corresponding sucrose controls (Figure 18, A and B). The Doxy treatment induced similar downregulation of NaPi-IIc in males (Figure 18, A and B) and females (Figure 18, C and D). These changes in the expression of NaPi-IIc at the protein level were paralleled by the changes observed at the mRNA level. All together, the down regulated mRNA and protein expression of type IIc Na/Pi-cotransporter suggested that the Doxy induction effectively depleted the abundance of NaPi-IIc protein in NaPi-IIc$^{f/f}$ and reduced it in NaPi-IIc$^{f/+}$ mice, which was paralleled by changes in mRNA expression.

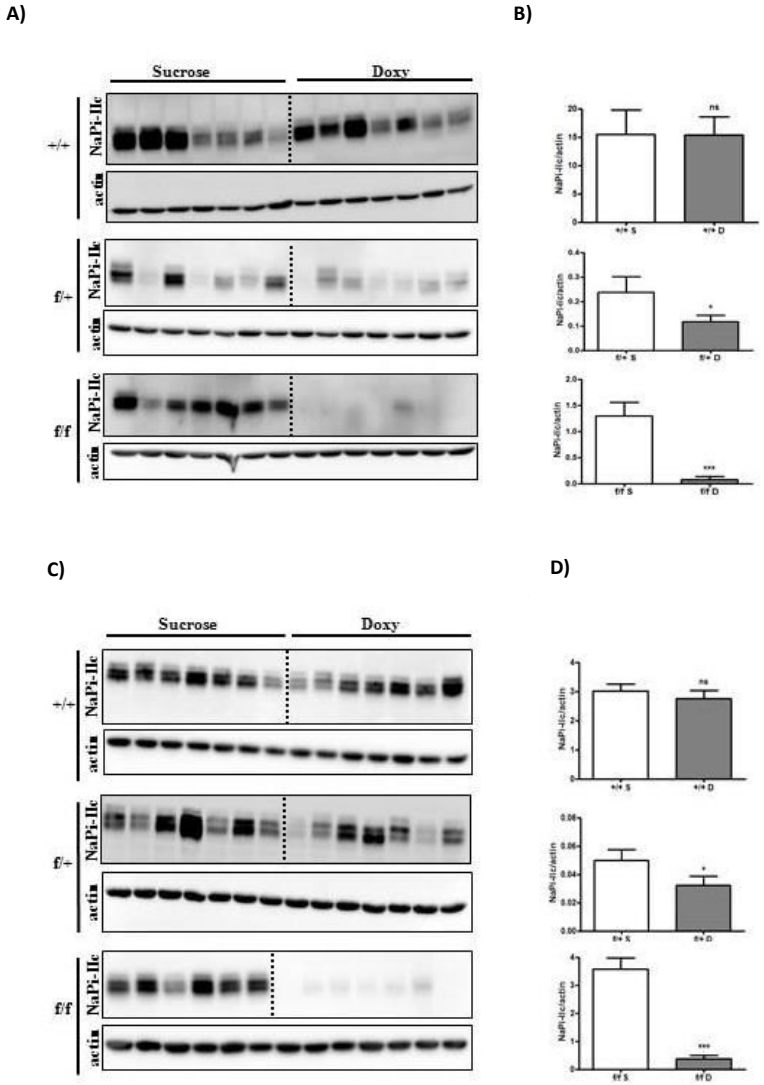

Figure 18 Abundance of NaPi-IIc protein in renal BBM of) males (A,B) and females (C, D) subjected to the final Doxy induction protocol. Quantification of NaPi-IIc expression was corrected by actin. The data are presented as mean ± SEM (n = 6 to 7 per group) and significances between the two groups were calculated by t-test. *P < 0.05, ***P < 0.001, no significance (ns).

In addition to the BBM we also analyzed the expression of NaPi-IIc protein in total homogenates. As expected the abundance of NaPi-IIc protein was similar in all NaPi-IIc$^{+/+}$ (Figure 19A), whereas the cotransporter was almost completely absent in NaPi-IIc$^{f/f}$ mice treated with Doxy (Figure 19B). The downregulated expression of NaPi-IIc in homogenates was similar in males and females (data not shown).

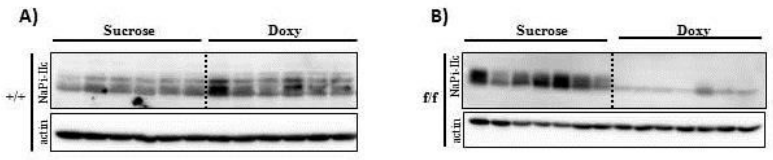

Figure 19 Abundance of NaPi-IIc protein in total renal homogenates of male NaPi-IIc$^{+/+}$ (A) and NaPi-IIc$^{f/f}$ (B) mice subjected to the final Doxy induction protocol. (n = 6 to 7 per group).

6.4.4 Localization of Na/Pi-cotransporters in kidneys upon doxycycline induction

Immunofluroscence staining was performed in kidney sections to observe the expression pattern of renal Na/Pi- cotransporters NaPi-IIa and NaPi-IIc in our renal specific NaPi-IIc deficient mice. The sections were also labeled with phalloidin (green) in order to stain the brush borders. These studies were performed only in NaPi-IIc$^{f/f}$ and NaPi-IIc$^{+/+}$ mice that had drunk water supplemented with Doxy and 2% sucrose. The expression of NaPi-IIc was observed at the BBM of proximal tubules of NaPi-IIc$^{+/+}$ mice and this signal was completely abolished in kidneys obtained from NaPi-IIc$^{f/f}$ mice (Figure 20A). This observation confirmed our previous results of mRNA and protein levels, indicating that the Doxy induced Cre-activation abrogated the expression of NaPi-IIc in NaPi-IIc$^{f/f}$ mice. The expression of NaPi-IIa was abundant in apical membranes of proximal tubules and its expression was similar in both NaPi-IIc$^{f/f}$ and NaPi-IIc$^{+/+}$ mice (Figure 20B).

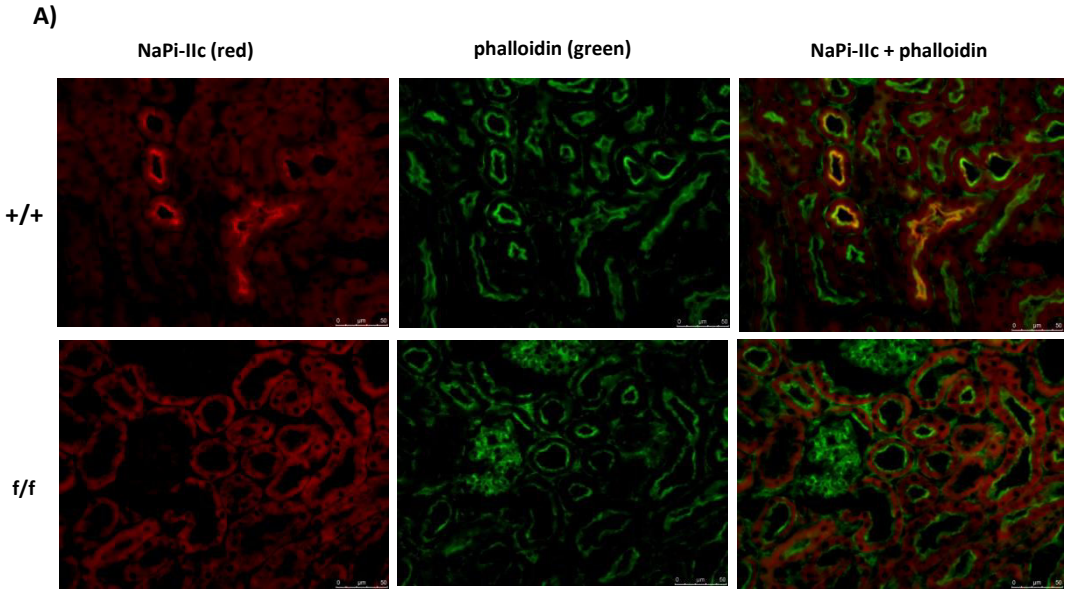

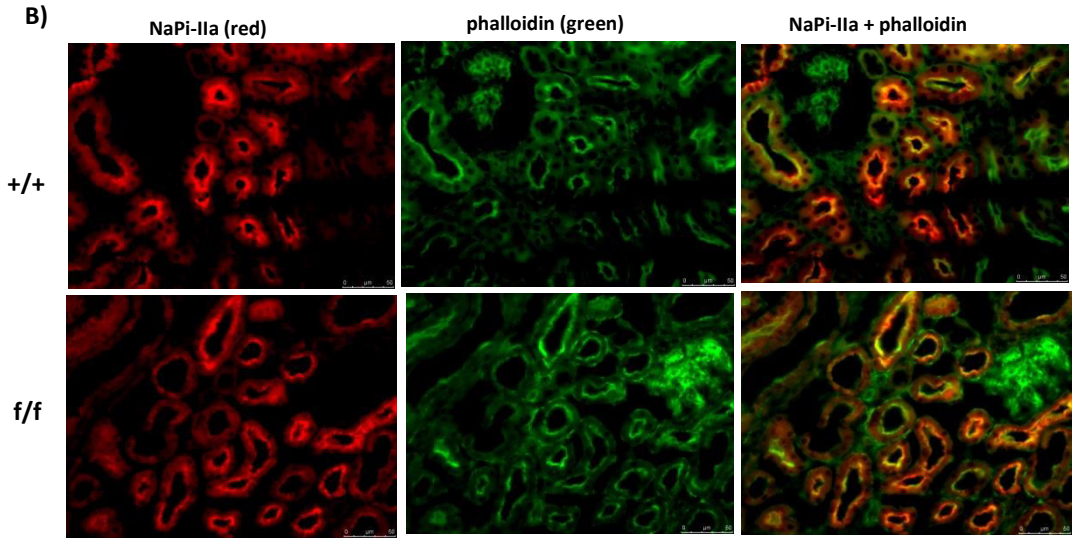

Figure 20 Pattern of expression of NaPi-IIc and NaPi-IIa protein in kidney. Immunostaining of NaPi-IIc (A) and NaPi-IIa (B) on renal cryosections of NaPi-IIc$^{+/+}$ and NaPi-IIc$^{f/f}$ mice treated with 0.5 + 0.25 mg/ml Doxy. The Na/Pi-cotransporters signals were shown in red. The renal sections were stained with phalloidin (green) to indicate the brush borders. The fluorescent signal was detected with a fluorescence microscope (Leica Microsystems) using 40X magnification (50 µm).

6.4.5 Effect of NaPi-IIc depletion on Pi uptake into isolated BBMVs

In kidney, active reabsorption of Pi takes place across the proximal tubule. The reabsorption is mediated by members of the SLC34 (NaPi-IIa and NaPi-IIc) and SLC20 (Pit-2) families of Na^+/Pi cotransporters. These cotransporters are predominantly expressed at the BBM of proximal tubules. To assess the relative contribution of NaPi-IIc to the total Pi transport in the proximal tubule, we performed ^{32}P uptake assay into isolated renal BBMVs from NaPi-IIc$^{+/+}$ and NaPi-IIc$^{f/f}$ males treated with Doxy and sucrose. The uptake of ^{32}P assay was performed under three different conditions: in the presence or absence of Na^+-ions and in the presence of Na^+-ions but with PFA (PFA is an inhibitor of SLC34 but not of SLC20 transporters; [34, 202]). These three conditions allowed us calculate the total ^{32}P uptake as well as the uptakes mediated by Na^+- independent and Na^+ - dependent (mediated by SLC34 and SLC20 transporters) mechanisms. The PFA sensitivity gives us the difference between the SLC34 and SLC20 mediated Pi uptake. The uptake ^3H glucose was also performed in parallel as a negative control. Equilibrium values has been determined (Data not shown) and were similar in all vesicular preparations indicating that same vesicles were prepared from the different mice.

Total and Na^+ dependent ^{32}P uptakes did not show significant differences between BBM`s isolated from NaPi-IIc$^{+/+}$ and NaPi-IIc$^{f/f}$ Doxy-treated mice compared to BBM's isolated from sucrose controls (Figure 21, A and B). Similarly, there were no significant changes in the PFA-sensitive or PFA-insensitive ^{32}P uptake neither between genotypes nor between the Doxy/sucrose groups (Figure 21, C and D). The data suggest that the absence of NaPi-IIc did not change the Na^+-dependent, PFA- sensitive or PFA-insensitive ^{32}P uptake in NaPi-IIc$^{f/f}$ Doxy treated mice. As expected the depletion of NaPi-IIc did not affect the uptake of ^3H-D-glucose that was comparable in NaPi-IIc$^{+/+}$ and NaPi-IIc$^{f/f}$ Doxy or sucrose treated mice (Figure 21E).

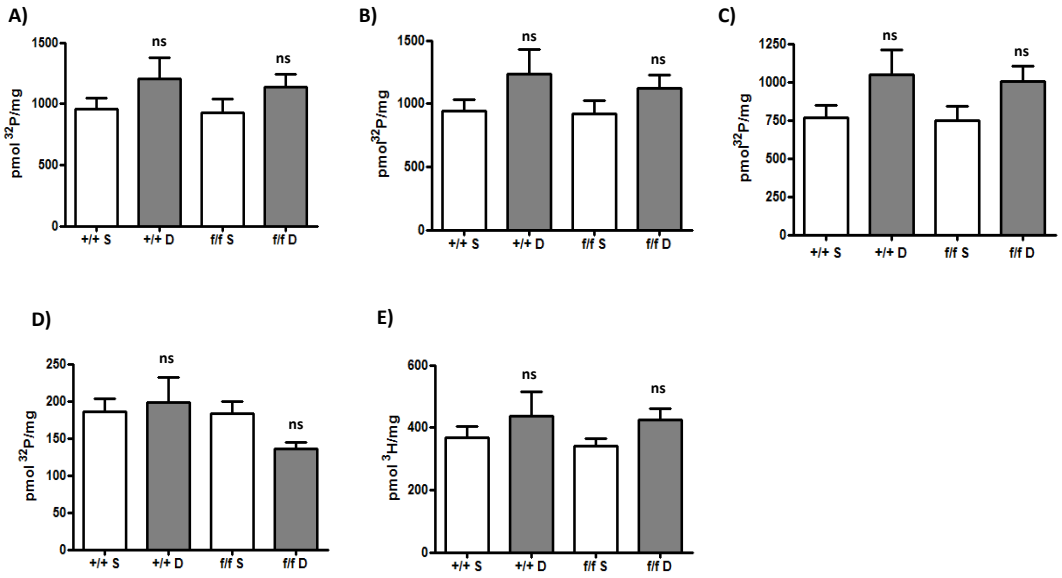

Figure 21 Transport of Pi into renal BBMVs isolated from the kidney of NaPi-IIc$^{+/+}$ and NaPi-IIc$^{f/f}$ mice treated with Doxy or sucrose. A) Total uptake of Pi was measured in the presence and absence of Na^+ B) Na^+-dependent uptake of Pi: represents the transport mediated by SLC34 and SLC20 transporters. C) PFA sensitive uptake of Pi: represents the transport of Pi mediated only by SLC34 transporters D) PFA insensitive uptake of Pi: represents the uptake mediated only by SLC20 transporters. E) Total uptake of D-glucose measured in the presents of Na+ with 3H-D-glucose. The data are presented as mean ± SEM (n = 7 to 8 per group) and statistical significances were calculated by ANOVA. No significant differences (ns) were observed between groups.

6.4.6 Effect of NaPi-IIc depletion on the expression of other Na/Pi-cotransporters

As shown above, the absence of NaPi-IIc did not affect Pi uptake of BBMVs. The transport activity mediated by NaPi-IIa and NaPi-IIc cannot be discriminated by ^{32}P uptake studies since both transporters are inhibited by PFA. The absence NaPi-IIc in the proximal tubular

BBM may lead to compensatory mechanism by increasing the expression of other known Na/Pi-cotransporters which also mediate the active reabsorption of Pi. Therefore, we were interested to analyse the BBM abundance of NaPi-IIa and Pit-2 in the kidney.

The abundance of NaPi-IIa in renal BBM was identical in Doxy and sucrose treated NaPi-IIc$^{+/+}$ mice and similar expression was also found in NaPi-IIc$^{f/f}$ mice (Figure 22A). In addition, the abundance of Pit-2 in NaPi-IIc$^{+/+}$ and NaPi-IIc$^{f/f}$ was also similar in Doxy treated mice compared with the corresponding sucrose treated controls (Figure 22B).

It is known that the intestine may compensate for impaired renal reabsorption of Pi by either increasing or decreasing the expression of NaPi-IIb. Therefore, we also analyzed the expression of NaPi-IIb in the ileum of Doxy/sucrose treated mice. The abundance of NaPi-IIb in intestinal BBM did not show differences between the groups (Figure 22C), similar to the observations on the renal cotransporters. Similar data were obtained in both male (Figure 22A - 22C) and female mice (data not shown). These data suggest that the absence of NaPi-IIc in the kidney did not alter expression of other known Na^+/Pi cotransporters in the kidney and intestine.

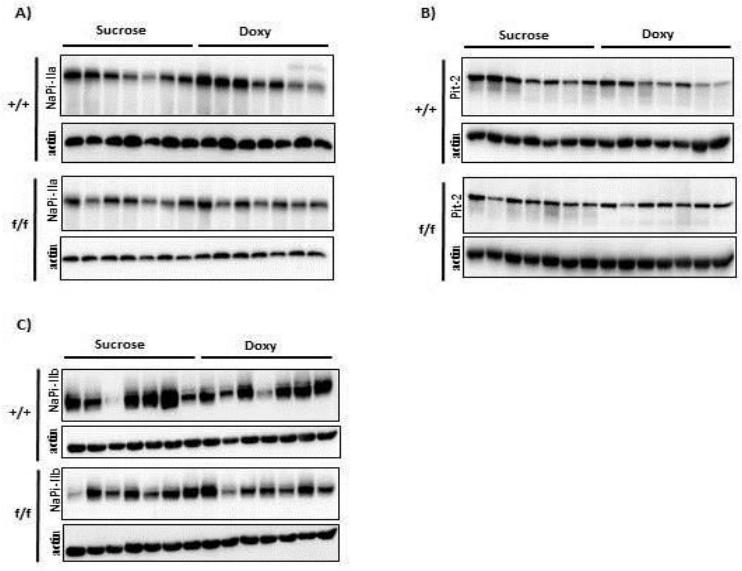

Figure 22 Effect of NaPi-IIc knockdown on the abundance of other Na^+/Pi cotransporters. Expression of A) NaPi-IIa, B) Pit-2 and C) NaPi-IIb in renal (A, B) or intestinal (C) BBM isolated NaPi-IIc$^{+/+}$ and NaPi-IIc$^{f/f}$ mice treated with Doxy or sucrose. Mice received 0.5 + 0.25 mg/ml Doxy or sucrose alone for 10 days followed by 15 days recovery period. All the membrane blots were incubated with β-actin (n = 7 per group).

6.4.7 Effect of NaPi-IIc depletion on plasma and urinary Pi

To analyse potential phenotypic changes upon Doxy induced depletion of NaPi-IIc, we measured the concentration of Pi in the urine and plasma. Urine samples were collected during the last 24 hours and plasma samples were collected after termination of the experimental protocol.

The urinary excretion of Pi did not change significantly in the NaPi-IIc$^{+/+}$ Doxy treated mice compared with their corresponding sucrose controls. Moreover, the excretion Pi was also identical in the NaPi-IIc$^{f/+}$ and NaPi-IIc$^{f/f}$ Doxy and sucrose treated mice (Figure 23A). The serum concentration of Pi was also similar in all groups of mice (Figure 23B). Similar results for urinary and plasma Pi were observed in both male (Figure 23 A and B) and female mice (data not shown). Therefore the deletion of NaPi-IIc in the kidney did not alter the plasma and urinary concentrations of Pi. Together these data indicate that the NaPi-IIc deficiency did not affect Pi homeostasis.

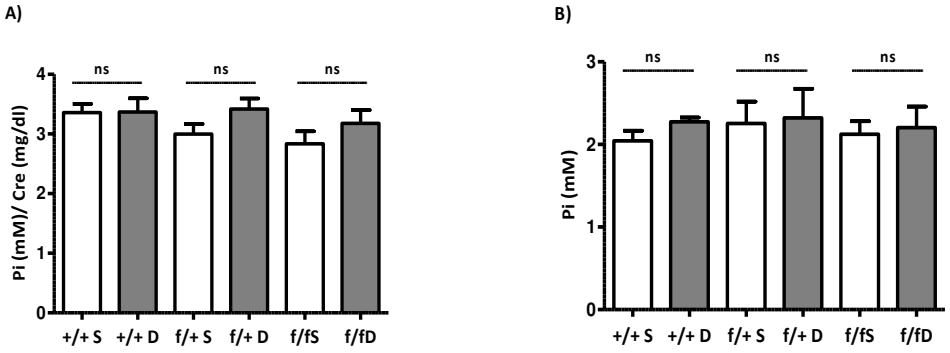

Figure 23 Effect of NaPi-IIc knockdown on the urinary excretion of Pi and plasma Pi. Pi concentration in A) urine and B) plasma of NaPi-IIc$^{+/+}$, NaPi-IIc$^{f/+}$ and NaPi-IIc$^{f/f}$ mice treated with Doxy (D) or sucrose (S). Urine was collected during the last 24 hours in metabolic cages and plasma was collected immediately after termination of experimental protocol. Mice received 0.5 + 0.25 mg/ml Doxy (gray bars) or sucrose alone (white bars) for 10 days followed by 15 days recovery period. The excretion of Pi (mM) was normalized to the concentration of creatinine (mg/dl). The data are presented as mean ± SEM (n = 8 to 10 per group) and statistical significances were calculated by ANOVA. No significant (ns) differences were observed between groups.

6.4.8 Effect of NaPi-IIc depletion on phosphaturic hormones

The maintenance of normal serum Pi depends, among other factors, on the balance between the phosphaturic hormones PTH and FGF23. PTH and FGF23 are known regulators of Pi homeostasis and act in response to different physiological stimuli. These hormones

regulate Pi reabsorption in the proximal tubules by controlling the abundance of apically located Na/Pi-cotransporters. To identify potential changes of these phosphaturic hormones due to the absence of NaPi-IIc, we determined the concentration of PTH and FGF23 in the plasma collected from NaPi-IIc$^{+/+}$, NaPi-IIc$^{f/+}$ and NaPi-IIc$^{f/f}$ mice.

The plasma levels of FGF23 (Figure 24A) and PTH (Figure 24B) were not changed significantly in NaPi-IIc$^{+/+}$ and NaPi-IIc$^{f/f}$ mice administered with Doxy compared to their corresponding sucrose controls. Together these data suggests that the depletion of NaPi-IIc did not affect the plasma levels of the phosphaturic hormones. The absence of changes in the hormonal levels correlates with the absence of changes in the urinary and serum Pi and with NaPi-lla abundance.

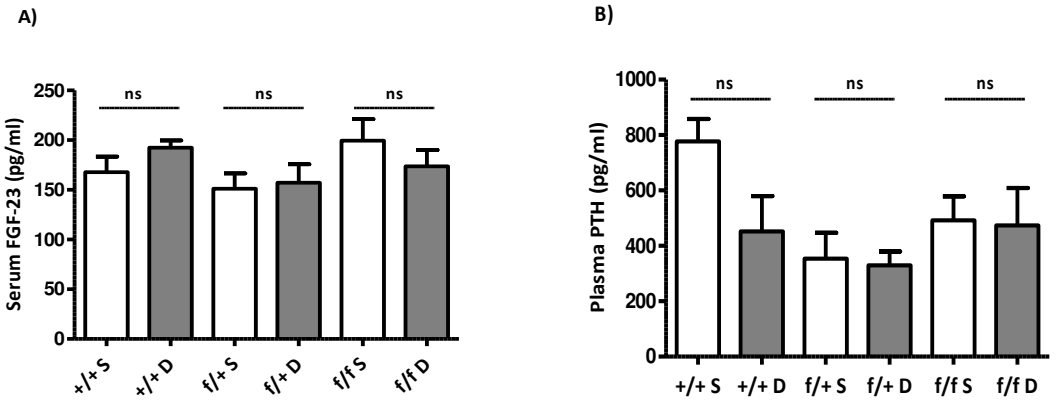

Figure 24 Effect of NaPi-IIc knockdown on circulating levels of phosphaturic hormones. Concentration of A) FGF-23 and B) PTH in plasma collected from NaPi-IIc$^{+/+}$, NaPi-IIc$^{f/+}$ and NaPi-IIc$^{f/f}$ mice drinking Doxy (D) or sucrose (S). Mice received 0.5 + 0.25 mg/ml Doxy (gray bars) or sucrose alone (white bars) for 10 days followed by 15 days recovery period. Plasma samples were collected immediately after termination of Doxy induction protocol. The data are presented as mean ± SEM (n = 6 to 8 per group) and statistical significances were calculated by ANOVA. No significant (ns) differences were observed between all the groups of mice.

6.4.9 Effect of NaPi-IIc depletion on plasma and urinary Ca^{2+}

Recently it was reported that the constitutive depletion of NaPi-IIc in mice causes hypercalcemia with hypercalciuria [69]. The changes in the calcium balance were probably due to the effect of increased circulating levels of $1,25(OH)_2D_3$. Furthermore, expression of 24-hydroxylase mRNA was reduced and 1α-hydroxylase remained unchanged in the described mutant mice. Therefore the increased $1,25(OH)_2D_3$ levels in constitutive NaPi-IIc depleted mice is probably due to reduced catabolism rather than increased production.

The urinary excretion of Ca^{2+} remained unchanged in NaPi-IIc$^{+/+}$ and NaPi-IIc$^{f/f}$ Doxy treated mice compared with their sucrose treated controls (Figure 25A). The plasma Ca^{2+} concentration was also not affected and was similar in all groups of mice (Figure 25B). Similar results were observed in both male (Figure 25 A and B) and female mice (data not shown).

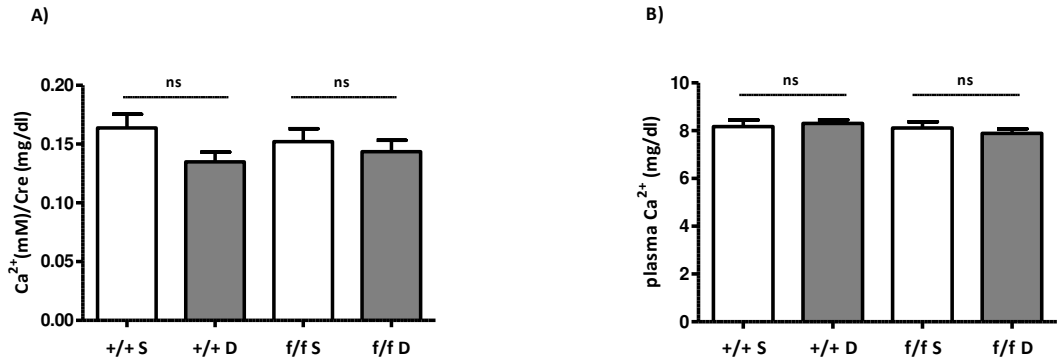

Figure 25 Effect of NaPi-IIc knockdown on the excretion of Ca^{2+} and plasma Ca^{2+} concentrationCa^{2+} concentration in urine A)and plasma B) of NaPi-IIc$^{+/+}$, NaPi-IIc$^{f/+}$ and NaPi-IIc$^{f/f}$ mice drinking Doxy (D) or sucrose (S). Urine was collected during the last 24 hours in metabolic cages and plasma was collected immediately after termination of experimental protocol. Mice received 0.5 + 0.25 mg/ml Doxy (gray bars) or sucrose alone (white bars) for 10 days followed by 15 days recovery period. The excretion of Ca^{2+} (mM) was normalized to the concentration of creatinine (mg/dl). The data are presented as mean ± SEM (n = 8 to 10 per group) and statistical significances were calculated by ANOVA. No significant (ns) differences were observed between groups.

6.4.10 Effect of NaPi-IIc depletion on plasma $1,25(OH)_2D_3$ and mRNA expression of $1,25(OH)_2D_3$ regulating genes

Finally we determined the concentration $1,25(OH)_2D_3$ in plasma and also analyzed the expression of mRNA's of $1,25(OH)_2D_3$ regulating genes in the kidney. As expected, the concentration of $1,25(OH)_2D_3$ was similar in NaPi-IIc$^{+/+}$ mice drinking Doxy and sucrose alone (Figure 26A). The renal specific depletion of NaPi-IIc did not lead to significant differences in $1,25(OH)_2D_3$ as similar concentrations were found in NaPi-IIc$^{f/f}$ mice drinking Doxy and sucrose (Figure 26A). In addition, we did not observe significant changes in the expression of both 1α- hydroxylase (Cyp27b1) and 24-hydroxylase (Cyp24a1) mRNAs between all the groups of mice (Figure 26B, C). Together, the absence of changes the mRNA expression of both 1α-hydroxylase and 24-hydroxylase correlates with the levels of $1,25(OH)_2D_3$ that were similar in all groups. Hence these data indicate that the renal specific depletion of NaPi-IIc did not alter circulating $1,25(OH)_2D_3$ which is in agreement with the absence of changes in

urinary Ca^{2+}.

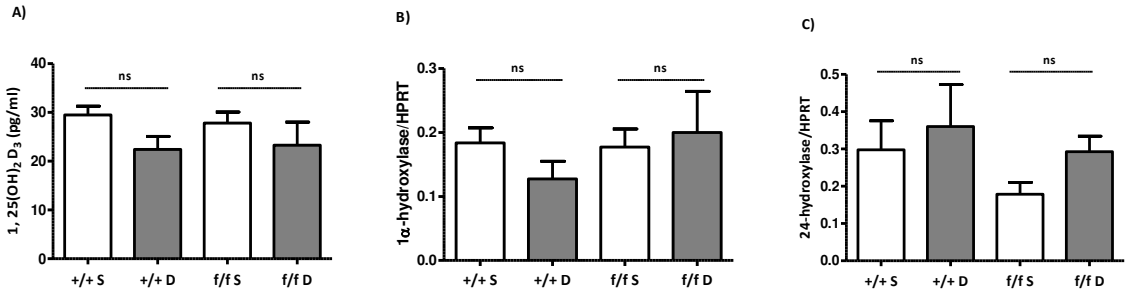

Figure 26 Effect of NaPi-IIc knockdown on the $1,25(OH)_2D_3$ metabolism in the kidney. A) Concentration of $1,25(OH)_2D_3$ in plasma and mRNA expression of $1,25(OH)_2D_3$ regulating enzymes B) 1α-hydroxylase and C) 24-hydroxylase in the kidney of NaPi-$IIc^{+/+}$ and NaPi-$IIc^{f/f}$ mice. Mice received 0.5 + 0.25 mg/ml Doxy (gray bars) or sucrose alone (white bars) for 10 days followed by 15 days recovery period. The relative expression of 1α-OHase and 24OHase was calculated and data are presented as mean ± SEM (n = 6 to 8 per group) and significances were calculated by ANOVA. No significant (ns) differences were observed between groups.

7 Discussion

Inorganic phosphate (Pi) is essential for cellular functions in the organism. The concentration of Pi in plasma is regulated by the modulation of intestinal absorption from the dietary source, renal reabsorption and storage of Pi in the skeleton and soft tissues (Figure 1). The maintenance of plasma Pi concentration is mainly achieved by the rate of Pi reabsorption in the proximal tubule of the kidney and to a limited extend by the intestinal absorption of dietary Pi. The renal reabsorption of Pi depends on the abundance of the Na/Pi-cotransporters NaPi-IIa, NaPi-IIc and Pit-2 that are localized at the brush border membrane (BBM) of proximal tubular epithelial cells [24]. In addition, the control of Pi homeostasis relies on secretory factors which regulate the abundance of these Na/Pi-cotransporters at the BBM. These factors are secreted by different organs including the parathyroid gland (PTH), bone (FGF-23) and kidney ($1,25(OH)_2D_3$) (see introduction). As mentioned in the introduction, these regulatory mechanisms form feedback networks such as the intestine-kidney or kidney-bone axis (Figure 7).

The renal reabsorption of Pi is an age-dependent process. In BBMVs isolated from kidneys of young animals Na/Pi cotransport activity is higher than in samples obtained from adult animals. Increased transport of Pi reflects a higher abundance of NaPi-IIa and NaPi-IIc proteins [7, 57]. It is thought that NaPi-IIa is the most important renal cotransporter in mice, since its absence in the kidney cannot be compensated by other cotransporters. Constitutive depletion of NaPi-IIa in mice leads to severe renal Pi wasting with hypophosphatemia although NaPi-IIc abundance is increased. In addition, the Pi uptake into renal BBMVs is reduced by 70% in the absence of NaPi-IIa [59]. This suggests that, in mice, the contribution of NaPi-IIa to Pi reabsorption is higher compared to NaPi-IIc and/or other apical cotransporters that altogether may reabsorb the remaining 30%. However, genetic defects in NaPi-IIc in humans lead to hereditary hypophosphatemic rickets with hypercalciuria (HHRH) suggesting a more important role of NaPi-IIc in Pi handling compared to mice [193].

In mice, the estimation of the relative contributions of NaPi-IIa and NaPi-IIc to renal Pi reabsorption is based on deficient models in which these cotransporters were constitutively knockedout [59, 69]. In these mouse models, compensatory upregulation of other

cotransporters in the intestine or kidney may have masked an initial effect on Pi handling. Therefore, the aim of this study was to investigate the role of NaPi-IIc by characterising a mouse model in which this cotransporter can be knocked out in an inducible and renal-specific manner. The inducible system used in this work is based on the activation of Cre-recombinase. In order to induce the recombinase activity, doxycycline (Doxy) was administered to 3 weeks old mice. It has been shown earlier that the abundance of NaPi-IIc is highest after weaning and continuously decreases with age [7].

Initially, mice received drinking water supplemented with 2 mg/ml Doxy and 2% sucrose or sucrose alone for 10 days. Compared to the sucrose controls, this protocol resulted in a decrease of 50% of the abundance of the NaPi-IIc protein and NaPi-IIc mRNA in NaPi-IIc$^{f/+}$ mice and an almost complete absence of NaPi-IIc protein and mRNA in NaPi-IIc$^{f/f}$ mice (males and females) (Figure 10, A and B, Figure 11).

Surprisingly, the urinary excretion of Pi was increased in both NaPi-IIc$^{+/+}$ and NaPi-IIc$^{f/f}$ after Doxy treatment (2mg/ml) (Figure 12, A and B). Furthermore, urinary excretion of several cations was changed. Thus, the excretion of Ca^{2+} was also higher in both NaPi-IIc$^{+/+}$ and NaPi-IIc$^{f/f}$ Doxy treated mice compared to the sucrose controls (Figure 13A, B) whereas the excretion of Na^{+} was reduced by 75% in all the groups of mice treated with Doxy (Figure 14 A). Similarly, K^{+} was also decreased significantly in urine collected from mice treated with Doxy compared to sucrose controls (Figure 14B). Together, these alterations in the urinary excretion of Pi and Ca^{2+} along with other cations (Na^{+} and K^{+}) in mice drinking 2mg/ml Doxy indicated that, this concentration of the antibiotic has nonspecific effects either in the kidney or in the intestine. A previous study indicated that, the treatment with Doxy at high concentration might have possible effects in the intestine by creating disturbances in the intestinal flora that lead to diarrhoea and colitis [203]. Thus, changes in the excretion of ions in urine might be secondary to disturbances in the intestine. We did not determine the concentration of Na^{+} and K^{+} in the feces. Nevertheless, these changes are unrelated to the deficiency of NaPi-IIc in the kidney.

Due to the nonspecific effects of the initial concentration of 2 mg/ml Doxy used, we had to optimize the concentration of the antibiotic in order to find a dosage which can efficiently

induce the depletion of NaPi-IIc without causing nonspecific effects. For that, we administered to NaPi-IIc$^{+/+}$ and NaPi-IIc$^{f/f}$ male mice different concentrations of Doxy (1, 0.5 and 0.25 mg/ml) for 10 days followed by a recovery period of 15 days during which mice drank normal tap water. Then, the NaPi-IIc mRNA expression was analysed in kidneys from NaPi-IIc$^{f/f}$ mice and the concentration of Na^+ was determined in urine of NaPi-IIc$^{+/+}$ mice. The expression of NaPi-IIc mRNA was almost completely depleted in mice that received 1 and 0.5 mg/ml Doxy whereas 25% expression remained in mice treated with 0.25 mg/ml Doxy compared with corresponding sucrose treated mice (Figure 15A). To monitor whether these concentrations of Doxy still lead to nonspecific effects, we determined the concentration of Na^+ in urine, which was used as an indicator for possible nonspecific effects. The urinary excretion of Na^+ was still reduced in NaPi-IIc$^{+/+}$ mice that received 1 and 0.5 mg/ml Doxy but no differences were observed in mice that received 0.25 mg/ml Doxy compared to sucrose controls (Figure 15B). Hence, the concentration of Doxy at which the NaPi-IIc mRNA expression was abolished still showed nonspecific effects whereas normal excretion of Na^+ was only found at the concentration of Doxy (0.25 mg/ml) at which NaPi-llc mRNA expression was not fully depleted. It may be of interest that even after a recovery phase of 10 days the effect on Na^+ excretion was still observed.

Therefore a new (and final Doxy) treatment was defined, consisting of administration of 0.5 mg/ml for 5 days followed by 0.25 mg/ml for the next 5 days, and extra 15 days as recovery period during which mice drank only normal tap water. Upon treatment with the final Doxy protocol, urinary excretion of Na^+ was comparable in all the Doxy treated animals and their respective sucrose controls (Figure 16A). Similarly, excretion of K^+ remained unchanged in all Doxy and sucrose mice (Figure 16B). The absence of changes in the urinary Na^+ excretion indicated that the final induction protocol (0.5 + 0.25 mg/ml Doxy + 15 days recovery) did not induce the non-specific effects which we observed in the mice treated with higher concentrations of Doxy. All results discussed below were obtained with animals treated with this final protocol.

In both males and females, the mRNA expression of NaPi-IIc was comparable in NaPi-IIc$^{+/+}$ mice drinking Doxy and sucrose. Instead, expression was reduced by 50% in NaPi-IIc$^{f/+}$ and almost fully absent in NaPi-IIc$^{f/f}$ Doxy treated mice compared with their corresponding

sucrose controls (Figure 17, A and B). The expression of NaPi-IIc protein in isolated renal BBM and total homogenates was also quantified. The results were similar to those of mRNA levels in all groups. Thus, while Doxy did not alter the abundance of NaPi-IIc in NaPi-IIc$^{+/+}$ mice, the expression was reduced by 50% and almost 100% in NaPi-IIc$^{f/+}$ and NaPi-IIc$^{f/f}$ mice respectively (Figure 18A - 18D). In addition, the abundance of NaPi-IIc protein in total homogenates paralleled the one observed in the BBM (Figure 19, A and B). The amount of NaPi-IIc protein in the renal BBM was highly variable in all the groups. In contrast, we did not observe such heterogeneity for other cotransporters namely NaPi-IIa and Pit-2. This suggests that the intra group variability of NaPi-IIc protein expression may not be due to a variable degree of protein degradation. The feeding behaviour may have an effect on expression of Na/Pi-cotransporters in the kidney. As mentioned earlier (see introduction) in response to dietary Pi restrictions the abundance of NaPi-IIa is regulated faster compared to changes of NaPi-IIc. Thus, the intra group variability of NaPi-IIc expression may not apply to changes in the diet. Circadian rhythm is also known to affect the expression of a number of proteins, although its potential effects on the translational regulation of NaPi-IIc are not known. Nevertheless, we collected samples between 9-11 am, so the heterogenic expression of the cotransporter may not relate to circadian variations.

In addition to Westernblot analysis, we also analysed the expression of NaPi-IIc by immunofluorescence. This study showed that the expression of NaPi-IIc in the proximal tubules remained detectable in kidneys from NaPi-IIc$^{+/+}$ mice, whereas the signal was absent in kidneys from NaPi-IIc$^{f/f}$ mice treated with Doxy (Figure20A). In contrast, NaPi-IIa protein was comparable in NaPi-IIc$^{+/+}$ and NaPi-IIc$^{f/f}$ mice treated with Doxy (Figure 20B). All together these results suggested that the optimized Doxy induction protocol efficiently depletes the expression of NaPi-IIc in NaPi-IIc$^{f/f}$ mice without non-specific effects and therefore allowed us to study the relative contribution of NaPi-IIc to Pi homeostasis in the kidney of weaning mice.

To study the effect of NaPi-IIc deficiency on the capacity of the kidney to reabsorb Pi, we isolated BBMVs from kidneys of NaPi-IIc$^{+/+}$ and NaPi-IIc$^{f/f}$ mice and measured Na/Pi-cotransport activity. We did not observe changes in the total, Na^+-dependent or Slc34-mediated Na/Pi-cotransport activity between the NaPi-IIc$^{+/+}$ and NaPi-IIc$^{f/f}$ Doxy treated mice

compared with their corresponding sucrose controls (Figure 21A - 21D). The transport of D-glucose which was used as a control for the integrity of the isolated membrane vesicles was also similar in BBMVs isolated from both NaPi-IIc$^{+/+}$ and NaPi-IIc$^{f/f}$ mice (Figure 21 E). These observations were similar to the previously reported data indicating that the constitutive depletion of NaPi-IIc did not alter Na/Pi-cotransport activity into renal BBMVs isolated from 9 weeks old mice [69]. Together, this data suggest that the deficiency of NaPi-IIc in the kidney did not alter Na/Pi-cotransport activity into proximal tubular BBMVs, suggesting a minimal role of this cotransporter in renal reabsorption of Pi, even in young animals. However, the transport studies in the BBMVs, discussed above cannot discriminate between the transport mediated by NaPi-IIa and NaPi-IIc as both proteins are sensitive to PFA. Therefore, we could not rule out a potential compensatory mechanism even though NaPiIIa abundance and total Pi transport activity into BBMV was unaltered.

In this regard, it has been demonstrated that the depletion of NaPi-IIa results in increased abundance of NaPi-IIc in the BBM probably to compensate urinary Pi losses [197]. However, this increased NaPi-IIc is not able to replace the lack of NaPi-IIa function, and the mice show hypophosphatemia secondary to renal loss of Pi. Similarly, compensatory mechanisms were also reported in mice deficient for NaPi-IIb, the SLC34 cotransporter responsible for the Na^+-dependent transcellular absorption of Pi across the small intestine. NaPi-IIb deficient mice did not exhibit changes in the serum Pi although faecal excretion was higher. The maintenance of normal serum Pi in these mice is achieved by a compensatory increased abundance of NaPi-IIa in the kidney [17]. Thus, the depletion of NaPi-IIc in the kidney could also lead to upregulation of other Na/Pi-cotransporters in order to maintain the Pi homoeostasis. However, renal-specific deficient NaPi-IIc mice did not show changes in the abundance of NaPi-IIa in the BBM as the amount of NaPi-IIa was similar in NaPi-II$^{f/f}$ mice treated with Doxy compared with respective sucrose controls (Figure 22A). In addition to NaPi-IIa and NaPi-IIc, Pit-2 is also expressed in the BBM of proximal tubules [8]. Pit-2 is also a Na/Pi-cotransporter, but belongs to the SLC20 family of solute carriers. Although its contribution to Pi reabsorption might be minimal, previous studies indicated that the expression of Pit-2 was regulated in response to dietary Pi, PTH and metabolic acidosis, three conditions known to regulate renal Pi reabsorption [8, 106].This data indicated the potential importance of Pit-2 activity in the kidney. The abundance of Pit-2 was not altered in NaPi-

IIc$^{f/f}$ mice treated with Doxy compared to sucrose controls (Figure 22B). Furthermore, the abundance of NaPi-IIb in the small intestine was also similar in NaPi-IIc$^{f/f}$ Doxy treated mice compared to corresponding sucrose controls (Figure 22C). Hence, the depletion of NaPi-IIc did not affect expression of other renal (NaPi-IIa and Pit-2) or intestinal (NaPi-IIb) Na/Pi-cotransporters.

Renal specific NaPi-IIc deficient mice had normal plasma concentration as well as urinary excretion of Pi (Figure 23, A and B). Thus, the absence of NaPi-IIc did not affect Pi homeostasis. These results were similar to previous findings observed in a constitutive NaPi-IIc deficient model, where the cotransporter deficiency did not induce changes in the urinary excretion and plasma concentration of Pi [69]. In contrast, constitutive NaPi-IIa deficient mice exhibited increased excretion of Pi and hypophosphatemia. In addition, the absence of NaPi-IIa affected Na/Pi-cotransport activity that was reduced by 70% in renal BBMVs [59] indicating the major role of NaPi-IIa. Together, the absence of changes in the urinary excretion of Pi and the normal expression levels of other cotransporters supports the conclusion that the contribution of NaPi-IIc to renal reabsorption of Pi must be minimal.

Several reports indicated that both PTH and FGF23 target the kidney to induce phosphaturia by reducing the BBM expression of NaPi-IIa and NaPi-IIc [116, 118, 122, 124, 204, 205]. In constitutive NaPi-IIa deficient mice both plasma PTH and FGF23 levels were reduced [59] whereas in constitutive NaPi-IIc deficient mice, FGF23 was reduced but PTH was unchanged [69]. Therefore, we measured the concentration of PTH and FGF23 in plasma. Both PTH and FGF23 levels were similar in NaPi-IIc$^{f/f}$ mice drinking either sucrose or Doxy (Figure 24, A and B). These results were consistent with the absence of changes in the expression of NaPi-IIa at the BBM.

We observed high variability of PTH within the groups. Recently it was reported that PTH levels could change rapidly in response to dietary Pi restrictions [110]. We know that the food intake was similar for all our mice because they were kept in single metabolic cage during the last 24 hours of the experimental protocol and food intake was recorded. However, we cannot estimate the latest time at which each mouse ate. Therefore, this variability in PTH levels could be the result of different feeding behaviours of the animals.

Together, these data indicate that renal-specific depletion of NaPi-IIc in weaning mice does not result in changes in Pi balance, circulating levels of PTH and FGF23, Na/Pi-cotransport activity of renal BBM and expression of other cotransporters.

As mentioned above that constitutive NaPi-IIc deficient mice showed lower FGF23 levels in plasma. In addition, expression of DMP-1 was increased in bone [69]. DMP-1 is a bone matrix protein known to inhibit the transcription of FGF23 and therefore might affect FGF23 synthesis [143]. In agreement with this hypothesis, it was also reported that the loss of DMP-1 in mice is associated with elevated plasma FGF23 levels and impaired maturation of osteocytes [184]. In humans, inactivating mutations in DMP-1 are associated with autosomal recessive hypophosphatemic rickets (ARHR) which leads to increased FGF23 production [184, 185]. This suggests that, the decreased FGF23 levels in constitutive NaPi-IIc deficient mice might be the effect of increased DMP-1 expression. However, is not clear how the NaPi-IIc deficiency leads to increased DMP-1 in the bone. Taken together, these observations suggest that the expression of NaPi-IIc in extra-renal tissues for instance like bone might be related to the changes in expression of DMP-1. Expression of NaPi-llc mRNA has been observed in osteoclasts (personal communication from D.Fuster, University of Bern, Switzerland). Further work, such as osteoclast specific knock outs will be needed to clarify the role of NaPi-llc in bone cells.

The constitutive depletion of either NaPi-IIa or NaPi-IIc in associated with hypercalcemia, hypercalciuria and elevated $1,25(OH)_2D_3$ in plasma [59, 69]. In the kidney, the active $1,25(OH)_2D_3$ is produced by the action of the anabolic enzyme 1α-hydroxylase and it is catabolised by the 24-hydroxylase. The absorption of calcium (Ca^{2+}) in the intestine is controlled by $1,25(OH)_2D_3$ via an increase of expression of TRPV6, a channel involved in the absorption of Ca^{2+} in the intestine [60]. In addition, $1,25(OH)_2D_3$ induces the expression of NaPi-IIb to promote the intestinal absorption of Pi [60]. Both PTH and FGF23 are known to regulate the plasma levels of $1,25(OH)_2D_3$ by modulating the expression of 1α- hydroxylase and 24-hydroxylase [206, 207]. In response to lower levels of plasma Ca^{2+} the synthesis of PTH increases which in turn acts on the kidney to enhance the 1α hydroxylase mRNA levels leading to higher $1,25(OH)_2D_3$. In contrast, FGF23 reduces $1,25(OH)_2D_3$ by decreasing the expression of 1α-hydroxylase and increasing 24-hydroxylase mRNA levels [208, 209].

Results obtained with a constitutive NaPi-IIc deficient mouse model indicated that 1α-hydroxylase mRNA levels were unchanged whereas 24-hydroxylase mRNA levels were significantly increased [69]. Furthermore, patients with mutations in the NaPi-IIc gene that are associated with hypophosphatemia and hypercalciuria showed elevated $1,25(OH)_2D_3$ levels [193]. Together these data suggest that a (constitutive) loss of NaPi-IIc function is associated with abnormal regulation of $1,25(OH)_2D_3$ metabolism which leads to changes in the Ca^{2+} homeostasis. Interestingly the urinary excretion and plasma Ca^{2+} were normal in NaPi-IIc$^{f/f}$ Doxy treated mice (Figure 25, A and B). Moreover, plasma $1,25(OH)_2D_3$ levels were similar in all groups of mice treated either with Doxy or sucrose (Figure 26A). Furthermore, the mRNA expression of the two key enzymes 1α-hydroxylase and 24-hydroxylase was undistinguishable in all the groups (Figure 26, B and C).

The marked differences in the Ca^{2+} phenotypes between constitutive and renal-specific NaPi-IIc deficient mouse models may result from an extra-renal knockdown of the cotransporter in the constitutive model. The expression of NaPi-IIc in several human and rat tissues was investigated by Northernblot [7]. In both species the expression of NaPi-IIc mRNA was detected only in the kidney. Recently, Nishimura et al. [70] analysed the mRNA expression of all the SLC members in several human tissues by real-time PCR. They observed highest mRNA expression levels of NaPi-IIc in the kidney whereas lower levels were detected in other tissues like testis, brain, lung and spinal cord [70]. Recently, NaPi-IIc mRNA has been also observed in osteoclasts (personal communication from D. Fuster). Thus, extra renal expression of NaPi-IIc might explain the disturbed Ca^{2+} metabolism observed in constitutive NaPi-IIc deficient mice. The distribution of NaPi-IIc protein in the other tissues is not known and needs to be examined. Our floxed-NaPi-IIc mouse model may be helpful to investigate the role of NaPi-IIc in different organs other than in kidney which might be responsible for the differences in the Ca^{2+} metabolism.

8. Conclusion

In summary, we have generated an inducible knockout mouse model that allows to knock-out NaPi-IIc in a tissue specific manner. Here NaPi-llc was knocked out specifically in renal proximal tubules in order to investigate its role renal handling of Pi and in overall Pi homeostasis. Our findings show that the absence of renal NaPi-IIc does not disturb Pi homeostasis in mice. These results are in agreement with previous studies performed with a constitutive NaPi-IIc deficient mouse model. Both, results obtained from a constitutive and renal-specific NaPi-IIc deficient mouse model suggest that NaPi-IIc might have a minor role in renal Pi reabsorption in mice. Interestingly, in humans, the deficiency of NaPi-llc cotransporter function leads to hereditary hypophosphatemic rickets with hypercalciurea. Thus, NaPi-IIc might be more important to renal reabsorption of Pi in humans as compared to mice.

Unlike the constitutive NaPi-IIc deficient mouse model, the renal-specific ablation of the cotransporter in weaning mice does not alter Ca^{2+} homeostasis, suggesting that extra-renal expression of NaPi-IIc may be responsible for changes in the Ca^{2+} metabolism that have been reported in the constitutive mouse model. The mouse model (floxed NaPi-llc) described in this work may be of help to investigate the role of the Na/Pi-cotransporter NaPi-llc in extrarenal tissues.

9 Future perspectives

PTH is one of the key regulatory phosphaturic factors that decrease the abundance of NaPi-IIa and NaPi-IIc at the BBM of proximal tubular cells. The regulation pattern of NaPi-IIa and NaPi-IIc in response to PTH is different. It has been described that PTH-induced internalization and lysosomal degradation of NaPi-IIa occurs by activating PKA and PKC signalling pathways [24, 118, 124]. NaPi-IIc is also internalized and degraded upon PTH treatment but degradation does not take place in lysosomes [119]. The intravenous injection of PTH leads to internalization of NaPi-IIa within 20 min and the cotransporter completely disappears from the BBM one hour after PTH administration [106]. In contrast, NaPi-IIc was observed in sub-apical compartments after 4 hours of PTH injection and complete degradation required up to 8 hours [119]. Our experimental data suggest that NaPi-IIc in weaning mice may not be accountable for significant Pi reabsorption in kidney. In contrast, and as already indicated NaPi-IIa deficient mice show a 70% reduction in Pi reabsorption. The remaining 30% must be reabsorbed by other Na/Pi-cotransporters and based on the present knowledge they are most probably NaPi-IIc and/or Pit-2. As indicated above NaPi-IIa is fully internalized 1 hour upon PTH injection whereas internalization of NaPi-IIc and Pit-2 takes 4 to 8 hours. This means that BBM isolated from kidneys of wild type mice acutely treated with PTH should contain NaPi-IIc and Pit-2 whereas BBM isolated from NaPi-IIc$^{f/f}$ would express only Pit-2. Therefore, short administration of PTH to NaPi-IIc$^{+/+}$ and NaPi-IIc$^{f/f}$ mice may be helpful to clearly define whether or not NaPi-IIc contributes, through minimally, to Pi reabsorption in the kidney.

As mentioned above that the NaPi-IIc mRNA expression was identified in several other organs like spinal cord, brain, lungs and testis where the cotransporter function was not yet characterized. Therefore, the generation of tissue-specific Cre-lines and our floxed-NaPi-IIc model may further helpful to investigate the NaPi-IIc function in different organs. For instance, NaPi-IIc mRNA was observed in osteoclasts. It is interesting to generate osteoclast specific knock outs to clarify the role of NaPi-llc in bone cells.

10 References

1. Cunningham, J., F. Locatelli, and M. Rodriguez, *Secondary hyperparathyroidism: pathogenesis, disease progression, and therapeutic options.* Clin J Am Soc Nephrol, 2011. **6**(4): p. 913-21.
2. Hruska, K.A., et al., *Hyperphosphatemia of chronic kidney disease.* Kidney Int, 2008. **74**(2): p. 148-57.
3. Tenenhouse, H.S., *Regulation of phosphorus homeostasis by the type IIa/phosphate cotransporter.* Annu Rev Nutr, 2005. **25**: p. 197-214.
4. Suyama, T., et al., *High phosphorus diet-induced changes in NaPi-IIb phosphate transporter expression in the rat kidney: DNA microarray analysis.* PloS One, 2012. **7**(1): p. e29483.
5. Magagnin, S., et al., *Expression cloning of human and rat renal cortex Na/Pi cotransport.* Proc Natl Acad Sci USA, 1993. **90**(13): p. 5979-83.
6. Hilfiker, H., et al., *Characterization of a murine type II sodium-phosphate cotransporter expressed in mammalian small intestine.* Proc Natl Acad Sci USA, 1998. **95**(24): p. 14564-9.
7. Segawa, H., et al., *Growth-related renal type II Na/Pi cotransporter.* J Biol Chem, 2002. **277**(22): p. 19665-72.
8. Villa-Bellosta, R., et al., *The Na^+/Pi cotransporter PiT-2 (SLC20A2) is expressed in the apical membrane of rat renal proximal tubules and regulated by dietary Pi.* Am J Physiol Renal Physiol, 2009. **296**(4): p. F691-9.
9. Danisi, G., J.P. Bonjour, and R.W. Straub, *Regulation of Na^+-dependent phosphate influx across the mucosal border of duodenum by 1,25-dihydroxycholecalciferol.* Pflugers Arch, 1980. **388**(3): p. 227-32.
10. Debiec, H. and R. Lorenc, *Effect of Lactose on phosphate-transport into rat intestinal brush border bembrane vesicles.* J Nutr, 1985. **115**(9): p. 1168-1172.
11. Kayne, L.H., et al., *Analysis of segmental phosphate absorption in intact rats. A compartmental analysis approach.* J Clin Invest, 1993. **91**(3): p. 915-22.
12. Amasheh, S., M. Fromm, and D. Gunzel, *Claudins of intestine and nephron - a correlation of molecular tight junction structure and barrier function.* Acta Physiol 2011. **201**(1): p. 133-40.
13. Balda, M.S., et al., *Assembly of the tight junction: the role of diacylglycerol.* J Cell Biol, 1993. **123**(2): p. 293-302.
14. Gonzalez-Mariscal, L., et al., *Tight junction proteins.* Prog Biophys Mol Biol, 2003. **81**(1): p. 1-44.
15. Benais-Pont, G., et al., *Identification of a tight junction-associated guanine nucleotide exchange factor that activates Rho and regulates paracellular permeability.* J Cell Biol, 2003. **160**(5): p. 729-740.
16. Will, C., M. Fromm, and D. Muller, *Claudin tight junction proteins: novel aspects in paracellular transport.* Perit Dial Int, 2008. **28**(6): p. 577-84.
17. Sabbagh, Y., et al., *Intestinal Npt2b plays a major role in phosphate absorption and homeostasis.* J Am Soc Nephrol, 2009. **20**(11): p. 2348-58.
18. Forster, I.C., et al., *Phosphate transport kinetics and structure-function relationships of SLC34 and SLC20 proteins.* Curr Top Membr, 2012. **70**: p. 313-56.
19. Kohler, K., et al., *The functional unit of the renal type IIa Na^+/Pi cotransporter is a monomer.* J Biol Chem, 2000. **275**(34): p. 26113-26120.

20. Gisler, S.M., et al., *Monitoring protein-protein interactions between the mammalian integral membrane transporters and PDZ-interacting partners using a modified split-ubiquitin membrane yeast two-hybrid system.* Mol Cell Proteomics, 2008. **7**(7): p. 1362-1377.
21. Fenollar-Ferrer, C., et al., *Structural Fold and Binding Sites of the Human Na^+-Phosphate Cotransporter NaPi-II.* Biophys J, 2014. **106**(6): p. 1268-79.
22. Bacconi, A., et al., *Renouncing electroneutrality is not free of charge: Switching on electrogenicity in a Na^+-coupled phosphate cotransporter.* Proc Natl Acad Sci USA, 2005. **102**(35): p. 12606-12611.
23. Andrini, O., et al., *Lithium interactions with Na^+-coupled inorganic phosphate cotransporters: insights into the mechanism of sequential cation binding.* Am J Physiol-Cell Physiol, 2012. **302**(3): p. C539-C554.
24. Forster, I.C., et al., *Proximal tubular handling of phosphate: A molecular perspective.* Kidney Int, 2006. **70**(9): p. 1548-59.
25. Busch, A.E., et al., *Properties of electrogenic Pi transport by a human renal brush border Na^+/Pi transporter.* J Am Soc Nephrol, 1995. **6**(6): p. 1547-51.
26. Forster, I.C., et al., *Electrogenic kinetics of a mammalian intestinal type IIb Na^+/Pi cotransporter.* J Membr Biol, 2006. **212**(3): p. 177-90.
27. Villa-Bellosta, R. and V. Sorribas, *Role of rat sodium/phosphate cotransporters in the cell membrane transport of arsenate.* Toxicol Appl Pharmacol, 2008. **232**(1): p. 125-34.
28. Virkki, L.V., et al., *Phosphate transporters: a tale of two solute carrier families.* Am J Physiol Renal Physiol, 2007. **293**(3): p. F643-54.
29. Forster, I.C., D.D. Loo, and S. Eskandari, *Stoichiometry and Na^+ binding cooperativity of rat and flounder renal type II Na^+/Pi cotransporters.* Am J Physiol, 1999. **276**(4): p. F644-9.
30. Virkki, L.V., H. Murer, and I.C. Forster, *Voltage clamp fluorometric measurements on a type II Na^+-coupled Pi cotransporter: shedding light on substrate binding order.* J Gen Physiol, 2006. **127**(5): p. 539-55.
31. Ghezzi, C., H. Murer, and I.C. Forster, *Substrate interactions of the electroneutral Na^+-coupled inorganic phosphate cotransporter (NaPi-IIc).* J Physiol, 2009. **587**(17): p. 4293-4307.
32. LoghmanAdham, M. and G.T. Motock, *Use of phosphonoformic acid to induce phosphaturia in chronic renal failure in rats.* Renal Failure, 1996. **18**(6): p. 855-866.
33. Villa-Bellosta, R., et al., *Characterization of phosphate transport in rat vascular smooth muscle cells: implications for vascular calcification.* Arterioscler Thromb Vasc Biol, 2007. **27**(5): p. 1030-6.
34. Ravera, S., et al., *Deciphering PiT transport kinetics and substrate specificity using electrophysiology and flux measurements.* Am J Physiol-Cell Physiol, 2007. **293**(2): p. C606-C620.
35. Virkki, L.V., et al., *Substrate interactions in the human type IIa sodium-phosphate cotransporter (NaPi-IIa).* Am J Physiol Renal Physiol, 2005. **288**(5): p. F969-81.
36. Forster, I., et al., *The voltage dependence of a cloned mammalian renal type II Na+/Pi cotransporter (NaPi-2).* J Gen Physiol, 1998. **112**(1): p. 1-18.
37. Ehnes, C., et al., *Functional studies on a split type II Na/P(i)-cotransporter.* J Membr Biol, 2002. **188**(3): p. 227-36.

38. Kohl, B., et al., *The Na^+-phosphate cotransport system (NaPi-II) with a cleaved protein backbone: implications on function and membrane insertion.* J Physiol, 1998. **508(2)**: p. 341-50.
39. Lambert, G., et al., *Studies on the topology of the renal type II NaPi-cotransporter.* Pflugers Arch, 1999. **437**(6): p. 972-8.
40. Radanovic, T., et al., *Topology of the type IIa Na^+/Pi cotransporter.* J Membr Biol, 2006. **212**(1): p. 41-49.
41. Lambert, G., et al., *Cleavage of disulfide bonds leads to inactivation and degradation of the type IIa, but not type IIb sodium phosphate cotransporter expressed in Xenopus laevis oocytes.* J Membr Biol, 2000. **176**(2): p. 143-9.
42. Hernando, N., et al., *Molecular determinants for apical expression and regulatory membrane retrieval of the type IIa Na/Pi cotransporter.* Kidney Int, 2001. **60**(2): p. 431-5.
43. Gisler, S.M., et al., *Interaction of the type IIa Na^+/Pi cotransporter with PDZ proteins.* J Biol Chem, 2001. **276**(12): p. 9206-13.
44. Weinman, E.J., et al., *Characterization of a protein cofactor that mediates protein-kinase-a regulation of the renal brush border membrane Na^+/H^+ Exchanger.* J Clin Invest, 1995. **95**(5): p. 2143-2149.
45. Murthy, A., et al., *NHERF, a regulatory cofactor for Na^+/H^+ exchange, is a common interactor for merlin and ERM (MERM) proteins.* J Biol Chem, 1998. **273**(3): p. 1273-1276.
46. Gisler, S.M., et al., *PDZK1: I. a major scaffolder in brush borders of proximal tubular cells.* Kidney Int, 2003. **64**(5): p. 1733-45.
47. Karim-Jimenez, Z., et al., *Molecular determinants for apical expression of the renal type IIa Na^+/Pi-cotransporter.* Pflugers Arch, 2001. **442**(5): p. 782-90.
48. Hernando, N., et al., *PDZ-domain interactions and apical expression of type IIa Na/Pi-cotransporters.* Proc Natl Acad Sci USA, 2002. **99**(18): p. 11957-62.
49. Shenolikar, S., et al., *Targeted disruption of the mouse NHERF-1 gene promotes internalization of proximal tubule sodium-phosphate cotransporter type IIa and renal phosphate wasting.* Proc Natl Acad Sci USA, 2002. **99**(17): p. 11470-5.
50. Kocher, O., et al., *Targeted disruption of the PDZK1 gene by homologous recombination.* Mol Cell Biol, 2003. **23**(4): p. 1175-80.
51. McWilliams, R.R., et al., *Shank2E binds NaPi cotransporter at the apical membrane of proximal tubule cells.* Am J Physiol-Cell Ph, 2005. **289**(4): p. C1042-C1051.
52. Reining, S.C., et al., *GABARAP deficiency modulates expression of NaPi-IIa in renal brush-border membranes.* Am J Physiol Renal Physiol, 2009. **296**(5): p. F1118-28.
53. Jamison, R.L., *Micropuncture study of superficial and juxtamedullary nephrons in the rat.* Am J Physiol, 1970. **218**(1): p. 46-55.
54. Knox, F.G., et al., *Phosphate transport in superficial and deep nephrons in phosphate-loaded rats.* Am J Physiol, 1977. **233**(2): p. F150-3.
55. Custer, M., et al., *Expression of Na/Pi cotransport in rat kidney: localization by RT-PCR and immunohistochemistry.* Am J Physiol, 1994. **266**(52): p. F767-74.
56. Ritthaler, T., et al., *Effects of phosphate intake on distribution of type II Na/Pi cotransporter mRNA in rat kidney.* Kidney Int, 1999. **55**(3): p. 976-83.
57. Taufiq, S., J.F. Collins, and F.K. Ghishan, *Posttranscriptional mechanisms regulate ontogenic changes in rat renal sodium-phosphate transporter.* Am J Physiol, 1997. **272**(12): p. R134-41.

58. Traebert, M., et al., *Distribution of the sodium/phosphate transporter during postnatal ontogeny of the rat kidney.* J Am Soc Nephrol, 1999. **10**(7): p. 1407-15.
59. Beck, L., et al., *Targeted inactivation of Npt2 in mice leads to severe renal phosphate wasting, hypercalciuria, and skeletal abnormalities.* Proc Natl Acad Sci USA, 1998. **95**(9): p. 5372-7.
60. Bouillon, R., et al., *Vitamin D and human health: lessons from vitamin D receptor null mice.* Endocr Rev, 2008. **29**(6): p. 726-76.
61. Chau, H., et al., *Renal calcification in mice homozygous for the disrupted type IIa Na/Pi cotransporter gene Npt2.* J Bone Miner Res, 2003. **18**(4): p. 644-57.
62. Prie, D., et al., *Nephrolithiasis and osteoporosis associated with hypophosphatemia caused by mutations in the type 2a sodium-phosphate cotransporter.* N Engl J Med, 2002. **347**(13): p. 983-91.
63. Virkki, L.V., et al., *Functional characterization of two naturally occurring mutations in the human sodium-phosphate cotransporter type IIa.* J Bone Miner Res, 2003. **18**(12): p. 2135-41.
64. Magen, D., et al., *A loss-of-function mutation in NaPi-IIa and renal Fanconi's syndrome.* N Engl J Med, 2010. **362**(12): p. 1102-9.
65. Ito, M., et al., *An apical expression signal of the renal type IIc Na^+-dependent phosphate cotransporter in renal epithelial cells.* Am J Physiol Renal Physiol, 2010. **299**(1): p. F243-F254.
66. Villa-Bellosta, R., et al., *Interactions of the growth-related, type IIc renal sodium/phosphate cotransporter with PDZ proteins.* Kidney Int, 2008. **73**(4): p. 456-64.
67. Silverstein, D.M., et al., *A putative growth-related renal Na^+/Pi cotransporter.* Am J Physiol, 1997. **273**(32): p. R928-33.
68. Nowik, M., et al., *Renal phosphaturia during metabolic acidosis revisited: molecular mechanisms for decreased renal phosphate reabsorption.* Pflugers Arch, 2008. **457**(2): p. 539-549.
69. Segawa, H., et al., *Type IIc sodium-dependent phosphate transporter regulates calcium metabolism.* J Am Soc Nephrol, 2009. **20**(1): p. 104-113.
70. Nishimura, M. and S. Naito, *Tissue-specific mRNA expression profiles of human solute carrier transporter superfamilies.* Drug Metab Pharmacokinet, 2008. **23**(1): p. 22-44.
71. Segawa, H., et al., *Npt2a and Npt2c in mice play distinct and synergistic roles in inorganic phosphate metabolism and skeletal development.* Am J Physiol Renal Physiol, 2009. **297**(3): p. F671-8.
72. Farrow, E.G. and K.E. White, *Recent advances in renal phosphate handling.* Nat Rev Nephrol, 2010. **6**(4): p. 207-217.
73. Segawa, H., et al., *The roles of Na/Pi-II transporters in phosphate metabolism.* Bone, 2009. **45**: p. S2-7.
74. Marks, J., E.S. Debnam, and R.J. Unwin, *Phosphate homeostasis and the renal-gastrointestinal axis.* Am J Physiol Renal Physiol, 2010. **299**(2): p. F285-96.
75. Homann, V., et al., *Sodium-phosphate cotransporter in human salivary glands: molecular evidence for the involvement of NPT2b in acinar phosphate secretion and ductal phosphate reabsorption.* Arch Oral Biol, 2005. **50**(9): p. 759-68.
76. Xu, Y., et al., *Sodium-inorganic phosphate cotransporter NaPi-IIb in the epididymis and its potential role in male fertility studied in a transgenic mouse model.* Biol Reprod, 2003. **69**(4): p. 1135-41.

77. Shibasaki, Y., et al., *Targeted deletion of the tybe IIb Na^+-dependent Pi-co-transporter, NaPi-IIb, results in early embryonic lethality.* Biochem Biophys Res Co, 2009. **381**(4): p. 482-6.
78. Corut, A., et al., *Mutations in SLC34A2 cause pulmonary alveolar microlithiasis and are possibly associated with testicular microlithiasis.* Am J Hum Genet, 2006. **79**(4): p. 650-6.
79. van Zeijl, M., et al., *A human amphotropic retrovirus receptor is a second member of the gibbon ape leukemia virus receptor family.* Proc Natl Acad Sci USA, 1994. **91**(3): p. 1168-72.
80. Miller, D.G., R.H. Edwards, and A.D. Miller, *Cloning of the Cellular Receptor for Amphotropic Murine Retroviruses Reveals Homology to That for Gibbon Ape Leukemia-Virus.* Proc Natl Acad Sci USA, 1994. **91**(1): p. 78-82.
81. Bottger, P., et al., *Characterization of transport mechanisms and determinants critical for Na^+-dependent Pi symport of the PiT family paralogs human PiT1 and PiT2.* Am J Physiol Cell Physiol, 2006. **291**(6): p. C1377-87.
82. Bai, L., J.F. Collins, and F.K. Ghishan, *Cloning and characterization of a type III Na-dependent phosphate cotransporter from mouse intestine.* Am J Physiol Cell Physiol, 2000. **279**(4): p. C1135-43.
83. Giral, H., et al., *Regulation of rat intestinal Na-dependent phosphate transporters by dietary phosphate.* Am J Physiol Renal Physiol, 2009. **297**(5): p. F1466-75.
84. Tatsumi, S., et al., *Molecular cloning and hormonal regulation of PiT-1, a sodium-dependent phosphate cotransporter from rat parathyroid glands.* Endocrinology, 1998. **139**(4): p. 1692-9.
85. Kavanaugh, M.P. and D. Kabat, *Identification and characterization of a widely expressed phosphate transporter/retrovirus receptor family.* Kidney Int, 1996. **49**(4): p. 959-63.
86. Beck, L., et al., *Identification of a novel function of PiT1 critical for cell proliferation and independent of its phosphate transport activity.* J Biol Chem, 2009. **284**(45): p. 31363-74.
87. Tenenhouse, H.S., et al., *Differential expression, abundance, and regulation of Na^+-phosphate cotransporter genes in murine kidney.* Am J Physiol, 1998. **275**(42): p. F527-34.
88. Leung, J.C., et al., *Expression of the rat renal PiT-2 phosphate transporter.* Horm Metab Res, 2005. **37**(5): p. 265-9.
89. Reining, S.C., et al., *Expression of renal and intestinal Na/Pi cotransporters in the absence of GABARAP.* Pflugers Arch, 2010. **460**(1): p. 207-17.
90. Beck, L., et al., *The Phosphate Transporter PiT1 (Slc20a1) Revealed As a New Essential Gene for Mouse Liver Development.* Plos One, 2010. **5**(2).
91. Villa-Bellosta, R. and V. Sorribas, *Compensatory regulation of the sodium/phosphate cotransporters NaPi-IIc (SCL34A3) and Pit-2 (SLC20A2) during Pi deprivation and acidosis.* Pflugers Arch, 2010. **459**(3): p. 499-508.
92. Wang, C., et al., *Mutations in SLC20A2 link familial idiopathic basal ganglia calcification with phosphate homeostasis.* Nat Genet, 2012. **44**(3): p. 254-6.
93. Khadeer, M.A., et al., *Na^+-dependent phosphate transporters in the murine osteoclast: cellular distribution and protein interactions.* Am J Physiol Cell Physiol, 2003. **284**(6): p. C1633-44.
94. Yang, H., G. Curinga, and C.M. Giachelli, *Elevated extracellular calcium levels induce smooth muscle cell matrix mineralization in vitro.* Kidney Int, 2004. **66**(6): p. 2293-9.

95. Kakita, A., et al., *Stimulation of Na-dependent phosphate transport by platelet-derived growth factor in rat aortic smooth muscle cells.* Atherosclerosis, 2004. **174**(1): p. 17-24.
96. Voelkl, J., et al., *Spironolactone ameliorates PIT1-dependent vascular osteoinduction in klotho-hypomorphic mice.* J Clin Invest, 2013. **123**(2): p. 812-22.
97. Honjo, S., et al., *Clinical outcome and mechanism of soft tissue calcification in Werner syndrome.* Rejuvenation Res, 2008. **11**(4): p. 809-19.
98. Salaun, C., et al., *Identification of a novel transport-independent function of PiT1/SLC20A1 in the regulation of TNF-induced apoptosis.* J Biol Chem, 2010. **285**(45): p. 34408-18.
99. Li, X., H.Y. Yang, and C.M. Giachelli, *Role of the sodium-dependent phosphate cotransporter, Pit-1, in vascular smooth muscle cell calcification.* Circ Res, 2006. **98**(7): p. 905-12.
100. Zoidis, E., et al., *Regulation of phosphate (Pi) transport and NaPi-III transporter (Pit-1) mRNA in rat osteoblasts.* J Endocrinol, 2004. **181**(3): p. 531-40.
101. Palmer, G., J.P. Bonjour, and J. Caverzasio, *Expression of a newly identified phosphate transporter/retrovirus receptor in human SaOS-2 osteoblast-like cells and its regulation by insulin-like growth factor I.* Endocrinology, 1997. **138**(12): p. 5202-9.
102. Hruska, K.A., *Regulation of renal phosphate reabsorption: concepts in evolution.* Pediatr Nephrol, 1987. **1**(4): p. 657-63.
103. Ullrich, K.J. and H. Murer, *Sulphate and phosphate transport in the renal proximal tubule.* Philos Trans R Soc Lond B Biol Sci, 1982. **299**(1097): p. 549-58.
104. Murer, H., I. Forster, and J. Biber, *The sodium phosphate cotransporter family SLC34.* Pflugers Arch, 2004. **447**(5): p. 763-7.
105. Alizadeh Naderi, A.S. and R.F. Reilly, *Hereditary disorders of renal phosphate wasting.* Nat Rev Nephrol, 2010. **6**(11): p. 657-65.
106. Picard, N., et al., *Acute parathyroid hormone differentially regulates renal brush border membrane phosphate cotransporters.* Pflugers Arch, 2010. **460**(3): p. 677-87.
107. Levine, B.S., et al., *Renal adaptation to phosphorus deprivation: characterization of early events.* J Bone Miner Res, 1986. **1**(1): p. 33-40.
108. Segawa, H., et al., *Internalization of renal type IIc Na-Pi cotransporter in response to a high-phosphate diet.* Am J Physiol Renal Physiol, 2005. **288**(3): p. F587-96.
109. Lotscher, M., et al., *Role of microtubules in the rapid regulation of renal phosphate transport in response to acute alterations in dietary phosphate content.* J Clin Invest, 1997. **99**(6): p. 1302-12.
110. Bourgeois, S., et al., *The phosphate transporter NaPi-IIa determines the rapid renal adaptation to dietary phosphate intake in mouse irrespective of persistently high FGF23 levels.* Pflugers Arch, 2013. **465**(11): p. 1557-72.
111. Custer, M., et al., *Identification of a new gene product (diphor-1) regulated by dietary phosphate.* Am J Physiol, 1997. **273**(52): p. F801-6.
112. Weinman, E.J., et al., *Parathyroid hormone inhibits renal phosphate transport by phosphorylation of serine 77 of sodium-hydrogen exchanger regulatory factor-1.* J Clin Invest, 2007. **117**(11): p. 3412-20.
113. Levi, M., et al., *Low-Pi diet increases the abundance of an apical protein in rat proximal-tubular S3 segments.* Pflugers Arch, 1994. **426**(12): p. 5-11.
114. Madjdpour, C., et al., *Segment-specific expression of sodium-phosphate cotransporters NaPi-IIa and -IIc and interacting proteins in mouse renal proximal tubules.* Pflugers Arch, 2004. **448**(4): p. 402-10.

115. Berndt, T. and R. Kumar, *Phosphatonins and the regulation of phosphate homeostasis.* Annu Rev Physiol, 2007. **69**: p. 341-59.
116. Bergwitz, C. and H. Juppner, *Regulation of phosphate homeostasis by PTH, vitamin D, and FGF23.* Annu Rev Med, 2010. **61**: p. 91-104.
117. Silver, J., et al., *Regulation of the parathyroid hormone gene by calcium, phosphate and 1,25-dihydroxyvitamin D.* Nephrol Dial Transpl, 1998. **13**: p. 40-44.
118. Lotscher, M., et al., *Rapid downregulation of rat renal Na/Pi cotransporter in response to parathyroid hormone involves microtubule rearrangement.* J Clin Invest, 1999. **104**(4): p. 483-94.
119. Segawa, H., et al., *Parathyroid hormone-dependent endocytosis of renal type IIc Na-Pi cotransporter.* Am J Physiol Renal Physiol, 2007. **292**(1): p. F395-403.
120. Bacic, D., et al., *The renal Na+/phosphate cotransporter NaPi-IIa is internalized via the receptor-mediated endocytic route in response to parathyroid hormone.* Kidney Int, 2006. **69**(3): p. 495-503.
121. Lanzano, L., et al., *Differential modulation of the molecular dynamics of the type IIa and IIc sodium phosphate cotransporters by parathyroid hormone.* Am J Physiol Cell Physiol, 2011. **301**(4): p. C850-61.
122. Keusch, I., et al., *Parathyroid hormone and dietary phosphate provoke a lysosomal routing of the proximal tubular Na/Pi-cotransporter type II.* Kidney Int, 1998. **54**(4): p. 1224-1232.
123. Hernando, N., et al., *PTH-induced downregulation of the type IIa Na^+/Pi-cotransporter is independent of known endocytic motifs.* J Am Soc Nephrol, 2000. **11**(11): p. 1961-1968.
124. Traebert, M., et al., *Internalization of proximal tubular type II Na/Pi-cotransporter by PTH: immunogold electron microscopy.* Am J Physiol Renal Physiol, 2000. **278**(1): p. F148-54.
125. Nagai, S., et al., *Acute Down-regulation of Sodium-dependent Phosphate Transporter NPT2a Involves Predominantly the cAMP/PKA Pathway as Revealed by Signaling-selective Parathyroid Hormone Analogs.* J Biol Chem, 2011. **286**(2): p. 1618-1626.
126. Bacic, D., et al., *Involvement of the MAPK-kinase pathway in the PTH-mediated regulation of the proximal tubule type IIa Na^+/Pi cotransporter in mouse kidney.* Pflugers Arch, 2003. **446**(1): p. 52-60.
127. Capuano, P., et al., *Defective coupling of apical PTH receptors to phospholipase C prevents internalization of the Na^+-phosphate cotransporter NaPi-IIa in Nherf1-deficient mice.* Am J Physiol Cell Physiol, 2007. **292**(2): p. C927-34.
128. Breusegem, S.Y., et al., *Differential regulation of the renal sodium-phosphate cotransporters NaPi-IIa, NaPi-IIc, and PiT-2 in dietary potassium deficiency.* Am J Physiol Renal Physiol, 2009. **297**(2): p. F350-61.
129. Zajicek, H.K., et al., *Glycosphingolipids modulate renal phosphate transport in potassium deficiency.* Kidney Int, 2001. **60**(2): p. 694-704.
130. Inoue, M., et al., *Partitioning of NaPi cotransporter in cholesterol-, sphingomyelin-, and glycosphingolipid-enriched membrane domains modulates NaPi protein diffusion, clustering, and activity.* J Biol Chem, 2004. **279**(47): p. 49160-71.
131. Perwad, F., et al., *Fibroblast growth factor 23 impairs phosphorus and vitamin D metabolism in vivo and suppresses 25-hydroxyvitamin D-1alpha-hydroxylase expression in vitro.* Am J Physiol Renal Physiol, 2007. **293**(5): p. F1577-83.

132. Shimada, T., et al., *Targeted ablation of Fgf23 demonstrates an essential physiological role of FGF23 in phosphate and vitamin D metabolism.* J Clin Invest, 2004. **113**(4): p. 561-568.
133. Taketani, Y., et al., *Regulation of type II renal Na^+-dependent inorganic phosphate transporters by 1,25-dihydroxyvitamin D3. Identification of a vitamin D-responsive element in the human NAPi-3 gene.* J Biol Chem, 1998. **273**(23): p. 14575-81.
134. Segawa, H., et al., *Intestinal Na/Pi cotransporter adaptation to dietary Pi content in vitamin D receptor null mice.* Am J Physiol Renal Physiol, 2004. **287**(1): p. F39-47.
135. Saito, H., et al., *Circulating FGF-23 is regulated by 1 alpha,25-dihydroxyvitamin D-3 and phosphorus in vivo.* J Biol Chem, 2005. **280**(4): p. 2543-2549.
136. Kolek, O.I., et al., *1alpha,25-Dihydroxyvitamin D3 upregulates FGF23 gene expression in bone: the final link in a renal-gastrointestinal-skeletal axis that controls phosphate transport.* Am J Physiol Gastrointest Liver Physiol, 2005. **289**(6): p. G1036-42.
137. Hamm, L.L. and E.E. Simon, *Roles and mechanisms of urinary buffer excretion.* Am J Physiol, 1987. **253**(42): p. F595-605.
138. Nowik, M., et al., *Genome-wide gene expression profiling reveals renal genes regulated during metabolic acidosis.* Physiol Genomics, 2008. **32**(3): p. 322-34.
139. Ambuhl, P.M., et al., *Regulation of renal phosphate transport by acute and chronic metabolic acidosis in the rat.* Kidney Int, 1998. **53**(5): p. 1288-98.
140. Cai, Q., et al., *Brief report: inhibition of renal phosphate transport by a tumor product in a patient with oncogenic osteomalacia.* N Engl J Med, 1994. **330**(23): p. 1645-9.
141. Econs, M.J. and M.K. Drezner, *Tumor-Induced Osteomalacia - Unveiling a New Hormone.* N Engl J Med, 1994. **330**(23): p. 1679-1681.
142. Biber, J., et al., *Regulation of phosphate transport in proximal tubules.* Pflugers Arch, 2009. **458**(1): p. 39-52.
143. Quarles, L.D., *Endocrine functions of bone in mineral metabolism regulation.* J Clin Invest, 2008. **118**(12): p. 3820-8.
144. White, K.E., et al., *Autosomal-dominant hypophosphatemic rickets (ADHR) mutations stabilize FGF-23.* Kidney Int, 2001. **60**(6): p. 2079-86.
145. Shimada, T., et al., *Cloning and characterization of FGF23 as a causative factor of tumor-induced osteomalacia.* Proc Natl Acad Sci USA, 2001. **98**(11): p. 6500-6505.
146. Nishi, H., et al., *Intravenous calcitriol therapy increases serum concentrations of fibroblast growth factor-23 in dialysis patients with secondary hyperparathyroidism.* Nephron Clin Pract, 2005. **101**(2): p. c94-9.
147. Schiavi, S.C. and R. Kumar, *The phosphatonin pathway: New insights in phosphate homeostasis.* Kidney Int, 2004. **65**(1): p. 1-14.
148. Bowe, A.E., et al., *FGF-23 inhibits renal tubular phosphate transport and is a PHEX substrate.* Biochem Bioph Res Co, 2001. **284**(4): p. 977-981.
149. Shimada, T., et al., *FGF-23 transgenic mice demonstrate hypophosphatemic rickets with reduced expression of sodium phosphate cotransporter type IIa.* Biochem Bioph Res Co, 2004. **314**(2): p. 409-414.
150. Gattineni, J., et al., *FGF23 decreases renal NaPi-2a and NaPi-2c expression and induces hypophosphatemia in vivo predominantly via FGF receptor 1.* Am J Physiol Renal Physiol, 2009. **297**(2): p. F282-F291.
151. Gattineni, J., et al., *Regulation of renal phosphate transport by FGF23 is mediated by FGFR1 and FGFR4.* Am J Physiol Renal Physiol, 2014. **306**(3): p. F351-F358.

152. Yamashita, T., et al., *Fibroblast growth factor (FGF)-23 inhibits renal phosphate reabsorption by activation of the mitogen-activated protein kinase pathway.* J Biol Chem, 2002. **277**(31): p. 28265-70.
153. Farrow, E.G., et al., *Initial FGF23-mediated signaling occurs in the distal convoluted tubule.* J Am Soc Nephrol, 2009. **20**(5): p. 955-60.
154. Li, S.A., et al., *Immunohistochemical localization of Klotho protein in brain, kidney, and reproductive organs of mice.* Cell Struct Funct, 2004. **29**(4): p. 91-9.
155. Kato, Y., et al., *Establishment of the anti-Klotho monoclonal antibodies and detection of Klotho protein in kidneys.* Biochem Biophys Res Commun, 2000. **267**(2): p. 597-602.
156. Liu, S., et al., *FGFR3 and FGFR4 do not mediate renal effects of FGF23.* J Am Soc Nephrol, 2008. **19**(12): p. 2342-50.
157. Baum, M., et al., *Phosphatonin washout in Hyp mice proximal tubules: evidence for posttranscriptional regulation.* Am J Physiol Renal Physiol, 2005. **288**(2): p. F363-70.
158. Martin, A., V. David, and L.D. Quarles, *Regulation and function of the FGF23/klotho endocrine pathways.* Physiol Rev, 2012. **92**(1): p. 131-55.
159. Andrukhova, O., et al., *FGF23 acts directly on renal proximal tubules to induce phosphaturia through activation of the ERK1/2-SGK1 signaling pathway.* Bone, 2012. **50**: p. S49-S50.
160. Kuro-o, M., et al., *Mutation of the mouse klotho gene leads to a syndrome resembling ageing.* Nature, 1997. **390**(6655): p. 45-51.
161. Kuro-o, M., *FGF23 and Klotho.* Endocr J, 2010. **57**: p. S243-S243.
162. Hu, M.C., et al., *Klotho: a novel phosphaturic substance acting as an autocrine enzyme in the renal proximal tubule.* Faseb J, 2010. **24**(9): p. 3438-3450.
163. Radanovic, T., et al., *Regulation of intestinal phosphate transport. I. Segmental expression and adaptation to low-Pi diet of the type IIb Na^+/Pi cotransporter in mouse small intestine.* Am J Physiol Gastrointest Liver Physiol, 2005. **288**(3): p. G496-500.
164. Marks, J., et al., *Intestinal phosphate absorption and the effect of vitamin D: a comparison of rats with mice.* Exp Physiol, 2006. **91**(3): p. 531-7.
165. Borowitz, S.M. and F.K. Ghishan, *Phosphate transport in human jejunal brush-border membrane vesicles.* Gastroenterology, 1989. **96**(1): p. 4-10.
166. Xu, H., et al., *Age-dependent regulation of rat intestinal type IIb sodium-phosphate cotransporter by 1,25-(OH)(2) vitamin D(3).* Am J Physiol Cell Physiol, 2002. **282**(3): p. C487-93.
167. Arima, K., et al., *Glucocorticoid regulation and glycosylation of mouse intestinal type IIb Na/Pi cotransporter during ontogeny.* Am J Physiol Gastrointest Liver Physiol, 2002. **283**(2): p. G426-34.
168. Sandberg, J.W., et al., *Improving Access to Intestinal Stem-Cells as a Step toward Intestinal Gene-Transfer.* Hum Gene Ther, 1994. **5**(3): p. 323-329.
169. Williams, K.B. and H.F. DeLuca, *Characterization of intestinal phosphate absorption using a novel in vivo method.* Am J Physiol-Endoc M, 2007. **292**(6): p. E1917-E1921.
170. Xu, H., et al., *Regulation of the human sodium-phosphate cotransporter NaPi-IIb gene promoter by epidermal growth factor.* Am J Physiol Cell Physiol, 2001. **280**(3): p. C628-36.
171. Xu, H., et al., *Regulation of intestinal NaPi-IIb cotransporter gene expression by estrogen.* Am J Physiol Gastrointest Liver Physiol, 2003. **285**(6): p. G1317-24.
172. Stauber, A., et al., *Regulation of intestinal phosphate transport. II. Metabolic acidosis stimulates Na^+-dependent phosphate absorption and expression of the Na^+/Pi*

cotransporter NaPi-IIb in small intestine. Am J Physiol Gastrointest Liver Physiol, 2005. **288**(3): p. G501-6.

173. Marks, J., et al., *Matrix extracellular phosphoglycoprotein inhibits phosphate transport.* J Am Soc Nephrol, 2008. **19**(12): p. 2313-20.
174. Miyamoto, K., et al., *Inhibition of intestinal sodium-dependent inorganic phosphate transport by fibroblast growth factor 23.* Ther Apher Dial, 2005. **9**(4): p. 331-5.
175. Capuano, P., et al., *Intestinal and renal adaptation to a low-Pi diet of type II NaPi cotransporters in vitamin D receptor- and 1alphaOHase-deficient mice.* Am J Physiol Cell Physiol, 2005. **288**(2): p. C429-34.
176. Katai, K., et al., *Regulation of intestinal Na^+-dependent phosphate cotransporters by a low-phosphate diet and 1,25-dihydroxyvitamin D3.* Biochem J, 1999. **343**: p. 705-12.
177. Nishida, Y., et al., *Acute effect of oral phosphate loading on serum fibroblast growth factor 23 levels in healthy men.* Kidney Int, 2006. **70**(12): p. 2141-7.
178. Hattenhauer, O., et al., *Regulation of small intestinal Na/Pi type IIb cotransporter by dietary phosphate intake.* Am J Physiol, 1999. **277**(41): p. G756-62.
179. Brown, A.J., F.J. Zhang, and C.S. Ritter, *The vitamin D analog ED-71 is a potent regulator of intestinal phosphate absorption and NaPi-IIb.* Endocrinology, 2012. **153**(11): p. 5150-5156.
180. Liu, S., et al., *Pathogenic role of Fgf23 in Hyp mice.* Am J Physiol Endocrinol Metab, 2006. **291**(1): p. E38-49.
181. Liu, S., et al., *Regulation of fibroblastic growth factor 23 expression but not degradation by PHEX.* J Biol Chem, 2003. **278**(39): p. 37419-26.
182. Econs, M.J. and P.T. McEnery, *Autosomal dominant hypophosphatemic rickets/osteomalacia: clinical characterization of a novel renal phosphate-wasting disorder.* J Clin Endocrinol Metab, 1997. **82**(2): p. 674-81.
183. Imel, E.A., S.L. Hui, and M.J. Econs, *FGF23 concentrations vary with disease status in autosomal dominant hypophosphatemic rickets.* J Bone Miner Res, 2007. **22**(4): p. 520-6.
184. Feng, J.Q., et al., *Loss of DMP1 causes rickets and osteomalacia and identifies a role for osteocytes in mineral metabolism.* Nat Genet, 2006. **38**(11): p. 1310-5.
185. Lorenz-Depiereux, B., et al., *DMP1 mutations in autosomal recessive hypophosphatemia implicate a bone matrix protein in the regulation of phosphate homeostasis.* Nat Genet, 2006. **38**(11): p. 1248-50.
186. Feng, J.Q., et al., *The dentin matrix protein 1 (Dmp1) is specifically expressed in mineralized, but not soft, tissues during development.* J Dent Res, 2003. **82**(10): p. 776-780.
187. Ye, L., et al., *Periodontal breakdown in the Dmp1 null mouse model of hypophosphatemic rickets.* J Dent Res, 2008. **87**(7): p. 624-9.
188. Liu, S., et al., *Pathogenic role of Fgf23 in Dmp1-null mice.* Am J Physiol Endocrinol Metab, 2008. **295**(2): p. E254-61.
189. Folpe, A.L., et al., *Most osteomalacia-associated mesenchymal tumors are a single histopathologic entity - An analysis of 32 cases and a comprehensive review of the literature.* Am J Surg Pathol, 2004. **28**(1): p. 1-30.
190. Ryan, E.A. and E. Reiss, *Oncogenous osteomalacia. Review of the world literature of 42 cases and report of two new cases.* Am J Med, 1984. **77**(3): p. 501-12.
191. Riminucci, M., et al., *FGF-23 in fibrous dysplasia of bone and its relationship to renal phosphate wasting.* J Clin Invest, 2003. **112**(5): p. 683-92.

192. Tieder, M., et al., *Hereditary hypophosphatemic rickets with hypercalciuria.* N Engl J Med, 1985. **312**(10): p. 611-7.
193. Bergwitz, C., et al., *SLC34A3 mutations in patients with hereditary hypophosphatemic rickets with hypercalciuria predict a key role for the sodium-phosphate cotransporter NaPi-IIc in maintaining phosphate homeostasis.* Am J Hum Genet, 2006. **78**(2): p. 179-92.
194. Lorenz-Depiereux, B., et al., *Hereditary hypophosphatemic rickets with hypercalciuria is caused by mutations in the sodium-phosphate cotransporter gene SLC34A3.* Am J Hum Genet, 2006. **78**(2): p. 193-201.
195. Levi, M., *Novel NaPi-2c mutations that cause mistargeting of NaPi-2c protein and uncoupling of Na^+/Pi cotransport cause HHRH.* Am J Physiol Renal Physiol, 2008. **295**(2): p. F369-F370.
196. Hsu, S.C., et al., *Mutations in SLC20A2 are a major cause of familial idiopathic basal ganglia calcification.* Neurogenetics, 2013. **14**(1): p. 11-22.
197. Tenenhouse, H.S., et al., *Differential effects of Npt2a gene ablation and X-linked Hyp mutation on renal expression of Npt2c.* Am J Physiol Renal Physiol, 2003. **285**(6): p. F1271-F1278.
198. Tenenhouse, H.S., et al., *Na/Pi cotransporter (Npt2) gene disruption increases duodenal calcium absorption and expression of epithelial calcium channels 1 and 2.* Pflugers Arch, 2002. **444**(5): p. 670-6.
199. Traykova-Brauch, M., et al., *An efficient and versatile system for acute and chronic modulation of renal tubular function in transgenic mice.* Nat Med, 2008. **14**(9): p. 979-84.
200. Biber, J., et al., *Isolation of renal proximal tubular brush-border membranes.* Nat Protoc, 2007. **2**(6): p. 1356-9.
201. Stoll, R., R. Kinne, and H. Murer, *Effect of dietary phosphate intake on phosphate transport by isolated rat renal brush-border vesicles.* Biochem J, 1979. **180**(3): p. 465-70.
202. Villa-Bellosta, R. and V. Sorribas, *Different effects of arsenate and phosphonoformate on Pi transport adaptation in opossum kidney cells.* Am J Physiol Cell Physiol, 2009. **297**(3): p. C516-25.
203. Riond, J.L. and J.E. Riviere, *Pharmacology and toxicology of doxycycline.* Vet Hum Toxicol, 1988. **30**(5): p. 431-43.
204. Biber, J., N. Hernando, and I. Forster, *Phosphate transporters and their function.* Annu Rev Physiol, 2013. **75**: p. 535-550.
205. Matsumoto, N., et al., *Immunohistochemical analyses of parathyroid hormone-dependent downregulation of renal type II Na^+/Pi-cotransporters by cryobiopsy.* J Med Invest, 2010. **57**(1-2): p. 138-45.
206. Bai, X., et al., *Transgenic mice overexpressing human fibroblast growth factor 23 (R176Q) delineate a putative role for parathyroid hormone in renal phosphate wasting disorders.* Endocrinology, 2004. **145**(11): p. 5269-79.
207. Xue, Y.B., et al., *Genetic models show that parathyroid hormone and 1,25-dihydroxyvitamin D-3 play distinct and synergistic roles in postnatal mineral ion homeostasis and skeletal development.* Hum Mol Genet, 2005. **14**(11): p. 1515-1528.
208. Shimada, T., et al., *FGF-23 is a potent regulator of vitamin D metabolism and phosphate homeostasis.* J Bone Miner Res, 2004. **19**(3): p. 429-435.

209. Larsson, T., et al., *Transgenic mice expressing fibroblast growth factor 23 under the control of the alpha1(I) collagen promoter exhibit growth retardation, osteomalacia, and disturbed phosphate homeostasis.* Endocrinology, 2004. **145**(7): p. 3087-94.

11. Appendix

Renal-specific and inducible depletion of NaPi-IIc/Slc34A3, the cotransporter mutated in HHRH, does not affect phosphate or calcium homeostasis in mice

Komuraiah Myakala, Sarah Motta, Heini Murer, Carsten A Wagner, Robert Koesters, Jürg Biber and Nati Hernando

Institute of Physiology and Zurich Center for Integrative Human Physiology (ZIHP). University of Zurich, Switzerland

The proximal renal epithelia express three different Na-dependent inorganic phosphate (Pi) cotransporters: NaPi-IIa/SLC34A1, NaPi-IIc/SLC34A3, and PiT2/SLC20A2. Constitutive mouse knockout models of NaPi-IIa and NaPi-IIc suggested that NaPi-IIa mediates the bulk of renal reabsorption of Pi whereas the contribution of NaPi-IIc to this process is minor and probably restricted to young mice. However, many reports indicate that mutations of NaPi-IIc in humans lead to hereditary hypophosphatemic rickets with hypercalciuria (HHRH). Here, we report the generation of a kidney-specific and inducible NaPi-IIc-deficient mouse model based on the loxP-Cre system. We found that the specific removal of the cotransporter from the kidneys of young mice does not impair the capacity of the renal epithelia to transport Pi. Moreover, the levels of Pi in plasma and urine as well as the circulating levels of parathyroid hormone, FGF-23, and vitamin D3 remained unchanged. These findings are in agreement with the data obtained with the constitutive knockout model and suggest that, under steady-state conditions of normal dietary Pi, NaPi-IIc is not an essential Na-Pi cotransporter in murine kidneys. However, and unlike the constitutive mutants, the kidney-specific depletion of NaPi-IIc does not result in alteration of the homeostasis of calcium. This suggests that the calcium-related phenotype observed in constitutive knockout mice may not be related to inactivation of the cotransporter in kidney

12. Acknowledgements

Foremost, I would like to express my sincere gratitude to my doctorial adviser Prof. Jürg Biber for accepting me as a grade student in his lab and supporting me to perform this research study during last 4 years, indeed it was a pleasure to work in your epithelial phosphate transporters lab. I would like to thank him for continuous support, mentoring, for his patience, immense knowledge in the area of phosphate transport mechanisms, his suggestions and comments during my work. His guidance helped me in all the time of research and writing of this thesis.

It is not enough to simply acknowledge, I will forever be sincere and special thanks to Dr. Nati Hernando. It was great opportunity to working under such a best supervision that I ever had. Nati has been supportive and encouragement was invaluable throughout my research. I am also very grateful for her scientific inputs, careful edits, knowledge and discussions regarding work and helping me to writing of my thesis. I have learned many things from you to be as enthusiastic researcher, organising the experiments without being waste of time. She remains my best role model for a scientist, mentor and teacher. Nati, I hope that I would implement and improve my strategies in the scientific research which I have learned from you.

Beside Jürg and Nati, I would also especially thank to Prof. Carsten Wagner for not only being as my thesis committee member, for also valuable scientific suggestions during the lab and committee meetings. I thank also to Dr. Daniel fuster (University of Bern) as my external thesis committee member and his suggestions during committee meetings. I am also wants to acknowledge honourable Prof. Heini Murer and his scientific advice for my paper.

My special thanks also goes to Gerti Stange for taught me the phosphate uptake experiments and indeed, it was tough and best but learned well. Udo. S has been really helpful with Ion chromatography and vitamin D analysis. I gratefully thank to Matthew. Adjei for his nice and kind help for taking care of my little NaPi-IIc animals in the animal facility.

I would also take this opportunity to thank my master thesis supervisors Prof. Dr. Paul Mohacsi and Dr. Melinda Orozlan from University hospital (InselSpital) of Bern for their first encouragement to take a step ahead in the doctoral research. I also thank to my lab colleague Nathali. Ligeti for heartful support.

Life would have been very difficult if I did not have the scientific and super friendly support of my dear fellow colleagues/or friends in our Lab. I gratefully thanks to my gentleman colleague Thomas. K for his help with perfusion of animals, written the thesis summary in German and more than that, as a nice friend, I remembered the chill outs during outings in downtown, it was nice fun time that we always poke or being mean to each other, like a little brothers. Linto, T. I would say, you are not only a colleague but as my good friend to share many things since I knew you better in Zurich although I met you before in Sweden. Porto girl, Marta. F you are really very friendly and good to have a friend like you, nice to discuss many things during lunch time. Justina. R, it was also good time in the lab with you that, you always make scientific discussions and complains regarding work and beside that, discussion about your things.

I am very glad to have best friend like Dr. Madan and his life partner Rithika madan who push, support and motivate me throughout my studies from Sweden until now and it is obvious that I share many of my activities with them. It's been a great time with my heartful friend Dr. Affy from Sweden to Basel, and especial thank to him. I always had happy moments and talk each other not only about science and share many things from both sides. It was good journey from Denmark with Dr. Anjan, Bern till Switzerland. It was great motivation for me from our discussions which makes me to take a step head in studies to become success. I cheerfully convey my thanks to Dr. Ramesh also from Bern.

Especial faces Sarah. M and Fabia. S for me to introduce here and we know each other for more than 12 months. It is not just enough to convey my acknowledgements here, in fact you always been special. It's a great pleasure to meet and work with such amicable and delightful friends like you in lab. It's always been fun and nice time with you; I thank both for making such special moments.

Finally, but top of everything, I would not have such wonderful moments from India to Europe without blessing from my hard-working parents Amma (Mom), Nanna (Dad). Their unconditional love is infinite and invaluable. I would not have made this far without them. Special members of my family to introduce here: From the beginning to till, immense encouragement from the bottom of heart by my lovely elder Brother (Ravi) and my Vadhina (Dr. Anuradha, Angel: Saanvi). All the situations, their love, huge support and motivation were really incredible and impressive. I love them forever. I also like to huge thanks to my sister Manju and her family and I love her dearly. Special thanks to my younger brother (Mahendar. K), more than, he is like my best friend, I really love him. I truly wish him to fulfil his strong aspirations in his life. I love you all dearly.

Last but not the least, I would like to thank to friends and people in J-flour for creating such wonderful environment to make my research. It`s been a nice memory for me to work with you all.

13. CURRICULUM VITAE

Personal information

Name (surname):	MYAKALA
Name:	komuraiah
Date of birth:	26th August 1982
Nationality:	Indian
Address:	Bergstrasse 57, Zimmer num. 218, 8032 Zürich, Switzerland
Email:	komuraiah.myakala@uzh.ch, gytkumar@gmail.com

Education

Since 05/2010	PhD student in Physiology, Institute of Physiology, University of Zurich, Switzerland Supervisors: Prof. Jürg Biber and Prof. Dr. Carsten Wagner
08/2008- 03/2010	Masters in Biomedicine, University of Skövde, Skövde, Sweden
2007- 2008	Exchanged study, University of Roskilde, Denmark
2003 - 2005	Masters in Microbiology, Osmania University, Hyderabad, Telangana, India.
1999 - 2002	Bachelors in Microbiology, Chemistry, Kakatiya University, Warangal, India.
1999	Intermediate education, Loyola Junior college, Karimnagar, AP, India

Master thesis

"PSI-associated proteinuria in renal transplant recipient: Dysfunction of proximal tubular epithelial cells is a result of decreased megalin andcubilin expression"?.
Prof. Dr. Paul Mohacsi and Dr. Melinda Oroszlan, Department of Cardiology, University Hospital (InselSpital), Bern.

Publications

- Renal-specific and inducible depletion of NaPi-IIc/Slc34a3, the cotransporter mutated in HHRH, does not affect phosphate or calcium homeostasis in mice
  Myakala. K, Motta. S, Murer. H, Wagner CA, Biber J, Hernando N
  Am J Physiol Renal Physiol. 2014 Apr.

- Intestinal depletion of NaPi-IIb/Slc34a2 in mice: renal and hormonal adaptation
  Hernando N, **Myakala. K,** Simona F, Murer. H, Wagner CA, Biber. J
  Manuscript submitted to JBMR